# REPORT DOCUMENTATION PAGE.

form Approved OMB No. 0704-0138

Applic recording burden for this collection of information is estimated to average 1 hour per response, including the time for ferinaving instructions, learning enting data sources, darkening and maintaining the data needed, and completing and remaining the collection of information. Send comments regarding this burden estimate or any other tribulations reasonables services. Sendon the data needed, and completing and remaining the data needed, and completing and remaining the data needed, and completing and remaining the data needed, and completing are services. gton Headquarters Services, Directorate for into the con Operations and Peports, 13 hent and Biudges, Paperwork Beduction Project (07:34-0158), Washington, OC 10503. Collection of information, including suggestions for reducing this ourcest, to Washin Daws nightway, Suita 1204, Amington, VA 22202-4302, and to the Office of Manager

1. AGENCY USE ONLY (Leave blank)

2. REPORT DATE 3/18/98

3. REPORT TYPE AND DATES COVERED

FINAL REPORT (10/1/93 - 9/30/97)

A TITLE AND SUBTITLE

High Temperature Superconductor MCM Process Development

F49620-93-1-0605

& AUTHOR(S)

Leonard W. Schaper

AFRL-SR-BL-TR-98-

7. PERFORMING ORGANIZATION NAME(S) AND ADDRESS(ES)

High Density Electronics Center (HiDEC) University of Arkansas

Fayetteville, AR 72701

9. SPONSORING MONITORING AGENCY NAME(5) AND ADORESS(ES)

Air Force Office of Scientific Research 110 Duncan Avenue, Room B115 Bolling AFB, DC 20332-8080



10. SPONSORING/MONITORING AGENCY REPORT NUMBER

11. SUPPLEMENTARY NOTES

12s. DISTRIBUTION / AVAILABILITY STATEMENT

125 DISTRIBUTION CODE

ilmited

### 13. ABSTRACT (Maximum 200 words)

Two types of high-temperature superconducting (HTS) multichip modules (MCMs), utilizing yttrium-barium-copper oxide (YBCO) as the superconductor, were developed under this grant. The first was a "flip mesh" MCM, in which two superconducting layers, one containing X-running and one Y-running wire segments, were fabricated on separate substrates and joined in a manner similar to flip chips.

The second module was a monolithic MCM, again using layers of X- and Y-running conductors, but patterned on a single substrate, with a thick layer of SiO, serving as interlayer dielectric. Deposition of the second superconducting (YBCO) layer was effected by the use of an ion beam-assisted deposition (IBAD) buffer layer.

> DING QUALITY LINGS BOTH 15. HUMBER OF PAGES

14. SUBJECT TERMS

Superconductivity, multichip module, ion beam-assisted deposition, flip-mesh, monolithic, vias, HTS, MCM, YBCO, YSZ

18. SECURITY CLASSIFICATION

14. PRICE CODE

17. SECURITY CLASSIFICATION of report

OF THIS PAGE UNLIMITED UNLIMITED

19. SECURITY CLASSIFICATION OF ABSTRACT UNLIMITED

20. LIMITATION OF ABSTRACT UNLIMITED

KN 7540-01-280-5500

Standard Form 298 (Rev. 2-39)

# (AASERT-93) HTCS MCM Process Development

Final Technical Report

15 March 1998

Air Force Office of Scientific Research

F49620-93-1-0605

University of Arkansas High Density Electronics Center

Approved for Public Release: Distribution Unlimited

The views, opinion, and/or findings contained in this report are those of the author(s) and should not be construed as an official United States Air Force position, policy, or decision, unless so designated by other documentation.

# **ABSTRACT**

Two types of high-temperature superconducting (HTS) multichip modules (MCMs), utilizing yttrium-barium-copper oxide (YBCO) as the superconductor, were developed under this grant. The first was a "flip mesh" MCM, in which two superconducting layers, one containing X-running and one Y-running wire segments, were fabricated on separate substrates and joined in a manner similar to flip chips.

The second module was a monolithic MCM, again using layers of X- and Y-running conductors, but patterned on a single substrate, with a thick layer of SiO<sub>2</sub> serving as interlayer dielectric. Deposition of the second superconducting (YBCO) layer was effected by the use of an ion beam-assisted deposition (IBAD) buffer layer.

# **RESULTS**

A great deal of progress was made toward realizing the flip-mesh MCM and the monolithic MCM, although neither were totally successful. Rather than repeat previously published material, the reader is referred to the enclosed papers presented at the May 1997 Electrochemical Society meeting. Presentation [11](principle author Cooksey, funded under this grant) describes the monolithic MCM, and presentation [12] (principal author Scott, funded under this grant) describes the "flip-mesh".

Although the final goal of reliably producing superconducting MCMs proved illusive, a great deal was learned about two important aspects of the creation of complex thin-film HTS structures: the deposition of superconducting layers over thick amorphous dielectric layers, and the process of creating vias between superconducting layers. These results, which go a long way in solving the most difficult problems associated with HTS multilayer structures, are discussed in Publications [11], [12], and [13].

The via structure described in [11], though made of normal metal (gold), represents a significant advance over previously reported superconducting vias, because it occupies relatively little space in an MCM structure, and contributes very little resistance compared with the resistance of normal metal lines. It is the line, not the via, resistance which was the impetus for HTS MCMs, in the first place.

The HTS layers described in [12] and [13], which use IBAD yttria-stabilized zirconia (YSZ) buffer layers to allow the deposition of an upper HTS layer over a thick  ${\rm SiO_2}$  interlayer dielectric, are a significant advance over previously reported HTS MCM work, which attempted to maintain multilayer epitaxy. The latter, maintenance of

multilayer epitaxy, resulted in an extremely thin, high dielectric constant interlayer dielectric, which would make the fabrication of transmission lines of usable impedance ( $\sim 50-75~\Omega$ ) and reasonable propagation delay (< 100~pS/cm) impossible. However, the fabrication of reasonable transmission lines is possible in the structures which have been developed under this grant. A monolithic HTS MCM was produced which appeared to superconduct and function as anticipated, before ultimately failing. The student responsible left for a job in industry before a second module was fabricated and these tantalizing results verified. New personnel, under another grant, are working to replicate the MCM.

# CONCLUSION

Significant progress was made on two impediments to the realization of HTS MCMs. First, HTS YBCO was deposited and patterned atop a thick, amorphous dielectric (SiO<sub>2</sub>). Second, functional gold vias between superconducting layers were developed. A multilayer HTS MCM was produced that appeared to function before its untimely failure. A complete set of the publications and presentations produced under this grant is included with this report.

# **PUBLICATIONS and PROCEEDINGS**

[1] J. W. COOKSEY, W. D. BROWN, S. S. ANG, H. A. NASEEM, R. K. ULRICH, AND L. WEST, "Gamma-ray and fast neutron radiation effects on thin film superconductors," *IEEE Trans. Nucl. Sci.*, vol. 41, pp. 2521-2524, 1994.

- [2] D. E. FORD, S. S. SCOTT, S. S. ANG, AND W. D. BROWN, "A comparison of high-temperature superconductors in multichip module applications," *Proc. Ark. Acad. Sci.*, vol. 48, pp. 45-49, 1994.
- [3] R. G. FLORENCE, S. S. ANG, AND W. D. BROWN, "The effects of rapid thermal annealing on the properties of sputtered YBCO superconducting films," *Supercond. Sci. Technol.*, vol. 7, pp. 741-744, 1994.
- [4] S. S. SCOTT, S. S. ANG, AND W. D. BROWN, "The effects of low-energy blanket ion milling on the properties of superconducting YBCO films," *Electrochem. Soc. Proc.*, vol. 95-9, *Proceedings of the Symposium on Low Temperature Electronics and High Temperature Superconductivity*, pp. 105-112, 1995.
- [5] G. FLORENCE, S. ANG, AND W. D. BROWN, "Ion beam assisted sputter deposition of CeO<sub>2</sub> buffer layers for superconducting multichip module (MCM) applications," *Electrochem. Soc. Proc.*, vol. 95-9, *Proceedings of the Symposium on Low Temperature Electronics and High Temperature Superconductivity*, pp. 113-120, 1995.
- [6] G. FLORENCE, S. ANG, AND W. D. BROWN, "Ion-beam-assisted sputter deposition of YSZ buffer layers for superconducting interconnect applications," *Supercond. Sci. & Tech.*, vol. 8, pp. 546-551, 1995.
- [7] R. G. FLORENCE, S. S. ANG, W. D. BROWN, G. SALAMO, L. W. SCHAPER, AND R. K. Ulrich, "Sputter-deposited yttrium-barium-copper-oxide multilayer structures incorporating a thick interlayer dielectric material," *J. Appl. Phys.*, vol. 79, pp. 2003-2005, 1996.
- [8] S. AFONSO, F. T. CHAN, K. Y. CHEN, G. J. SALAMO, Y. Q. TANG, R. C. WANG, X. L. XU, Q. XIONG, G. FLORENCE, S. SCOTT, S. ANG, W. D. BROWN, AND L. W. SCHAPER, "Magnetic field and temperature dependence of critical current densities in multilayer YBa<sub>2</sub>Cu<sub>3</sub>O<sub>7-δ</sub> films," J. Appl. Phys., vol. 79, pp. 6593-6595, 1996.
- [9] Q. XIONG, S. AFONSO, F. T. CHAN, K. Y. CHEN, G. J. SALAMO, G. FLORENCE, J. COOKSEY, S. SCOTT, S. ANG, W. D. BROWN, AND L. SCHAPER, "Fabrication of highly textured superconducting thin films on polycrystalline substrates using ion beam assisted deposition," *Proceedings of the 10th Anniversary HTS Workshop on Physics, Materials and Applications*, B. BATLOGG, C. W. CHU, W. K. CHU, D. U. GUBSER, and K. A. MÜLLER eds. World Scientific: New Jersey 1996, pp. 167-170.

[10] J. W. COOKSEY, S. S. SCOTT, W. D. BROWN, S. S. ANG, R. G. FLORENCE, AND S. AFONSO, "Recent advances in high temperature superconductor multichip modules," *Proc.* 1997 *ICEMCM*, pp. 115-120, 1997.

- [11] J. W. COOKSEY, S. AFONSO, W. D. BROWN, L. W. SCHAPER, S. S. ANG, R. K. ULRICH, G. J. SALAMO, AND F. T. CHAN, "Fabrication and characterization of vias for contacting YBa<sub>2</sub>Cu<sub>3</sub>O<sub>7x</sub> multilayers," *Physica C*, vol. 282-287, pp. 683-684, 1997.
- [12] S. AFONSO, K. Y. CHEN, Q. XIONG, F. T. CHAN, G. J. SALAMO, J. W. COOKSEY, S. SCOTT, S. ANG, W. D. BROWN, AND L. W. SCHAPER, "Fabrication techniques and electrical properties of YBa<sub>2</sub>Cu<sub>3</sub>O<sub>7-x</sub> multilayers with rf sputtered amorphous SiO<sub>2</sub> interlayers," *Physica C*, vol. 282-287, pp. 685-686, 1997.
- [13] S. AFONSO, K. Y. CHEN, Q. XIONG, Y. Q. TANG, G. J. SALAMO, F. T. CHAN, J. COOKSEY, S. SCOTT, Y. J. SHI, S. ANG, W. D. BROWN, AND L. W. SCHAPER, "Y<sub>1</sub>Ba<sub>2</sub>Cu<sub>3</sub>O<sub>7-x</sub> multilayer structures with a thick SiO<sub>2</sub> interlayer for multichip modules," *J. Mater. Res.*, vol. 12, pp. 2947-2951, 1997.

# **PRESENTATIONS**

- [1] D. E. FORD, S. S. SCOTT, S. S. ANG, AND W. D. BROWN, "A comparison of high-temperature superconductors in multi-chip module applications," 78th Annual Meeting of the Arkansas Academy of Science, April 8-9, 1994, Jonesboro, AR, 1994.
- [2] J. W. COOKSEY, W. D. BROWN, S. S. ANG, H. A. NASEEM, R. K. ULRICH, AND L. WEST, "Gamma-ray and fast neutron radiation effects on thin film superconductors," 31st Annual International Nuclear and Space Radiation Effects Conference, July 18-22, 1994, Tucson, AZ, 1994.
- [3] J. W. COOKSEY, W. D. BROWN, L. W. SCHAPER, S. S. ANG, AND R. K. ULRICH, "Development of vias for use in high temperature superconductor multichip modules," 187<sup>th</sup>. Meeting of the Electrochemical Society, May 21-26, 1995, Reno, NV, 1995.
- [4] G. FLORENCE, S. ANG, AND W. D. BROWN, "Ion beam assisted sputter deposition of CeO<sub>2</sub> buffer layers for superconducting multichip module (MCM) applications," Symposium on Low Temperature Electronics and High Temperature Superconductivity at the 187<sup>th</sup> Meeting of the Electrochemical Society, May 21-26, 1995, Reno, NV, 1995.
- [5] S. S. SCOTT, S. S. ANG, AND W. D. BROWN, "The effects of low-energy blanket ion milling on the properties of superconducting YBCO films," Symposium on Low Temperature Electronics and High Temperature Superconductivity at the 187th Meeting of the Electrochemical Society, May 21-26, 1995, Reno, NV, 1995.

[6] S. AFONSO, F. T. CHAN, K. Y. CHEN, G. J. SALAMO, Y. Q. TANG, R. C. WANG, X. L. XU, Q. XIONG, G. FLORENCE, S. SCOTT, S. ANG, W. D. BROWN, AND L. W. SCHAPER, "The magnetic field and temperature dependence of critical current densities in multilayer YBa<sub>2</sub>CuO<sub>4+δ</sub>," 40<sup>th</sup> Annual Conference on Magnetism and Magnetic Materials, November 6-9, 1995, Philadelphia, PA, 1995.

- [7] Q. XIONG, S. AFONSO, F. T. CHAN, K. Y. CHEN, G. J. SALAMO, G. FLORENCE, J. COOKSEY, S. SCOTT, S. ANG, W. D. BROWN, AND L. SCHAPER, "Fabrication of highly textured superconducting thin films on polycrystalline substrates using ion beam assisted deposition," 10th Anniversary HTS Workshop on Physics, Materials and Applications, March 12 16, 1996, Houston, TX, 1996.
- [8] J. W. COOKSEY, S. AFONSO, W. D. BROWN, L. W. SCHAPER, S. S. ANG, R. K. ULRICH, G. J. SALAMO, AND F. T. CHAN, "Fabrication and characterization of vias for contacting YBa<sub>2</sub>Cu<sub>3</sub>O<sub>7-x</sub> multilayers," 5<sup>th</sup> International Conference on Materials and Mechanisms of Superconductivity and High-Temperature Superconductors, M<sup>2</sup>S-HTSC-V, February 28 March 4, 1997, Beijing, China, 1997.
- [9] S. AFONSO, K. Y. CHEN, Q. XIONG, F. T. CHAN, G. J. SALAMO, J. W. COOKSEY, S. SCOTT, S. ANG, W. D. BROWN, AND L. W. SCHAPER, "Fabrication techniques and electrical properties of YBa<sub>2</sub>Cu<sub>3</sub>O<sub>7-x</sub> multilayers with rf sputtered amorphous SiO<sub>2</sub> interlayers," 5<sup>th</sup> International Conference on Materials and Mechanisms of Superconductivity and High-Temperature Superconductors, M<sup>2</sup>S-HTSC-V, February 28 March 4, 1997, Beijing, China, 1997.
- [10] J. W. COOKSEY, S. S. SCOTT, W. D. BROWN, S. S. ANG, R. G. FLORENCE, AND S. AFONSO, "Recent advances in high temperature superconductor multichip modules," 6<sup>th</sup> International Conference on Multichip Modules, ICEMCM '97, April 2-4, 1997, Denver, CO, 1997.
- [11] J. W. COOKSEY, W. D. BROWN, L. W. SCHAPER, R. G. FLORENCE, S. S. SCOTT, AND S. AFONSO, "Fabrication and characterization of a high temperature superconducting multichip module," Fourth Symposium on Low Temperature Electronics and High Temperature Superconductivity at the 191<sup>st</sup> Meeting of the Electrochemical Society, May 4-9, 1997, Montreal, Canada, 1997.
- [12] S. S. SCOTT, S. S. ANG, W. D. BROWN, L. W. SCHAPER, AND S. AFONSO, "The flip-mesh superconducting MCM," 191st Meeting of the Electrochemical Society, May 4-9, 1997, Montréal, Québec, Canada, 1997.

# Gamma-ray and Fast Neutron Radiation Effects on Thin Film Superconductors\*

J. W. Cooksey, W. D. Brown, S. S. Ang, H. A. Naseem, and R. K. Ulrich High Density Electronics Center (HiDEC) University of Arkansas, Fayetteville, AR 72701

and

L. West

Department of Mechanical Engineering University of Arkansas, Fayetteville, AR 72701

Abstract

II. EXPERIMENTAL PROCEDURES

The gamma-ray and neutron radiation hardness of YBa<sub>2</sub>Cu<sub>3</sub>O<sub>7-x</sub>, Tl<sub>2</sub>Ba<sub>2</sub>CaCu<sub>2</sub>O<sub>8+x</sub>, and Tl<sub>2</sub>Ba<sub>2</sub>Ca<sub>2</sub>Cu<sub>3</sub>O<sub>10+x</sub> superconducting thin films deposited by off-axis sputtering and laser-ablation deposition techniques on substrates of MgO and LaAlO<sub>3</sub> was investigated. The unbiased samples were irradiated with 662 keV gamma-rays up to a cumulative dose of 1.5 Mrad(Si) and with neutron fluences up to 1 x 10<sup>14</sup> neutrons/cm<sup>2</sup>.

It was determined through nondestructive critical temperature transition,  $T_{\rm c}$ , and critical current density,  $J_{\rm c}$ , measurements and x-ray diffraction analysis that the thin film superconductors were radiation hard up to moderate levels of neutrons and gamma-rays. It was also determined that extended exposure to moderately humid air degraded the critical current density of all the films.

### I. INTRODUCTION

Space applications of multichip modules (MCMs) appear to be part of the driving force for their development. In the future, thin film superconductors (TFSCs) will potentially be used as interconnects for MCMs. As a result of this application of TFSCs, their response to a radiation environment is of great interest. In the past, studies of radiation effects on superconductor materials have been restricted to the bulk form [1-5], but if superconducting interconnects are to be used in future MCMs, the impact of exposure to gamma-rays and fast neutrons on the properties of TFSC materials must be examined. In addition to the effects of radiation on the superconductor material, the substrate material on which the superconductor is deposited, as well as the dielectric material used to separate the multiple levels of interconnects, must also be examined for sensitivity to radiation exposure.

In the work reported here, YBa<sub>2</sub>Cu<sub>3</sub>O<sub>7-x</sub> (YBCO), Tl<sub>2</sub>Ba<sub>2</sub>CaCu<sub>2</sub>O<sub>8+x</sub> (Tl-2212), and Tl<sub>2</sub>Ba<sub>2</sub>Ca<sub>2</sub>Cu<sub>3</sub>O<sub>10+x</sub> (Tl-2223) thin films on substrates of MgO and LaAlO<sub>3</sub>, some of the more common superconductor/substrate combinations, were subjected to both gamma-ray and neutron radiation in an electrically unbiased state. Although radiation without bias does not fully explore the impact on dielectric substrates, it does examine the impact on high temperature superconductors. The samples were deposited using laserablation and off-axis sputtering techniques, and were of varying quality and thickness in order to determine if their radiation hardness varied accordingly. The thin film thicknesses ranged from about 200 to 1000 nm.

The superconductors were characterized by their critical temperature transition, T<sub>c</sub>, and critical current density, J<sub>c</sub>, measured using a nondestructive inductance method as described by Claassen et al. [6]. This measurement technique involves placing a thin, multiturn copper coil next to the film surface and driving the coil with a low distortion audiofrequency sine-wave current. In turn, the driving current induces shielding currents in the film. The nonlinearity in the coil-film system increases abruptly when the induced current in the film reaches its critical level. A schematic of the measurement system used is shown in Figure 1. The resulting voltage across the coil is filtered by a passive twintee notch filter with a center frequency the same as the drive current frequency, 1 kHz, and analyzed by the lock-in amplifier for third harmonics. Either a single or double coil can be used. A single coil acts as "both the drive and pickup coil." We have used a single coil setup in our measurements since it functions as well as a two coil setup according to Claassen et al. The samples were measured down to liquid nitrogen temperature (77 K). This type of measurement was chosen over the four point contact method because the samples had to be measured after each irradiation. Any probe technique would destroy a large surface area of the film after each subsequent measurement since we were dealing with samples less than 1 cm<sup>2</sup>. A Philips x-ray diffractometer was also used in an attempt to detect any atomic disorder in the superconductor films resulting from neutron bombardment.

The superconductor/substrate structures were irradiated with gamma-rays up to a cumulative dose of 1.5 Mrad(Si)

<sup>\*</sup>We would like to acknowledge the assistance of Tim Welty of the Southwest Radiation Calibration Center in the radiation experiments. We would also like to acknowledge Conductus, Inc. and Superconductor Technologies Inc. for their donation of superconductor samples. This research was funded by E-Systems, Inc. and the Advanced Research Projects Agency.

using a Cs-137 radioisotope emitting 662 keV gamma-rays at a dose rate of 24.2 krad(Si)/hr. The gamma-ray source was contained in a JL Shepherd Model 81-12A Irradiator. The neutron irradiations involved exposing the samples to cumulative fluences up to 1 x 10<sup>14</sup> neutrons/cm<sup>2</sup> from a 0.68 Ci Cf-252 source which had an average neutron flux throughout the experiment of 1.966 x 10<sup>8</sup> neutrons/cm<sup>2</sup>·s. All irradiations were performed in air at room temperature.

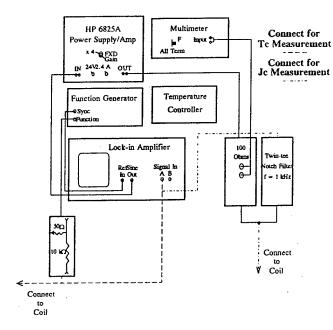


Figure 1. Critical temperature and critical current density measurement system schematic.

# III. RESULTS AND DISCUSSION

The pre-irradiation critical temperature transitions for the Tl-based films ranged from about 85-113 K and from about 86-90 K for the YBCO films. The pre-irradiation critical current densities at 77 K for all the samples ranged from on the order of  $10^4$  A/cm<sup>2</sup> up to on the order of  $10^6$  A/cm<sup>2</sup>.

# A. Gamma-ray Irradiations

The structures proved to be hard to gamma-rays up to very high doses and exhibited relatively little change in their critical temperature or critical current density characteristics. The measurements were taken 30 minutes after the films were removed from the source. This did not permit short term transient effects, possibly occurring during the irradiations, to be observed.

The critical temperature and critical current density characteristics of a typical sample of YBCO on a LaAlO<sub>3</sub> substrate after several gamma-ray irradiations up to a cumulative dose of 1.5 Mrad(Si) are shown in Figures 2 and 3. As shown in these figures, there was very little change in the critical temperature transition region (~89.4 K) or in the critical current density (~1.5 x 10<sup>6</sup> A/cm<sup>2</sup> at 77 K). This was

typical for all samples that underwent gamma-ray irradiations and seemed to be independent of the initial quality of the superconductor. The critical temperature and critical current density measurement data for a typical sample of each superconductor/substrate combination that underwent gamma-ray irradiations are listed in Table I.

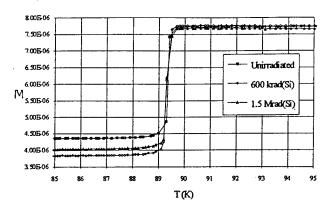


Figure 2. Critical temperature transition of YBa<sub>2</sub>Cu<sub>3</sub>O<sub>7-x</sub> on a LaAlO<sub>3</sub> substrate after gamma irradiations.

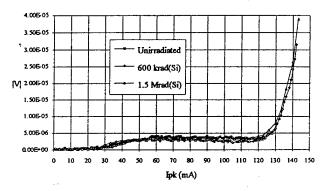


Figure 3. Critical current density measurement of  $YBa_2Cu_3O_{7-x}$  on a LaAlO<sub>3</sub> substrate after gamma irradiations.

# **B.** Neutron Irradiations

The various sample types were exposed to cumulative neutron fluences up to 1014 n/cm2. An accompanying total gamma dose of 237.9 krad(Si) was also emitted by the Cf-252 source. However, this was neglected knowing that the same types of samples had been exposed to much higher gamma doses with the Cs-137 source. X-ray diffraction analyses failed to show any atomic disorder as a result of the neutron irradiations. In Figures 4 and 5, critical temperature and critical current density measurements of a typical sample of TI-2212 on an MgO substrate are shown after undergoing neutron exposures. As seen in Figure 5, there was a decrease in critical current density thought to be caused by exposure to moderately humid air for an extended period of time. After exposure to the highest fluences, where longer environmental exposure times (on the order of up to two weeks) were necessary for the samples to radioactively decay, the critical current density degradation, as shown in Figure 6, was

observed. This environmental degradation was confirmed by leaving samples open to the environment for an equal amount of time (two weeks) and then remeasuring the superconductors. Thus, the degradation observed in this work, although similar to that resulting from proton bombardment by Lombardo et al. and Weaver et al. [7,8], is caused by moisture absorption. Critical temperature and critical current density measurement data for samples of each superconductor/substrate combination irradiated with neutrons and exposed to the environment appear in Table II.

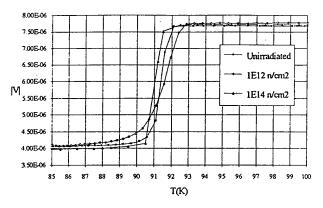


Figure 4. Critical temperature transition of  $Tl_2Ba_2CaCu_2O_{8+x}$  on a MgO substrate after various neutron fluences.

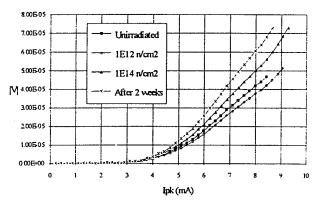


Figure 5. Critical current density measurement of  $Tl_2Ba_2CaCu_2O_{8+x}$  on a MgO substrate after various neutron fluences.

Exposure to moisture in the surrounding air had no adverse effects on the critical temperature of YBCO samples, but seemed to have a slight effect on the critical temperature of the Tl-2212 superconductors although it was independent of their initial critical temperature and critical current density values. This is illustrated in Figure 4 where the temperature transition fluctuates slightly and, at  $10^{12} \text{ n/cm}^2$ , the transition region widens from 2 K to 4.2 K. This may be due to larger grain boundaries in the Tl-2212 film which were deposited by laser-ablation as opposed to sputtering. However, this has yet to be verified.

As shown in Figure 6, further environmental degradation, which can probably be attributed to corrosion taking place at the surfaces of the superconductors from exposure to moderately humid air, occurred [9,10]. Samples of varying thick-

nesses (other than those listed in Table II) were irradiated to the same neutron fluences. Thickness was determined not to be a factor in our experiments. Unirradiated samples were also exposed to the same environment and showed essentially the same degradation in critical current density with time. No moisture exposure effects were seen up to fluences of 10<sup>12</sup> n/cm<sup>2</sup>, probably because of the short time the samples were exposed to air (approximately 1.4 hours for the exposure time and about 1 day for the decay time). Zhou and McDevitt have shown that TI-2223 bulk samples tend to degrade more slowly than YBCO bulk samples (by a factor of 3) when exposed to high humidity (85%) with the primary corrosion products being CuO, BaCO<sub>3</sub>, Tl<sub>2</sub>O<sub>3</sub>, and CaCO<sub>3</sub> [10]. X-ray diffraction analyses were also performed but did not show any detectable levels of atomic disorder as a result of the neutron irradiations. Degradation was not seen during the gammaray irradiations because of the much shorter exposure times that involved no radioactivation of the samples. There were no noticeable changes in the temperature transitions of the materials due to irradiations or exposure to air.

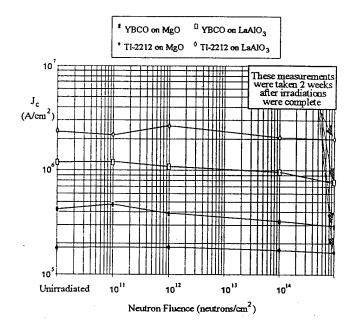


Figure 6. Critical current density variation of various superconductor/substrate combinations for different neutron fluences (also shown is the variation due to air exposure.)

# C. Improvements for Future Studies

Biasing the superconducting thin films and measuring their characteristics at cryogenic temperatures would have been much more realistic, but this was not possible because of the limitations on the containment necessary for the radiation sources. In particular, the application of a voltage across a dielectric during gamma irradiation is known to enhance degradation of dielectric type materials because of charge creation, separation, and trapping in a dielectric or at a semi-conductor/dielectric interface. However, these initial experiments performed at room temperature in air showed that the

Table I. T<sub>c</sub> and J<sub>c</sub> measurement data for gamma-ray irradiated samples. (J<sub>c</sub> values were measured at 77 K.)

						and the second		
HTSC		Film	Unirradiated		600 krad(Si)		1.5 Mrad(Si)	
Film	Substrate	Thickness (Å)	T <sub>c</sub> (K)	J <sub>c</sub> (A/cm <sup>2</sup> )	T <sub>c</sub> (K)	$J_c(A/cm^2)$	$T_c(K)$	$J_c(A/cm^2)$
YBCO	MgO	~2000	82.6	7.2 x 10 <sup>4</sup>	82.6	8.4 x 10 <sup>4</sup>	82.6	6.6 x 10 <sup>4</sup>
YBCO	LaAlO.	~10.000	89.4	1.54 x 10 <sup>6</sup>	89.4	1.51 x 10 <sup>6</sup>	89.4	1.49 x 10 <sup>6</sup>
TI-2223	MgO	~3000	112	$6.0 \times 10^4$	112.3	9.6 x 10 <sup>4</sup>	111.6	7.6 x 10 <sup>4</sup>
TI-2212	LaAlO,	~5000	86.2	1.92 x 10 <sup>6</sup>	86.4	1.87 x 10 <sup>6</sup>	86.5	1.87 x 10 <sup>6</sup>

Table II.  $T_c$  and  $J_c$  measurement data for neutron irradiated samples. ( $J_c$  values were measured at 77 K.)

·		<del>                                     </del>			<u> </u>				J <sub>2</sub> (2 weeks
HTSC		Film	Unirradiated		10 <sup>12</sup> n/cm <sup>2</sup>		10 <sup>14</sup> n/cm <sup>2</sup>		after irradiations)
Film	Substrate	Thickness (Å)	T <sub>c</sub> (K)	J <sub>c</sub> (A/cm <sup>2</sup> )	T <sub>c</sub> (K)	$J_c(A/cm^2)$	T <sub>c</sub> (K)	$J_c(A/cm^2)$	(A/cm <sup>2</sup> )
YBCO	MgO	~2000	84.2	4.2 x 10 <sup>5</sup>	84.5	3.84 x 10 <sup>5</sup>	84.4	3.24 x 10 <sup>5</sup>	2.88 x 10 <sup>5</sup>
YBCO	LaAlO.	~10,000	89.5	1.19 x 10 <sup>6</sup>	89.6	1.08 x 10 <sup>6</sup>	89.5	9.6 x 10 <sup>5</sup>	7.68 x 10 <sup>5</sup>
T1-2212	MgO	~3000	91.3	1.8 x 10 <sup>5</sup>	91.6	1.84 x 10 <sup>5</sup>	91.0	1.72 x 10 <sup>5</sup>	1.64 x 10 <sup>5</sup>
T1-2212	LaAlO.	~5000	102.6	2.38 x 10 <sup>6</sup>	102.9	2.64 x 10 <sup>6</sup>	102.9	$2.06 \times 10^6$	1.99 x 10 <sup>6</sup>

superconducting thin film structures are hard to the levels of radiation described. Such information is a necessary initial step in understanding how superconducting multichip modules will perform in a radiation environment.

## IV. CONCLUSIONS

Gamma-rays and neutrons had little to no effect on the critical temperature and critical current density of thin films of YBCO, Tl-2212, and Tl-2223. Since these properties of superconductors are highly sensitive to atomic displacement effects in the material, it can be concluded that very little damage occurred in the unbiased superconductors at room temperature as a result of the irradiations performed. Although the outcome may have been different if the films were biased and were irradiated and measured at 77 K, the results presented here are encouraging.

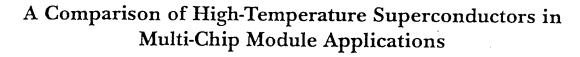
It was also determined that the films were more susceptible to degradation by the environment than by radiation. The results suggest that the surrounding air and humidity caused a decrease in the critical current density of the materials due to surface corrosion [9,10].

As mentioned previously, we are currently working on the development of a multichip module utilizing superconducting interconnects. If our efforts are successful, it will be of great interest to perform radiation experiments on such a device to gain some insight into its hardness to space radiation effects. The experiments performed here have provided a good foundation for making a more detailed study on such a superconducting device.

# V. REFERENCES

[1] J.R. Cost, J.O. Willis, J.D. Thompson, and D.E. Peterson, "Fast-neutron irradiation of YBa<sub>2</sub>Cu<sub>3</sub>O<sub>x</sub>," *Phys. Rev. B*, 37, pp. 1563-1568, (1988).

- [2] A. Wieniewski, M. Baran, P. Przystupski, H. Szmczak, A. Pajaczkowska, B. Pytel, and K. Pytel, "Magnetization studies of YBa<sub>2</sub>Cu<sub>3</sub>O<sub>7-x</sub> irradiated by fast neutrons," Solid State Communications, 65(7), pp. 577-580, (1988).
- [3] A. Umezawa, G.W. Crabtree, J.Z. Liu, H.W. Weber, W.K. Kwok, L.H. Nunez, T.J. Moran, C.H. Sowers, and H. Claus, "Enhanced critical magnetization currents due to fast neutron irradiation in single-crystal YBa<sub>2</sub>Cu<sub>3</sub>O<sub>7-x</sub>," Phys. Rev. B, 36(13), pp. 7151-7154, (1987).
- [4] J. Bohandy, J. Suter, B.F. Kim, K. Moorjani, and F.J. Adrian, "Gamma radiation resistance of the high T<sub>c</sub> superconductor YBa<sub>2</sub>Cu<sub>3</sub>O<sub>7-x</sub>," Appl. Phys. Lett., 51(25), pp. 2161-2163, (1987).
- [5] L. Luo, Y.H. Zhang, S.H. Hu, W.H. Liu, G.L. Zhang, W.X. Hu, "Gamma radiation effects on some properties of YBCO," *Physica C* 178, pp. 11-14, (1991).
- [6] J.H. Claassen, M.E. Reeves, and R.J. Soulen, Jr., "A contactless method for measurement of the critical current density and critical temperature of superconducting films," Rev. Sci. Instrum. 62 (4), pp. 996-1004, (1991).
- [7] L. Lombardo, A. Kapitulnik, and A. Leone, "Alteration in the superconducting properties of Bi<sub>2</sub>Sr<sub>2</sub>CaCu<sub>2</sub>O<sub>8</sub> crystals due to proton irradiation," *IEEE Trans. Nucl. Sci.*, vol. 38, no. 6, pp. 1089-1093, (1991).
- [8] B.D. Weaver, E.M. Jackson, G.P. Summers, D.B. Chrisey, J.S. Horwitz, J.M. Pond, H.S. Newman, and E.A. Burke, "Radiation effects in high temperature superconducting films and devices for the NRL high temperature superconductivity space experiment," *IEEE Trans. Nucl. Sci.*, vol. 38, no. 6, pp. 1284-1288, (1991).
- [9] T.H. Buyuklimanli and J.H. Simmons, "Surface degradation of YBa<sub>2</sub>Cu<sub>3</sub>O<sub>7-x</sub> superconductors on exposure to air and humidity," *Phys. Rev. B* 44, p. 727-733, (1991).
- [10] J.P. Zhou and J.T. McDevitt, "Corrosion reactions of YBa<sub>2</sub>Cu<sub>3</sub>O<sub>7-x</sub> and Tl<sub>2</sub>Ba<sub>2</sub>Ca<sub>2</sub>Cu<sub>3</sub>O<sub>10+x</sub> superconductor phases in aqueous environments," *Chem. Mater.*, vol. 4, no. 4, p. 953-959, (1992).





D.E. Ford, S.S. Scott, S.S. Ang and W.D. Brown High-Density Electronics Center (HiDEC) Department of Electrical Engineering University of Arkansas Fayetteville, AR 72701

### **Abstract**

In the application of high-temperature superconductors (HTSCs) in multi-chip module (MCM) technology, it is first necessary to investigate the advantages and disadvantages of the various HTSC compounds. The standard criteria for comparing the suitability of HTSCs in electronics applications has been critical temperature ( $T_c$ ) and critical current density ( $J_c$ ). It is also necessary to consider the physical properties of HTSCs in relation to the various processing techniques required in fabrication of MCMs. These techniques can be grouped into four main areas: deposition, patterning, packaging, and characterization. The four main HTSC materials, Y-Ba-Cu-O, Bi-Sr-Ca-Cu-O, Tl,Ba-Ca-Cu-O and Hg-Ba-Ca-Cu-O, will be compared to determine which is most suitable for MCM application.

### Introduction

In the decades since the popular advent of the transistor in the 1960s, there has been continual and steady improvement in both the performance and cost of electronics equipment through miniaturization. This effort has given us the multi-chip module (MCM) as the latest and most promising technique to be introduced. MCM technology improves the speed at which devices can operate and decreases the power lost by eliminating as much length as possible from the interconnection between the individual devices. With this new technology some new barriers to increased speed and performance have arisen. By concentrating all of the devices in one area, the problems due to Joulean heating (I2R losses) and electromigration are increased. Also, the lack of recent improvements may indicate that the upper limit of the speeds that can be expected from current semiconductor devices using conventional interconnects have been reached.

All of these problems can be addressed by combining high-temperature superconductors (HTSCs) with MCMs. Some of the interconnecting lines may typically carry 50-100 mA of current. Therefore, they account for a major portion of the heat generated (Burns et al., 1993). Replacing the lines with zero resistance HTSCs eliminates these I<sup>2</sup>R losses. This means less heat and less power consumed. The refrigeration required for HTSC operation further limits the overall heat production to less than that produced by the individual devices. All of this allows for an even greater decrease in the interconnection lengths which, in turn, maximizes the operating speed of the MCM.

HTSC devices have been shown to be more than 2.5

times faster than their semiconductor counterparts, use three orders of magnitude less power, and do not suffer from electromigration problems (Van Duzer and Tuner, 1981). Their use in MCMs should produce the next quantum jump in performance. A cross-sectional schematic of an MCM is shown in Figure 1.

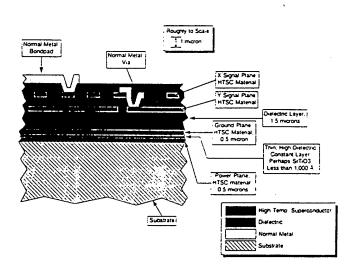


Fig. 1. Cross-sectional Schematic of a Superconducting Multi-Chip Module.

But, which HTSC offers the best overall prospects for MCM applications? This is the first question to be answered in the search for a viable superconducting MCM. When comparing HTSCs, the standard for suitability in electronics applications has been the materials critical temperature,  $(T_c)$ , and critical current density,  $(J_c)$ . It is

also necessary to consider the additional requirements and effects due to the different fabrication steps such as erial deposition, patterning, packaging and characterization. This paper is the result of our research in each of these areas.

Using the initial criterion of T<sub>c</sub>, a great number of HTSCs can be eliminated. The cost of cooling below liquid nitrogen temperature (77K) tends to preclude using HTSCs with T<sub>c</sub>'s any lower. The currently viable HTSC materials with T<sub>c</sub>'s above liquid nitrogen temperature can be separated in to four groups: yttrium-based, bismuth-based, thallium-based, and mercury-based. These four groups will be dealt with in this paper.

### Yttrium

There are at least three variations to the yttrium-based HTSCs with the only significant differences being the T<sub>c</sub>s (40K, 80K, 90K) and the ease of production. Fortunately, the highest T<sub>c</sub> (90K) belongs to the phase of yttrium material that is the easiest to produce. YBa<sub>2</sub>Cu<sub>2</sub>O<sub>x</sub>, known commonly as either YBCO or 123, was the first material discovered to superconduct above liquid nitrogen temperature (Wu et al., 1989). This fact and the relatively low toxicity of the component materials seem to be the only really good characteristics that YBCO possesses.

An ongoing study by our group at the University of 'kansas indicates that to achieve an effective current den-

, a given HTSC must be held to 10 - 20% below its  $T_c$  (Ulrich, 1994). While this is better than the 30% or  $T_c/2$  values commonly accepted in the scientific community (Doss, 1989), it still puts YBCO at the very borderline for use with liquid nitrogen.

Most of the drawbacks encountered in the production of YBCO thin films can be tied to one problem. Due to critical mismatches in lattice parameters, it is difficult to get good epitaxial growth for YBCO on the viable low dielectric substrates in use today (Werder, 1991). This means that, no matter how good a deposition technique, YBCO films will tend to be comparatively rough in texture and have a limited  $J_c$  due to internal flaws in the achievable crystalline structure.

The deposition of YBCO on a substrate has typically been accomplished using off-axis sputter deposition. While this method can produce usable thin films, it is often necessary to anneal these films in an oxygen ambient at approximately 450°C after deposition in order to correct for oxygen depletion and to achieve an acceptable T<sub>c</sub>. Fortunately, an on-axis method has been demonstrated that produces thin films with T<sub>c</sub>s of 88K and J<sub>c</sub>s of greater than 10<sup>6</sup> A/cm<sup>2</sup> with no post annealing required (Blue and Boolchand, 1991). It should be noted however, that the current density for this material is only 10<sup>4</sup> A/cm<sup>2</sup> at 77K as for most YBCO films (Jin et al., 1988).

Another successful method for the deposition of YBCO has been demonstrated using metalorganic chemical vapor deposition (MOCVD) combined with rapid isothermal processing (RIP) (Singh et al., 1991). With  $T_{cs}$  of 89K and  $J_{cs}$  of 1.5 x 10<sup>6</sup> A/cm<sup>6</sup> at 77K, this is by far the best method for producing YBCO films seen to date.

Pulsed laser deposition has also been used successfully to cover small areas, but this technique has proven to be a very costly and a difficult process to control (Burns et al., 1993). Laser deposition does seem to be an excellent choice for spot deposition of YBCO in applications such as individual connections between layers commonly called vias.

In the areas of patterning, packaging and characterization, there is another major drawback. YBCO has a very high affinity for water. When exposed to moisture, the properties of YBCO tend to degrade. This process is accelerated by flaws in the crystalline structure so common to current processing techniques. Another aspect of this fault is that YBCO tends to form an oxide skin layer. This means an added difficulty for any patterning process. Also, this creates a problem in making direct contact to YBCO films as is necessary for multilayer applications, metalization for packaging purposes, or just testing the material. With some small difficulty, this can be dealt with using a procedure consisting of a solution of bromine in methanol that will remove the skin layer (Vasquez et al., 1988). A non-superconducting surface layer can also be removed by brief exposure to a low-energy cleaning ion bombardment.

Yttrium-based HTSCs have been successfully etched using weak acidic solutions such as phosphoric, nitric and hydrochloric acids. However, YBCO's reactivity with the various substrates, while not notably greater than for other HTSCs, when combined with the noted skin effect creates a scum layer between the substrate and the YBCO thin film that seems impervious to these enchants.

Yttrium-based HTSCs can also be dry etched using either a reactive process with a halogen such as chlorine, or by argon ion milling. Both of these methods suffer from the same structural distortions found in deposition techniques. For the reactive process, it is necessary to either post-etch anneal or use a mask that can keep oxygen from escaping during the etching process. In argon ion milling, the problem can be solved by cooling the sample during the etching process, preferably with liquid nitrogen. But, since photoresist are often used for masking in both dry etching processes, the problem with moisture is still present.

## Bismuth

There are several different bismuth based HTSCs, with

the highest T<sub>c</sub> being ~114K for Bi<sub>2</sub>Sr<sub>2</sub>Ca<sub>2</sub>Cu<sub>3</sub>O<sub>x</sub>, but it is very difficult to produce the higher Tc phase of this compound (Bi 2223). This is due to the intergrowth of the Bi 2212 phase which has a  $T_c$  of 85K. Many attempts to enhance growth of the 2223 phase have been made with varied results (Endo et al., 1988; 1989; Tarascon et al., 1988; Huang et al., 1990). One procedure produces good thin films, but requires a heating period of one week (Sleight, 1988). The most promising method seems to be the addition of lead in the form Bi2-yPbySr2Ca2Cu3Ox to stabilize the Tc. This method has produced Tcs in the usable range of 104 - 112K (Xin and Sheng, 1991). This is the most commonly encountered form of the bismuth compound and can be deposited using the same methods as described for YBCO. Most of the information gathered about the bismuth-based system has been for this lead mixed form. As other easily produced phases of the bismuth compound have lower Tcs than YBCO, they are of little interest to the MCM field.

of

ni-

ì

 $\Gamma_{cs}$ 

he

lly

: a

ıl.,

nt

ch

ed

:ry

he

el-

to

ılt

ıis

śs.

to

ıs,

ıe

ιh

in

)e

d

d

ıe

r

:s

n

g

·r

n

0

a

1

The addition of lead to bismuth HTSCs defeats one of the bismuth compound's major benefits. That is, the relatively low toxicity of the elements used. While the lead can be incorporated easily, it will still require special handling like the thallium and mercury compounds.

Most reports of J<sub>c</sub>s are somewhere above 10<sup>4</sup> A/cm<sup>2</sup> at 77K which is similar to YBCO (Doss, 1989). This is probably due, in part, to the difficulty in producing a pure phase of this material. The lattice parameters of the bismuth compounds, though not exact, are better matched to the low dielectric substrates than YBCO's. This would indicate better epitaxial growth and better J<sub>c</sub>s. Comparison of the thermal power properties also indicates this conclusion (Xin et al., 1992). Indeed, a 110K sample with a J<sub>c</sub> of 3.4 x 10<sup>6</sup> Z/cm<sup>2</sup> at 77K has been reported (Grenwald, 1991), but it should be noted that this sample did not contain lead and is not easily reproduced.

Bismuth-based HTSCs can be etched with the same methods as YBCO and slow none of the problems due to YBCO's affinity for moisture. Most forms of this compound appear to be fairly stable and much less brittle than YBCO. It should be noted that bismuth compounds require the same precautions for dry etching methods as YBCO, and although the etching damage is generally of a lesser extent, bismuth compounds can easily be destroyed during any annealing process.

Bismuth compounds have shown a tendency to flake in layers similar to mica (Doss, 1989). This could cause some slight problems in packaging, but should not prove to be a major concern.

The only problems with the characterization of bismuth based HTSCs are directly related to the ability to produce a pure phase material.

### Thallium

Like bismuth, thallium-based HTSCs exist in many ( ferent phases. Unlike bismuth, however, the highest (125K) phase is relatively easy to produ Tl<sub>2</sub>Ba<sub>2</sub>Ca<sub>2</sub>Cu<sub>3</sub>O<sub>x</sub>, commonly referred to as Tl2223, 1 one major drawback. Thallium is a very toxic substan that can be absorbed through the skin. It can be absorb over a period of time and is not normally purged from t body. Therefore, proper precautions must be taken wh dealing with this material. Special precautions should taken when working with lead or mercury. However, the precautions required for working with these materials a only slightly more than those normally observed in a co scientious production facility (Chelton et al., 1991). these facilities are already dealing with arsenide, cyanide and many other toxic compounds, the addition of thalliu should present no insurmountable problems.

Excellent quality thin films of the 2223 phase have bee deposited by several methods such as spin coating, spr. pyrolysis, sputtering, thermal evaporation, electron bear laser ablation, and MOCVD (Shih and Qiu, 1988; Ichikav et al., 1988; Ginely et al., 1989; Hammond et al., 199 Collins et al., 1991; Liu et al., 1991; Malandrino et a 1991), but the method of choice seems to be the po deposition annealing technique. First, a precursor layer BaCaCuO of the desired stoichiometry is sputter deposied onto a substrate. Then the film is annealed in thallium vapor which drives the thallium into the matrix formir. the actual HTSC. While a one step sputter deposition possible, the two step method consistently provides bette results with average T<sub>c</sub>s of 125K and J<sub>c</sub>s typically above 1( A/cm<sup>2</sup> at 77K (Grenwald, 1991). This includes the bequality samples to date with a  $J_c$  of over  $10^7$  A/cm<sup>2</sup> at 77 (Chu et al., 1991). The two step method may also have hidden benefit in that it isolates thallium contamination t the furnace used for the drive-in procedure.

The lattice parameters for the 2223 phase are muc. closer to those of the low dielectric substrates with as littl as 0.75% mismatch for CeO<sub>2</sub> (Holstien et al., 1992). Thi means better epitaxial growth and smoother films that possible with either YBCO or bismuth (Lee et al., 1992).

Thallium-based HTSCs can be etched using the same methods as yttrium-based and bismuth-based compounds but because of the greater stability, require less attention to reactivity and oxygen loss. The preliminary results from a wet etch process our group is currently investigating indicates that the extra strength and consistency of 2225 films makes the etching process much easier to control.

Other than the special precautions for dealing with thallium 2223 makes no special demands on packaging or characterization. Indeed, the additional strength can only serve to make these processes easier. A comparison of T curves for Yttrium, Bismuth and Thallium superconduc

tors is shown in Fig. 2.

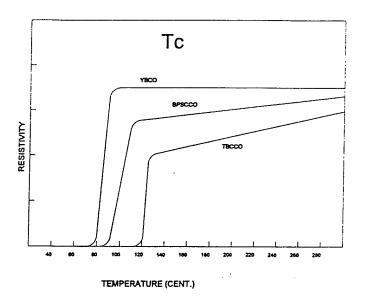


Fig. 2. Comparison of Typical T<sub>c</sub> Curves.

# Mercury

The recent discovery of mercury based HTSCs with nossible T<sub>c</sub>s above the 145K boiling point of Freon<sup>™</sup> is ly exciting. But, as of yet, little is known of the characteristics of the mercury-based compounds. The HgBa<sub>2</sub>Ca<sub>2</sub>Cu<sub>3</sub>O<sub>x</sub> phase (Hg 1223) with the highest T<sub>c</sub> of 135K at ambient pressure has been shown to increase to a T<sub>c</sub> of over 150K under hydrostatic pressure (Chu et al., 1993). However, 1223 is not produced without some amount of effort. 1223 thin films have currently been produced only by post deposition annealing under special pressure controlled conditions. With the additional cost due to current government efforts to ban the use of Freon™, the added effort necessary to produce the material and then maintain the hydrostatic pressure, means that practical Freon<sup>™</sup>-cooled HTSCs are still far in the future. Indeed, the added effort required just to achieve an additional 10K increase in T<sub>c</sub> from thallium's 125K to 135K seems to serve no purpose, but improvements could be just over the horizon.

The reported lattice parameters combined with the initial troubles in separating out the different phases, tend to indicate that 1223 will have a  $J_c$  somewhat less than the thallium-based HTSCs (Huang et al., 1993), but this remains to be confirmed. The bottom line with mercury-based HTSCs is that we just don't know yet. A comparison of the  $J_c$ 's of the four materials is shown in table 1.

Table 1. Critical Current Density (Jc) in A/cm2.

	УВСО	BSCCO	ТВССО	нвссо
TYPICAL	10 <sup>4</sup>	104	106	?
MAXIMUM	$1.5 \times 10^6$	3.4 x 10 <sup>6</sup>	2.8 x 10 <sup>7</sup>	;

# **Summary and Conclusion**

Yttrium base HTSCs, while having several drawbacks, have only one advantage. The comparatively low toxicity of the component materials. While, bismuth-based HTSCs have much more to offer than the yttrium based compounds, the current production of viable bismuth thin films requires the additional of lead. This tends to nullify any benefits relative to thallium-based HTSCs. Most processes used in MCM production have been demonstrated for thallium HTSVs with significantly better results than any other material. Mercury-based materials have shown some prospects and raised some new questions, but until they can be produced with more ease and characterized more definitively, they offer no apparent advantages. However, they definitely warrant more research.

While the evidence does not totally rule out any of the candidate HTSCs, the majority of the information indicates that thallium-based HTSCs should be the HTSC of choice in MCM applications.

## Acknowledgements

This research was funded by E-Systems, Melpar Division.

### Literature Cited

Blue, C. and P. Boolchand, 1991, Appl. Phys, Lett., vol. 58,p. 2036-2038.

Burns, M.J., K. Char, B.F. Cole, W.S. Ruby and S.A. Sachtjen. 1993. Appl. Phys. Lett., vol. 62, p. 1435.

Chelton, C.F., M. Glowatz and J.A. Mosovsky. 1991. IEEE Trans. on Educ., vol. 34, p. 269-288.

Chu, M.L., H.L. Chang, C. Wang, J.Y. Juang, T.M. Uen and Y.S. Gou. 1991. Appl. Phys. Lett., vol. 59, p. 1123-1125.

Chu, C.W., L. Gao, F. Chen, Z.J. Huang, R.L. Meng and Y.Y. Xue. 1993. Nature.

Collins, B.T., J.A. Ladd and J.R. Matey. 1991. J. Appl. Phys., vol. 70, p. 2458.

Doss, J.D. 1989. Engineer's Guide to High-Temperature Superconductivity, John Wiley and Sons, New York.

Endo, U., S. Koyama and T. Kawai. 1988. Jpn. J. Appl. Phys., vol. 27, p. L1467.

Endo, U., S. Koyama and T. Kawai. 1989. Jpn. J. Appl. Phys., vol. 28, p. L190.

Ginely, D.S., J.F. Kwak, E.L. Venturini, B. Morosin and R. J. Baughman. 1989. Physics C., vol. 160, p. 42.

Grenwald, A.C. 1991. Microelec. Manuf. Tech., p. 25.

Hammond, R.B., G.V. Negrete, L.C. Bourne, D.D. Strother, H. Cardona and M.M. Eddy. 1990. Appl. Phys. Lett., vol. 57, p. 825.

Holstien, W.L., L.A. Parisi and D.W. Face. 1992. Appl. Phys. Lett., vol. 61, p. 982-984.

Huang, Y.T., C.Y. Shei, W.N. Wang, C.K. Chiang and W.H. Lee. 1990. Physics C, vol. 76, p. 169.

Huang, Z.J., R.L. Meg, X.D. Qiu, Y.Y. Sun, J. Kulick Y.Y. Xue and C.W. Chu. 1993. Physics C.

Ichikawa, Y., H. Adachi, K. Setsune, S. Hatta, K. Hirochi and K. Wasa. 1988. Appl. Phys. Lett., vol. 53, p. 919.

Jin, S., T.H. Tiefel, R.C. Sherwood, R.B. van Dover, M.E. Davis, G.W. Kammlott and R.A. Fastnacht. 1988. Phys. B, vol. 37, p. 7850-7853.

Lee, W.Y., S.M. Garrison, M.Kawasaki, E.L. Venturini, B.T. Ahn, R. Boyers, J. Salem, R. Savoy and J. Vazquez. 1992. Appl. Phys. Lett., vol. 60, p. 772-774.

Liu, R.S., J.L. Tallon and P.P. Edwards. 1991. Physics C, vol. 182, p. 119.

Malandrino, G., D.S. Richeson, T.J. Marks, D.C. Degroot, J.L. Schindler, C.R. Kannewurf. 1991. Appl. Phys. Lett., vol. 58, p. 182.

Shih, I. and C.X. Qiu. 1988. Appl. Phys. Lett., vol. 53, p. 523.

Singh, R., S. Sinha, N.J. Hsu, J.T.C. Ng, P. Chou and R.P.S. Thakur. 1991. J. Vac. Sci. Technol., vol. A-9, p. 401-404.

Sleight, A.W. 1988. Science, vol. 242, p. 1519-1527.

Tarascon, J.M., W.R. McKinnon, P. Barboux, D.M. Hwang, B.G. Bagley, L.G. Greene, G.W. Hull, Y. LePage, N. Stoffel and M. Giroud. 1988. Phys. Rev. B, vol. 38, p. 8885.

Ulrich, R. 1994. Private communication, Chemical Engineering Dept. University of Arkansas.

Van Duzer, T. and C.W. Turner. 1981. Principles of Superconductive Devices and Circuits, Elsevier, New York.

Vasquez, R.P., B.D. Hunt and M.C. Foote. 1988. Appl. Phys. Lett., vol. 53, p. 2692-2694.

Werder, D.J. 1991. Physics C, vol. 179, p. 430-436.

Wu, M.K., J.R. Ashburn, C.J. Torng, P.H. Hor, R.L. Meng, L. Gao, Z.J. Huang, Y.Q. Wang and C.W. Chu. 1989. Phys. Rev. Lett., vol. 58, p. 908-910.

Xin, Y. and Z.Z. Sheng. 1991. Physics C, vol. 176, p. 179-188.

Xin, Y., D. Ford and Z.Z. Sheng. 1992. Rev. Sci. Instrum.,

vol. 63, p. 2263-2267.

# The effects of rapid thermal annealing on the properties of sputtered YBCO superconducting films

# R G Florence, S S Ang and W D Brown

University of Arkansas, High Density Electronics Center and Department of Electrical Engineering, Fayetteville, AR 72701, USA

Received 18 May 1994, in final form 25 July 1994

Abstract. The effects of rapid thermal annealing on the material and electrical properties of sputter deposited yttrium barium copper oxide  $(YBa_2Cu_3O_{7-x})$  superconducting films were investigated. Rapid thermal annealing increased the critical current density but decreased the critical transition temperature of the films. The maximum increase in critical current density, an order of magnitude, occurred at  $800\,^{\circ}$ C, while no increase was observed at  $700\,^{\circ}$ C, below the growth temperature of  $735\,^{\circ}$ C, or at  $900\,^{\circ}$ C. The increase in critical current density is due to a reduction in the density of misaligned grains as evidenced by a decreasing c-axis parameter and a decrease in the full width at half maximum (FWHM) of the (005) peak. The critical temperature decreased for all annealing times and temperatures above the growth temperature due, presumably, to oxygen effusion from the films.

### 1. Introduction

Thin superconducting yttrium barium copper oxide (YBCO) films have been grown by various techniques including ion-beam sputtering [1], magnetron sputtering [2], electron-beam evaporation [3], molecular-beam epitaxy [4], metalorganic chemical vapour deposition [5], and laser ablation [6]. Most of these techniques require either post-deposition oxygen annealing or growth at an elevated substrate temperature to convert the YBCO films from the tetragonal phase to the orthorhombic phase. In order to optimize postdeposition annealing conditions, it is necessary to understand the thermodynamics of the structural and chemical changes that occur during annealing. Davidson et al [7] investigated the resistance of e-beam-evaporated as-deposited YBa<sub>2</sub>Cu<sub>3</sub>O<sub>7-x</sub> films with different heating rates and O2 partial pressures. They reported that fast annealing is preferable over slow annealing in converting the as-deposited YBa<sub>2</sub>Cu<sub>3</sub>O<sub>7-x</sub> into an orthorhombicphase superconducting film.

In order for superconducting thin films to be used in electronics, they must undergo numerous processing steps such as patterning, etching, and subsequent depositions and passivation. It is generally known that processing steps, performed subsequently to the deposition of superconducting thin films, have a pronounced effect on their material and electrical properties. Sheats et al [8] reported severe degradation in the critical current density  $(J_c)$  of multitarget-sputtered YBCO films to less than 4% of the initial value after

a small amount of ion milling (approximately 375 Å). They also found that a conventional photoresist bake at  $105\,^{\circ}$ C resulted in as much as a 94% decrease in the  $J_c$ . Ichikawa et al [9] found that the  $J_c$  of their sputtered YBCO films degraded after overcoating with aluminum oxide,  $Al_2O_3$ , by sputtering. They attributed this degradation to the interdiffusion between the YBCO and dielectric, which modified the crystal structure of the YBCO films. In general, the  $J_c$  of YBCO films has been observed to degrade severely with post-deposition processing [10], although some modest increases in  $J_c$  after processing have been reported [11].

Rapid thermal annealing (RTA) has been shown to be a viable processing technology by which thermal annealing is performed for a short duration, usually for a few minutes or less. The main advantage of RTA is a reduced thermal processing budget. The reduced thermal budget mitigates interdiffusion problems associated with the YBCO/dielectric layers. This is especially beneficial in the fabrication of superconducting multichip modules (MCMs) where at least two layers of YBCO interconnects, sandwiched between a thick dielectric, are required.

RTA was investigated in this work as a potential process for improving the electrical characteristics of YBCO films. In this paper, the effects of RTA on the material and electrical properties of sputtered YBCO thin films are reported. In addition, the effects of post-RTA annealing at a low temperature in an  $O_2$  ambient on the transition temperature ( $T_c$ ) of these films are also discussed.

# 2. Experimental details

YBCO films were deposited by off-axis DC magnetron sputtering from a two-inch-diameter stoichiometric  $Y_1Ba_2Cu_3O_{7-x}$  target. The substrates used were polished 1 cm<sup>2</sup> yttria-stabilized zirconia (YSZ) of (100) orientation. The deposition parameters were as follows: base pressure,  $10^{-6}$  Torr, deposition pressure, 200 mT with 80% Ar and 20%  $O_2$ , substrate temperature, 735 °C, and sputter power, 100 W. A deposition rate of about 1000 Å  $h^{-1}$  was achieved using these parameters, and nominal film thicknesses were 4000 Å. After deposition, the films were cooled in 100%  $O_2$  at about 600 Torr and held at 400 °C for 30 min before being ramped down to room temperature. The total cooling time was about 2 h.

Two different groups of films, referred to hereafter as group A and group B, were annealed using a computercontrolled Heatpulse 210-T rapid thermal processor. Each film was placed on a two-inch silicon wafer for support inside a double-walled quartz furnace. annealing temperature was measured using a type-K thermocouple pressed against the surface of the film. Films were annealed at temperatures ranging from 700 °C to 900 °C in 50 °C increments; sample group A was annealed for 10 s, and sample group B for 30 s. A fresh film was used for each annealing increment. Annealing and cooling were performed in the presence of 50 sccm of oxygen (limited by the volume of the furnace), and were allowed to cool to 200 °C before being removed from the furnace. Typical cooling times required were about 5 min for the 10 s annealed films and about 7 min for the 30 s annealed films. Some samples were O2 annealed at a low temperature after RTA. The annealing temperature was ramped up to 450 °C in 30 min and held at this temperature for 2 h under 700 Torr of O<sub>2</sub>. The samples were then cooled to room temperature in about 1 h.

A contactless method was used to measure the  $J_c$ and  $T_c$  of the films. In this technique, the sample is placed between two coils and then cooled to 77 K. A current is passed through one of the coils, which induces current flow in the film. The other coil detects the signal produced when  $J_c$  is exceeded [12]. This technique has the important benefit of not requiring patterning of the films in order to perform the measurement. Furthermore, it is only sensitive to intergranular critical current. The transition temperature of the sample is measured by the reactive component of the coil voltage at the fundamental drive frequency, as the inductance drops substantially at the transition temperature due to the induced shielding current in the film. The YBCO films were also analysed using a Philips PW-1830 x-ray diffractometer (XRD) equipped with a Eulerian cradle. The c-axis parameters were measured using the d-spacing of the (0011) peaks located near  $2\theta = 92.5^{\circ}$  to minimize systematic errors of the diffractometer. Rocking curves about the (005) peak were also observed. This peak was selected because of its relatively high intensity. The starting and finishing  $\theta$ angles were 18° and 21°, respectively, with a step size of 0.01° and a dwell time of 1.5 s/step. The fixed  $2\theta$ 

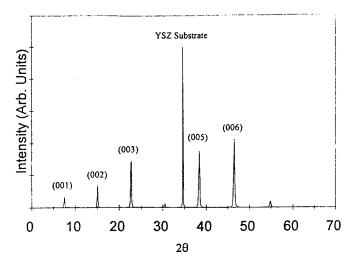


Figure 1. The XRD pattern of a typical as-deposited YBCO film

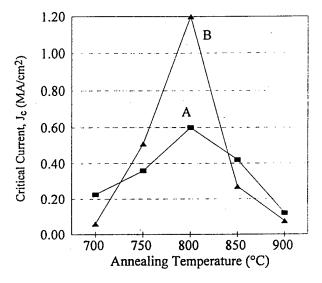


Figure 2. Critical current density versus annealing temperature plots for groups A and B of the YBCO samples.

position of the detector was determined by noting the maximum intensity. Furthermore, the collimating slit in front of the detector was removed to maximize detected diffraction. All XRD measurements were performed at 27 °C.

## 3. Results and discussion

All of the as-deposited YBCO films yielded very uniform  $T_{\rm c}$  and  $J_{\rm c}$  data, due to the excellent repeatability of the deposition parameters. The mean value of  $T_{\rm c}$  and  $J_{\rm c}$  for both groups of films was 85 K and  $1.4 \times 10^5$  A cm<sup>-2</sup>, respectively. Figure 1 shows the XRD pattern of a typical as-sputtered film. As can be seen, the strongest peak intensity occurs for the (006) peak. The (020) peak is much smaller in intensity than the peaks corresponding to c-oriented grains. Thus, the predominant growth is c-axis-oriented grains.

Figure 2 shows  $J_c$ -versus-annealing-temperature curves for both groups of samples. No change in  $J_c$  is noted for films annealed at 700 °C, which is below the

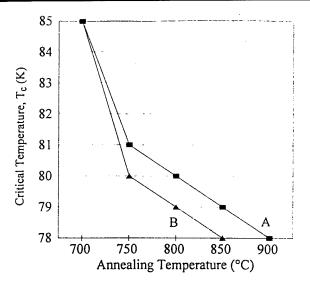
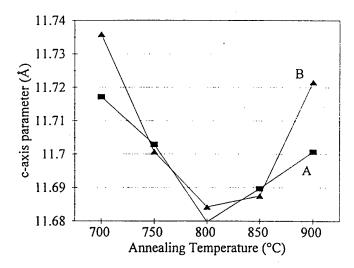


Figure 3. Critical transition temperature versus annealing temperature plots for groups A and B of the YBCO samples.



**Figure 4.** The *c*-axis parameter of the yaco films as a function of annealing temperature.

deposition temperature of 735 °C. Above the deposition temperature, the  $J_c$  of the annealed films increases to a maximum at 800 °C for both groups. The  $J_c$  of the sample subjected to a 30 s annealing at 800 °C increases from  $1 \times 10^{5}$  A cm<sup>-2</sup> to about  $1.2 \times 10^{6}$  A cm<sup>-2</sup>. The amount of increase in  $J_c$  with annealing then decreases for annealing temperatures above 800 °C. At 900 °C, no increase and, in fact, a slight degradation in  $J_c$  is observed. Also, annealing for longer durations (60 s and 90 s) resulted in smaller increases in  $J_c$ . While the  $J_c$  of these films increases with annealing, their  $T_c$  decreases for all annealing times and temperatures. Figure 3 shows the reduction in  $T_c$  for annealed films. No change in  $T_c$ is noted for films annealed at 700 °C. However, a sharp decrease in T<sub>c</sub> (from 85 K to 81 K) is noted for films annealed at 750 °C for 30 s. Furthermore, films annealed for 30 s show a larger decrease in Tc than those annealed for 10 s at all anneal temperatures. The T<sub>c</sub> of the 800 °C, 30 s annealed sample recovered to its original value after O<sub>2</sub> annealing at 450 °C for 2 h.

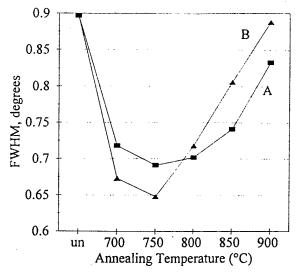


Figure 5. The FWHM versus annealing temperature for groups A and B of the YBCO samples.

Figure 4 shows the c-axis parameter of the films as a function of annealing temperature. The c-axis lattice parameter decreases from 11.74 Å to 11.69 Å upon annealing at 800 °C for 10 s. Even though only a small change in the c-axis parameter is noted, the data indicate that the c-axis parameter generally decreases with annealing with a minimum occurring at 800°C for both anneal temperatures. For temperatures higher than about 800 °C, the decrease in the c-axis parameter with annealing is smaller. For example, the c-axis parameter decreases from 11.72 Å to about 11.7 Å for the film annealed at 900 °C for 30 s. Reduction in the c-axis parameter is indicative of a reduction in grain misalignment. According to Jorgensen et al [13], a reduction in the c-axis parameter is accompanied by an increase in  $T_c$ , and thus, is also a measured of increased oxidation. However, all of our data reveal that a decrease in c-axis parameter is accompanied by a decrease in  $T_c$ . This may be attributed to lattice strain, since it is well known that, in general, RTA imparts strain to films.

Rocking curves of the (005) peak were obtained using the XRD. The full width at half maximum (FWHM) for each film was measured and is plotted in figure 5. YBCO films of similar thickness (i.e., 4000 Å) were used to facilitate comparison. The FWHM is a direct measure of the number of misaligned grains present in the film and is, therefore, useful for quantifying the amount of misalignment. It is interesting to note that, while no change in  $T_c$  or  $J_c$  is noted for films annealed at 700 °C (below the deposition temperature of 735 °C), the FWHM decreases from 0.9° for the unannealed film to 0.73° for 10 s annealed films or 0.67° for 30 s annealed films. This indicates that minute restructuring of the films occurs at this annealing temperature resulting in a reduction in the density of misaligned grains. As the figure indicates, the amount of misalignment decreases for all annealing temperatures with a minimum occuring for 750°C. However, the decrease in misalignment as a function of annealing temperature is smaller for 800 °C and higher temperatures.

Improvement in  $J_c$  after RTA can be attributed to a decrease in the density of misaligned grains or a

reduction in the density of weak links [14]. RTA at a temperature higher than the deposition temperature increases the atomic mobility in the as-deposited YBCO film. Eom et al [15] reported that, given sufficient mobility at a high temperature, c-axis grain growth is favoured over a-axis grain growth. The high mobility of the atoms favours c-axis growth and deters nucleation of a-axis grains. Thus, the decrease in c-axis parameter and FWHM of the (005) peak indicate an increase in the density of c-axis grains. Scanning-electronmicroscope (SEM) photographs of all the annealed films indicate larger grain sizes for the films annealed at higher temperatures, which further suggests a reduction in misaligned grains [16]. The smaller increase in  $J_c$  for annealing at temperatures above 800 °C is possibly due to partial eutectic melting at these temperatures [3].

The decrease in  $T_{\rm c}$  with RTA is probably attributable to the loss of O during annealing. Since RTA was performed at atmospheric pressure, O can easily effuse from the film [17]. O effusion is more pronounced for films annealed for a longer duration as indicated by the lower  $T_{\rm c}$  of these films. Annealing in an  $O_2$  ambient at 450 °C did have the effect of restoring the  $T_{\rm c}$  of these RTA-annealed films to nearly the original values, supporting the assumption that O effusion occurs during RTA. Unfortunately, the  $J_{\rm c}$  values were also reduced, but they remained higher than their original values.

# 4. Summary and conclusions

RTA was performed on superconducting YBCO films at temperatures ranging from  $700\,^{\circ}$ C to  $900\,^{\circ}$ C, and for 10 and 30 s durations. A general increase in  $J_{\rm c}$  occurred, with the greatest increase, a factor of 10, occurring at an anneal temperature of  $800\,^{\circ}$ C for 30 s. For all times and temperatures,  $T_{\rm c}$  decreased, which is attributable to 0 effusion from the films. Measurements of the FWHM of the (005) peak and the c-axis lattice parameter indicate that the increase in  $J_{\rm c}$  is due to a decrease in the number of misaligned grains present in the film. The reduction in  $T_{\rm c}$  with RTA was reversed by conventional low-temperature annealing in  $O_2$ . However, this also

caused  $J_c$  to decrease although the final values were greater than the as-deposited values.

# **Acknowledgments**

This work was supported by a research contract from ARPA through E-System, Melpar Division. Equipment donations from the Kurt J Lesker Company and Texas Instruments are gratefully acknowledged.

# References

- [1] Shah S I and Carcia P F 1987 Mater. Lett. 6 49
- [2] Shah S I and Carcia P F 1987 Appl. Phys. Lett. 51 2146
- [3] Shah S I 1988 Appl. Phys. Lett. 53 612
- [4] Kwo J, Hsieh T C, Hong M, Fleming R M, Liou S H, Davidson B A and Feldman L C 1987 MRS Symp. Proc. 99 339
- [5] Hamdi A H, Mantese J V, Micheli A L, Laugal R C O, Dungan D F, Zhang Z H and Padmanabhan K R 1987 Appl. Phys. Lett. 51 2263
- [6] Dijkkamp D, Vekatesan T, Wu X D, Shaheen S A, Jisrawi N, Min-Lee Y H, McLean W L and Croft M 1987 Appl. Phys. Lett. 51 619
- [7] Davidson A, Palevski A, Brady M J, Laibowitz R B, Kocj R, Scheuermann M and Chi C C 1988 Appl. Phys. Lett. 52 157
- [8] Sheats J R, Taber R C, Merchant P and Amano J 1993 J. Vac. Sci. Technol. A 11 574
- [9] Ichikawa Y, Adachi H, Mitsuyu and Wasa K 1988 Japan. J. Appl. Phys. 27 L381
- [10] Beall J A, Cromar M W, Harvey T E, Johansson M E, Ono R H, Reinstsema C D, Rudman D A, Asher S E, Nelson A J and Swartzlander A B 1991 IEEE Trans. Magn. MAG-27 1596
- [11] Sheats J R, Newman N, Taber R C and Merchant P 1994 J. Vac. Sci. Technol. A 12 388
- [12] Claassen J H, Reeves M E and Soulen R J Jr 1991 Rev. Sci. Instrum. 62 996
- [13] Jorgensen J D, Veal B W, Paulikas A P, Nowicki G W, Claus H and Kwok W K 1990 Phys. Rev. 41 1863
- [14] Shi D 1993 Appl. Supercond. 1 61
- [15] Eom C B, Marshall A F, Ladermann S S, Jacowitcz R D and Geballe T H 1990 Science 249 1549
- [16] Bhatt D, Basu S N, Westerheim A C and Anderson A C 1994 Physcia C 222 283
- [17] Jorgensen J D, Beno M A, Hinks D G, Soderholm L, Volin K J, Hitterman R L, Grace J D and Schuller I K 1987 Phys. Rev. 36 3608



# THE EFFECTS OF LOW-ENERGY BLANKET ION MILLING ON THE PROPERTIES OF SUPERCONDUCTING YBCO FILMS

S. S. Scott, S. S. Ang, and W. D. Brown High-Density Electronics Center (HiDEC) Department of Electrical Engineering University of Arkansas 3217 Bell Engineering Center Fayetteville, AR 72701

### **ABSTRACT**

The effects of low-energy blanket ion milling on the electrical and structural properties of superconducting yttrium-barium-copper-oxide (YBa<sub>2</sub>Cu<sub>3</sub>O<sub>7-x</sub>, or YBCO) were investigated. This process has proven not to have a detrimental effect on the electrical or structural properties of high-quality YBCO films. In fact, it has been found that, in many cases, the critical current density ( $I_c$ ) improves as a result of a brief exposure to a low-energy ion beam. Also, milling of high-quality films results in a reduction in RMS surface roughness. Lower-quality films are typically degraded by the same process.

# INTRODUCTION

The High-Density Electronics Center (HiDEC) at the University of Arkansas is conducting research directed at the fabrication of superconducting multi-chip modules (MCMs). These modules will consist of semiconducting ICs on a superconducting interconnect structure. The superconductor material of choice is YBCO. Due to the reactivity of YBCO with air and water, its surface develops a non-superconducting layer through processing and handling. It is desired that this layer be removed prior to metallization (preferably in-situ) to produce a low-resistance contact. Ion milling is under consideration to serve this purpose. Consequently, the effects of ion bombardment on the electrical and structural properties of YBCO must be investigated to determine the effectiveness of this process.

The proposed superconducting MCM interconnect structure consists of two superconducting planes separated by dielectric layers which are deposited on a substrate. This two-layer structure is based on the interconnected mesh power system (IMPS) MCM topology [1], in which the power, ground, and signal components are combined into two planes. Due to the high dependence on the crystallographic properties when interfacing ceramic materials, minimization of layers is critical in this structure.

The four-sided problem of lattice matching, coefficient of thermal expansion

Sel presentation



oic

er

of th (CTE), interdiffusion, and dielectric constant prevent the use of a single material for the dielectric layer in this structure. The currently proposed dielectric layer for the HiDEC superconducting MCM consists of silicon oxide  $(Si_2O_y)$  buffered by layers of cerium dioxide  $(CeO_2)$  grown either by an ion beam assisted sputtering or laser ablation technique.  $Si_2O_y$  has been chosen due to its low dielectric constant, and its extensive application in electronics. The  $Si_2O_y$  will be tailored by sputter deposition for the best trade-off between its dielectric constant and CTE.  $CeO_2$  has been chosen to buffer between  $Si_2O_y$  and YBCO because of its lattice parameter and CTE match with YBCO.

The superconductor planes are to be connected by metal vias. Previous publications have illustrated the severe degradation of the critical current density  $(J_c)$  of a superconducting YBCO via [2]. This reduction in  $J_c$  is due to the anisotropic nature of current flow in YBCO [3]. In order to keep the YBCO layers planar, the  $Si_rO_y$  will be planarized prior to the second YBCO deposition, and the YBCO layers will be connected by reach-through vias. The ideal metal for low-resistance contact to YBCO is gold (Au). Other options are silver (Ag), platinum (Pt), or a multi-layer metal. A cross-sectional representation of the superconducting MCM interconnect structure is shown in Figure 1.

An item of extreme importance, not considered in the previous section, is that of the reactivity of YBCO with its surroundings. YBCO has been shown to be reactive with many of its environmental components, especially air and water [4-6]. This results in the formation of a non-superconducting surface layer on YBCO films upon exposure to air and conventional wet processing steps, such as photolithography. This reacted layer results in higher-resistance contacts and defeats the purpose of lattice matching at the interface of a dielectric and a reacted YBCO surface. Avoidance of these reactions by shielding YBCO from a reactive atmosphere would be very time consuming as well as expensive. Figure 2 shows the interconnect structure of Figure 1 taking into account a non-superconducting surface on the YBCO planes of the superconducting MCM interconnect structure.

# **EXPERIMENTAL PROCEDURES**

Removal of the non-superconducting surface of YBCO is the most feasible solution to the reactivity problem. It is desirable for this removal process to be performed in the same chamber as the subsequent deposition step, so that the superconducting surface of the YBCO is not exposed to air. In the fabrication of the HiDEC module, where the CeO<sub>2</sub> layers are deposited by ion-beam assisted sputtering in the same chamber in which metallization is performed, the ion source may be used to etch the YBCO films until the superconducting bulk is exposed. This arrangement then allows for the deposition of the dielectric layer or metal following the in-situ milling process.

The use of inert ions to bombard a surface in order to remove material is called ion milling. Ion milling has been applied extensively to the patterning of YBCO films [7,8]. However, it has also been reported that it degrades the electrical properties of

YBCO (this is remain: YBCO. than th.

the elec measure property the surf for a 10

a currer duration mA/cm source v used to The etc about 21 approxi

zirconia or STO system Digital perform

non-sup properti and typ deposite remains exposur same sa which c

sputteri:

terial for the or the HiDEC is of cerium aser ablation its extensive i for the best ien to buffer with YBCO.

s. Previous ensity ( $J_e$ ) of pic nature of  $Si_xO_y$  will be be connected is gold (Au). oss-sectional in Figure 1.

on, is that of reactive with results in the posure to air eacted layer ching at the reactions by g as well as to account a sting MCM

ost feasible e performed rconducting EC module, ne chamber /BCO films ws for the

ial is called BCO films roperties of

YBCO [9]. Since the surface preparatory process exposes the entire surface of the film (this is where the term "blanket" comes from), a major concern is damage to the remaining film. In order to minimize the damage to the underlying superconducting YBCO, caused by exposure to ion milling, the process is performed at an energy lower than that common to bulk etching processes.

In order to evaluate the effects of low-energy blanket ion milling on YBCO films, the electrical properties of critical current density  $(J_c)$  and critical temperature  $(T_c)$  were measured prior to processing and after repeated exposures. The effects on the structural properties of YBCO were determined using atomic force microscopy (AFM) by which the surface structure was observed for changes and the surface roughness was calculated for a  $100 \ \mu m^2$  area.

Although bulk etching is generally performed at energies greater than 1000 eV and a current density of approximately 1 mA/cm², in this work milling steps of 2-minute duration were performed at a beam energy of 500 eV and a beam current density of 0.3 mA/cm² in order to minimize residual damage from the ion bombardment. The ion source was oriented normal to the sample surface at a distance of 15 cm. Argon gas was used to create the inert ions. The background pressure during milling was 1x10<sup>4</sup> Torr. The etch rate of YBCO for these etching parameters was approximately 100 Å/min, so about 200 Å were removed per 2-minute exposure. The initial thickness of the films was approximately 3000 - 4000 Å.

YBCO films were deposited by sputtering or laser ablation on yttria-stabilized zirconia (YSZ), lanthanum aluminate (LaAlO<sub>3</sub>, or LAO), or strontium titanate (SrTiO<sub>3</sub>, or STO) substrates. Measurements of J<sub>c</sub> and T<sub>c</sub> were performed using a non-contact system that employs a current induction technique [10]. AFM data was obtained with a Digital Instruments Dimension 3000 Scanning Probe Microscope. The ion milling was performed with an Ion Tech model FC3000 filament-type 3 cm ion source.

### **EXPERIMENTAL RESULTS**

As previously noted, the intent of the surface preparation process is to remove the non-superconducting surface from YBCO without degrading its electrical or structural properties. However, what has been discovered is an improvement of  $J_c$  in some cases and typically a degradation of  $T_c$ . Figure 3 shows the plot of  $T_c$  for a YBCO film deposited by laser ablation onto a LAO substrate. As can be seen, the onset temperature remains the same while the zero temperature has degraded from 88 K to 83 K after one exposure to the blanket ion milling. Figure 4 shows a plot of critical current ( $I_c$ ) for the same sample. For a crossover criterion of 20 V,  $I_c$  has increased from 11 mA to 25 mA, which corresponds to a  $I_c$  increase from  $3.77 \times 10^5$  A/cm² to  $8.57 \times 10^5$  A/cm².

Figures 5 and 6 show the  $T_e$  and  $I_e$ , respectively, of a YBCO film deposited by sputtering onto a YSZ substrate. After one exposure to blanket ion milling,  $T_e$  remained

unchanged at 88 K while L increased from 30 mA to 36 mA, which corresponds to a J<sub>c</sub> increase from  $1.029 \times 10^6$  A/cm<sup>2</sup> to  $1.234 \times 10^6$  A/cm<sup>2</sup>. Figures 7 and 8 show the T<sub>c</sub> and I<sub>c</sub>, respectively, of another YBCO film deposited by sputtering on YSZ. After milling, the T<sub>c</sub> remained unchanged at 87 K while the L increased from 32 mA to 52 mA, which corresponds to a J<sub>c</sub> increase from  $1.097 \times 10^6$  A/cm<sup>2</sup> to  $1.783 \times 10^6$  A/cm<sup>2</sup>.

Not all samples exposed to blanket ion milling behaved in this manner. Figure 9 plots the variation in  $I_c$  after each blanket mill for six samples. After one exposure to blanket ion milling, three of the films showed an increase in  $I_c$ , two showed a decrease, while one remained unchanged. After the second exposure, one film showed an increase in  $I_c$ , three showed a decrease, while one remained unchanged. One sample was milled three times and showed a continous decrease in  $I_c$ .

In addition to the electrical properties of YBCO, it is desirable that the surface roughness of the films not be degraded by the in-situ processing to promote epitaxy and planarity. Figure 10 plots the variation in RMS surface roughness ( $R_q$ ) after each blanket mill for six samples. After one exposure to the blanket ion milling, three of the films showed a decrease in  $R_q$ , while three showed an increase. The films consistently showed an increase in  $R_q$  after subsequent exposures.

### CONCLUSIONS

As discussed previously, the intent of the in-situ surface conditioning process described in this paper is to remove a non-superconducting surface without degrading the electrical or structural properties of YBCO. It has been shown that, in many cases, the  $J_c$  of YBCO films can be increased by a 2-minute exposure to an argon ion beam at 500 eV and 0.3 mA/cm<sup>2</sup>. The increase in  $J_c$  is believed to be due to damage caused by the argon ions which creates flux pinning centers on the surface of the YBCO [11,12].

The effect on surface roughness of low-energy blanket ion milling are intriguing. While the films studied here showed some increase in surface roughness, the amount of the increase is acceptable considering that these films initially are sufficiently smooth for patterning of lines as small as 5 µm. It has also been found that films with poor initial roughness (>30 nm RMS) are consistently smoothed by low-energy blanket ion milling. The films that did show an increase in roughness initially contained many pits on the surface which were progressively worsened by the milling. Films which were initially pit-free were shown to decrease in roughness after milling, even for films which were initially very smooth (<10 nm RMS).

The effects of ion milling on the electrical properties of YBCO films correlate well with changes in roughness. Films which exhibited high quality initially were more likely to be improved by low-energy blanket ion milling. On the other hand, poorer quality films typically degraded with ion milling. However, the results of these experiments show that YBCO films can be exposed to low-energy blanket ion milling

with it ma films

1.

2.

4.

5.

6.

\_

9.

10.

11.

12

The Ele

onds to a  $J_c$  ie  $T_c$  and  $I_c$ , milling, the mA, which

ner. Figure exposure to a decrease, an increase was milled

the surface epitaxy and each blanket of the films ntly showed

ing process sgrading the y cases, the seam at 500 used by the 11,12].

e intriguing. e amount of smooth for poor initial ion milling. pits on the ere initially which were

ns correlate were more and, poorer ts of these ion milling with relatively little detrimental effect on their electrical or structural properties. In fact, it may be reasonable to perform ion milling with the intent of increasing the  $J_c$  of YBCO films.

### REFERENCES

- Schaper, L., S. Ang, Y. Low, and D. Oldham, To be published in IEEE Trans. Comp., Hybrids, and Manuf. Tech.
- Burns, M., K. Char, B. Cole, W. Ruby, and S. Sachtjen, Appl. Phys. Lett., 62, 1435 (1993).
- 3. Braginski, A., Physica C, 153-155, 1598 (1988).
- 4. Bansal, N. and A. Sandkuhl, Appl. Phys. Lett., 52, 323 (1988).
- Behner, H., K. Rührnschopf, G. Wedler, and W. Rauch, Physica C. 208, 419 (1993).
- 6. Büyüklimanli, T. and J. Simmons, Phys. Rev. B, 44, 727 (1991).
- 7. Alff, L., G. Fischer, R. Gross, F. Kober, A. Beck, K. Husemann, and T. Nissel, Physica C, 200, 277 (1992).
- Ivanov, Z., P. Nilsson, E. Andersson, and T. Claeson, Supercond. Sci. Technol., 4, S112 (1991).
- 9. Xavier, P., T. Foumier, J. Chaussy, J. Richard, and M. Charalambous, J. Appl. Phys., 75, 1219 (1994).
- 10. Pena, O., Meas. Sci. Technol., 2, 470 (1991).
- Liu, J., Kulik, J., Zhao, Y., Chu, W., Nucl. Instrum. Methods Phys. Res. Sect. B, 80-81, 1255 (1993).
- 12. Abdullah, M., Shiraishi, K., Solid State Commun., 86, 109 (1993).

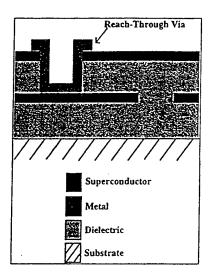


Figure 1: Interconnect Structure

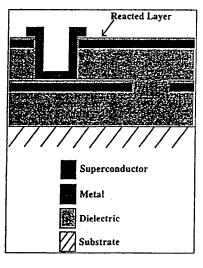


Figure 2: Reactivity of YBCO

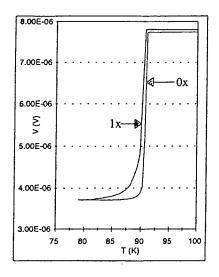


Figure 3: T<sub>C</sub> of laser-deposited YBCO on LAO

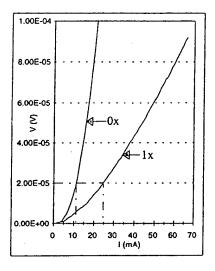


Figure 4: I<sub>c</sub> of laser-deposited YBCO on LAO

110

Fig

The I



YBCO



YBCO

110

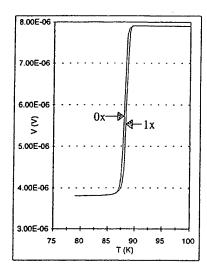


Figure 5:  $T_c$  of sputtered YBCO on YSZ

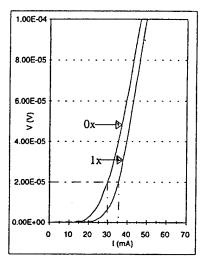


Figure 6:  $I_C$  of sputtered YBCO on YSZ

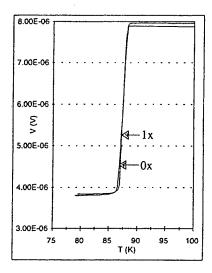


Figure 7:  $T_c$  of sputtered YBCO on YSZ

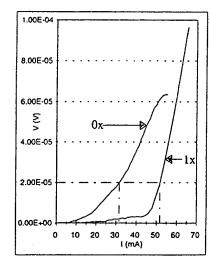


Figure 8: I<sub>C</sub> of sputtered YBCO on YSZ

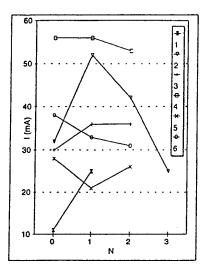


Figure 9: I<sub>C</sub> vs. number of mills

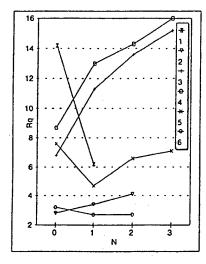


Figure 10: RMS roughness vs. number of mills

elec adv the allo sup onl pro cap laye app has deg diox

Hig thic:

prov

hav high laye PROCEEDINGS OF THE SYMPOSIUM ON

# LOW TEMPERATURE ELECTRONICS AND HIGH TEMPERATURE SUPERCONDUCTIVITY

# Editors

Cor L. Claeys IMEC Leuven, Belgium

Stan I. Raider IBM T.J. Watson Research center Yorktown Heights, New York, USA

Randall Kirschman Mountain View, California, USA

William D. Brown University of Arkansas Fayetteville, Arkansas, USA

ENERGY TECHNOLOGY, ELECTRONICS, AND DIELECTRIC SCIENCE AND TECHNOLOGY DIVISIONS

Proceedings Volume 95-9



THE ELECTROCHEMICAL SOCIETY, INC., 10 South Main St., Pennington, NJ 08534-2896



Ion Beam Assisted Sputter Deposition of CeO2 Buffer Layers for Superconducting Multichip Module (MCM) Applications

> Glenn Florence, Simon Ang, and W. D. Brown High Density Electronics Center (HiDEC) and Department of Electrical Engineering, University of Arkansas 3217 Bell Engineering Center, Fayetteville, AR 72701

Cerium dioxide (CeO<sub>2</sub>) buffer layers have been sputter deposited onto various substrates including silicon and nickel alloy using ion beam assisted deposition (IBAD). This technique has resulted in the formation of CeO2 which exhibits strong (100) phase growth as well as in-plane orientation as evidenced by X-ray diffraction. Subsequent YBCO depositions on these films exhibit T<sub>5</sub>'s of 86 K and biaxial texture with the c-axis normal to the surface. With further refinement, this technique may be used to fabricate the multilayer structure needed for superconducting multichip modules.

### INTRODUCTION

There is widespread interest in the use of superconducting interconnects in electronics, especially in multichip modules (MCMs). Superconductor interconnects have advantages of low signal loss and very low RC propagation delays. Furthermore, due to the reduction in interconnect resistance, the linewidths can be made much smaller, allowing for a reduction in the number of signal layers. One proposed structure for the superconducting MCM is the interconnected mesh power system (IMPS), which requires only two interconnect layers, thereby reducing the complexity of the manufacturing process (1). In order to achieve satisfactory electrical performance and reduce parasitic capacitances, these interconnects need to be separated by a thick (~2-5 µm) insulating layer with a low dielectric constant. Possible substrate and dielectric materials for these applications include silicon, silicon dioxide, or other polycrystalline materials. However, it has been shown that YBCO deposited directly onto these materials reacts with them and degrades the YBCO superconducting properties. The use of buffer layers such as cerium dioxide (CeO2) or yttria-stabilized zirconia (YSZ) can mitigate these problems, but they have high dielectric constants and need to exhibit a high degree of biaxial texture to reduce high-angle grain boundaries and improve the critical current density, Jc, of the YBCO layer.

One possible interconnect structure that has been proposed by researchers at the High Density Electronics Center (HiDEC) consists of two YBCO layers separated by a thick layer of SiO2, which exhibits a low dielectric constant. To prevent interdiffusion and provide for an epitaxial surface on which high quality YBCO can be deposited, the SiO2 is



see presentation

separated from the YBCO by a thin buffer layer of either cerium dioxide or yttriastabilized zirconia. Clearly, the ability to deposit aligned buffer layers on polycrystalline or amorphous substrates would greatly improve the manufacturability of superconducting MCMs.

Ion beams have been used previously to deposit aligned buffer layers for YBCO on polycrystalline substrates. Iijima et al. (2) reported a dual-ion beam process for depositing YSZ on Hastelloy C276, a nickel-based alloy. The ion beam position with respect to the substrate normal was varied from 30° to 60°, with bi-axially oriented films obtained at an angle of 45°. Reade et al. (3) also reported biaxial deposition of YSZ on nickel alloys when using ion beam assisted deposition in conjunction with laser ablation. The degree of orientation of the films was found to be strongly dependent on the incident angle of the ion beam, with the optimal results occurring at 55° from the substrate normal. Ion beam voltage and current also played important roles in determining the amount of orientation of the film. Oriented YSZ growth on Pyrex substrates using IBAD has also been reported by Sonnenberg et al (4). They reported detailed microstructural characterization, but did not subsequently deposit YBCO on these films. This paper reports our progress to date in the use of IBAD with magnetron sputtering, which has the advantage of producing larger area films than laser ablation.

### EXPERIMENTAL DETAILS

All of the buffer layer films were deposited by RF magnetron sputtering in a deposition system designed at the University of Arkansas for superconductor and related dielectric research. Briefly, it is a 22" diameter side-sputtering deposition system that is pumped with two cryopumps. The deposition pressure can be precisely controlled from high vacuum to above 1 Torr, independently of the amount of backfill gas present. This is achieved through the use of separate high- and low-conductance paths to the cryopumps. Both conductance paths utilize servo-controlled throttle valves to maintain a constant pressure regardless of the gas flow present. The chamber has multiple ports for mounting two sputter guns, an ion beam, and two substrate holders, which also serve as heaters. The chamber was pumped down to  $4 \times 10^{-7}$  Torr before each deposition.

The ion beam used in these experiments is an Anatech IS-3000 3" filamentless gun. It was positioned about 8 cm from the substrate and at an angle of 55° from the substrate normal. This corresponds to the angle of the [111] direction from the [100] direction for cubic CeO<sub>2</sub>, and it is believed that ions directed at this angle may suppress growth of the (111) phase while enhancing growth of the (100) phase (3). Argon gas was flowed through the gun and an acceleration potential of 200-300 eV was used, with a beam current of 2-5 mA.

The dielectric films were deposited from a stoichiometric 2" diameter CeO<sub>2</sub> target which was RF sputtered in 80% Ar and 20% O<sub>2</sub> at pressures ranging from 0.2 mTorr to 1 mTorr, and at power levels from 60-80 watts. The low pressures were required to create

de or yttriacrystalline or erconducting

or YBCO on or depositing espect to the btained at an nickel alloys he degree of gle of the ion. Ion beam of orientation een reported tion, but did ess to date in lucing larger

ittering in a and related stem that is itrolled from sent. This is cryopumps.

1 a constant or mounting as heaters.

nentless gun. the substrate direction for rowth of the was flowed with a beam

CeO<sub>2</sub> target mTorr to 1 red to create a long enough mean free path for the ion gun to maintain a collimated beam. According to basic vacuum theory, a mean free path of 8 cm requires a pressure lower than 0.61 mTorr. Special modifications were made to the sputtering guns to allow them to maintain plasmas at such low pressures. These modifications basically consisted of flowing the sputtering gas inside the dark space shield of the sputter guns, creating a localized high pressure region. The substrate was unheated, but its temperature generally increased to about 50 °C due to radiative heating from sputtering and the ion beam.

The YBCO films were deposited in the same system described above, using a 2" magnetron sputtering gun in an off-axis geometry; the parameters are described elsewhere (5). Briefly, substrates were mounted onto a heater block using silver paste. The deposition temperature was held at 735 °C in 80% Ar and 20% O<sub>2</sub>. After deposition, the samples were cooled in 700 Torr of oxygen.

The following substrates were used in this experiment: pieces of <100> prime silicon, 1" square Corning 7059 borosilicate glass (Pyrex), and 0.5" square Haynes alloy (#230). Haynes alloy is a nickel-based stainless steel which is a candidate substrate for YBCO films because of its low thermal expansion coefficient mismatch with YBCO. The Haynes alloy was mechanically polished using successively finer diamond paste to 0.25 µm. The three different materials represent crystalline, amorphous, and polycrystalline structures, respectively, and provide a thorough test of the ability of IBAD to deposit oriented films independently of the substrate structure or orientation.

Cerium dioxide films were deposited on the above substrates both with and without IBAD. All of the films in this study were grown to a thickness of about 2000 Å. The use of IBAD caused a decrease in the deposition rate, from about 16 Å/min to 13 Å/min. After all of the CeO<sub>2</sub> depositions were completed, the CeO<sub>2</sub> sputtering gun was removed and replaced with the YBCO sputtering gun. The CeO<sub>2</sub> films were removed for analysis, then remounted to the heater block for YBCO deposition. YBCO films of approximately 3500 Å thickness were deposited on the glass and Haynes substrates.

The thickness and index of refraction of the CeO<sub>2</sub> films deposited on bare silicon were measured using an ellipsometer. The structure of the films was analyzed with a Phillips PW-1830 four-circle x-ray diffractometer (XRD) using copper ka radiation, and the surface analysis was performed with a Digital Instruments atomic force microscope (AFM). Electrical characteristics were measured using a non-contact technique similar to the system described in (6).

### RESULTS AND DISCUSSION

The index of refraction of both the IBAD and non-IBAD films was around 2.3, compared to 2.2 for bulk CeO<sub>2</sub>. This indicates that the films are slightly oxygen deficient (7), but theta-two theta XRD scans show only evidence of the CeO<sub>2</sub> phase. The theta-two theta scan of CeO<sub>2</sub> on a silicon substrate without using IBAD is shown in figure 1. The presence of the (111), (200), and the (220) peaks are present at roughly the same

intensity, with the ratio of the (200) peak intensity to (111) peak intensity equal to 0.95. This suggests a polycrystalline film with no prevalent texture. The film consists of completely random oriented grains since the substrate does not provide epitaxy for the growing layers. Figure 2 shows the theta-two theta scan of CeO<sub>2</sub> on silicon using IBAD. As the figure indicates, IBAD causes a marked improvement in the texturing of the (100) phase. The other phases are significantly attenuated, with the ratio of (200) to (111) intensities equal to 14.5. One reason for this dramatic improvement in texture, besides the fact that IBAD was used, is that silicon is crystalline with very nearly the same lattice constant as CeO<sub>2</sub>.

Figure 3 shows a theta-two theta XRD scan of IBAD deposited CeO<sub>2</sub> on Pyrex. While the (111) and (220) peaks are still visible, the (200) peak is dominant; the ratio of (200) to (111) intensities is 1.4. Figure 4 shows a phi scan of the (111) family of CeO<sub>2</sub> peaks on Pyrex and indicates both in-plane and out-of-plane orientation, as evidenced by the four peaks spaced 90° apart. The full-width-at-half-maximum (FWHM) for these peaks is approximately 34°. The relatively high FWHM implies that some in-plane misorientation is present. A theta-two theta scan of YBCO/CeO<sub>2</sub>/Pyrex is presented in figure 5. Only c-axis YBCO growth is detected, which suggests that the CeO<sub>2</sub> deposition provides a well-aligned layer upon which the YBCO can be deposited. As a further demonstration of the alignment, figure 6 shows a phi scan of the YBCO (103) family of peaks with a FWHM of 22°. This indicates well-aligned grains in the a-b plane, which is parallel to the substrate. The presence of 45° misaligned grains would be indicated by peaks spaced 45° out of phase from the major peaks. Misaligned grains greatly reduce the J<sub>e</sub> of the films.

Next, data for CeO<sub>2</sub> and YBCO/CeO<sub>2</sub> structures deposited on Haynes alloy are presented. Figure 7 shows a theta-two theta scan for CeO<sub>2</sub> deposited without IBAD. In this case, the CeO<sub>2</sub> peaks are barely discernible above the noise of the substrate, with the (111), (200), and (220) peaks at about equal intensity. The ratio of (200) to (111) intensities is equal to 0.9. Figure 8 illustrates a theta-two theta scan of YBCO deposited on Haynes alloy with an IBAD-deposited CeO<sub>2</sub> buffer layer. As in figure 5, only c-axis YBCO growth is evident. In addition, the (200) peak of CeO<sub>2</sub> is 3.2 times more intense than the (111) peak.

YBCO was deposited on the three CeO<sub>2</sub>/substrate structures and their  $T_c s$  and  $J_c s$  were measured.  $T_c s$  (zero resistance) were 86 K, and  $J_c s$  ranged from  $1 \times 10^5$  A/cm<sup>2</sup> to  $5 \times 10^5$  A/cm<sup>2</sup> when measured at 77 K. These values are somewhat lower than  $T_c s$  and  $J_c s$  obtained for films deposited on single crystal substrates, such as yttria stabilized zirconia. The cause for the reduction in  $J_c s$  is most likely due to the presence of high-angle grain boundaries, which are evident from the scan shown in figure 6. These grain boundaries are known to act as weak links and reduce the critical current density (8)

It is not well understood how the ion beam provides oriented film growth, but three separate mechanisms have been postulated. First, the collimated ion beam may selectively sputter grains growing in undesirable directions. Second, the beam is believed men The the Fina mob

be a impr peak quali quali for h

using indication from direct

exhibi has b polyci manuf substr brittle.

- 1. L. 'Comp
- 2. Y.:
- 3. R 1 (1992)
- 4. N. :
- 5. R. ( (1994)

al to 0.95. consists of exy for the ing IBAD. f the (100) to (111) besides the ame lattice

on Pyrex. he ratio of y of CeO<sub>2</sub> denced by for these e in-plane esented in deposition a further family of ; which is licated by reduce the

alloy are BAD. In , with the to (111) deposited nly c-axis re intense

es and Jes /cm² to 5 es and Jes zirconia. gle grain pundaries

eam may believed to enhance film growth corresponding to the channeling direction of the film. As mentioned above, the [111] channeling direction is 55° away from the [100] direction. Therefore, a beam directed at this angle allows the (100) phase to become channeled to the growing film, while other phase growth is attenuated or slowly sputtered away. Finally, the ion beam imparts energy to the surface of the film, which provides increased mobility for the molecules to realign into the preferred orientation.

The average roughness R, of the IBAD films was measured by AFM and found to be about 2.6 nm, while the R, of the non-IBAD films was about 3.8 nm. This improvement in smoothness is most likely due to the tendency of the ion beam to etch peaked surfaces more rapidly than smooth areas (9). This enhances superconductor quality by providing a smooth surface for YBCO nucleation. The improved surface quality, along with the stronger presence of the (100) phase, is believed to be responsible for higher YBCO film quality.

### CONCLUSIONS

Cerium dioxide films have been sputter deposited onto several substrate materials using IBAD. These films exhibit bi-axial alignment with dominant (100) phase growth, as indicated by XRD theta-two theta and phi scans. The argon ion beam was positioned 55° from the substrate normal. This angle corresponds to the angle of separation of the [111] direction of cubic CeO<sub>2</sub> from the [100] direction.

High quality YBCO was deposited over the IBAD buffer layers. The YBCO exhibited  $T_c s$  around 86 K and  $J_c s$  ranging from  $1\times10^5~A/cm^2~to~5\times10^5~A/cm^2$ . IBAD has been shown to be a useful technique for depositing aligned films on crystalline, polycrystalline, and amorphous substrates. This capability allows greater flexibility in manufacturing superconductor-dielectric structures by enabling the use of low-cost substrates in place of lattice-matched single crystal substrates, which tend to be expensive, brittle, and have high dielectric constants.

## REFERENCES

- 1. L. W. Schaper, S. S. Ang, Y. L. Low, and D. Oldham, to appear in IEEE Trans. on Comp., Hyb., and Man. Tech.
- 2. Y. Iijima, N. Tanabe, O. Kohno, and Y. Ikeno, Appl. Phys. Lett., 60, 769 (1992).
- 3. R. P. Reade, P. Berdahl, R. E. Russo, and S. M. Garrison, Appl. Phys. Lett., 61, 2231 (1992).
- 4. N. Sonnenberg, A. S. Longo, M. J. Cima, B. P. Chang, K. G. Ressler, P. C. McIntyre, and Y. P. Liu, J. Appl. Phys., 74, 1027 (1993).
- 5. R. G. Florence, S. S. Ang, and W. D. Brown, Supercond. Sci. Technol., 7, 741, (1994).

J. H. Claassen, M. E. Reeves, and R. J. Soulen, Rev. Sci. Instrum., 62, 996 (1991).
 S. Yaegashi, T. Kurihara, H. Hoshi, H. Segawa, Jpn. J. Appl. Phys. 33, 270 (1994).
 K. Char, M. S. Colclough, S. M. Garrison, N. Newman, and G. Zaharchuk, Appl.

9. S. S. Scott, M.S. EE thesis, University of Arkansas, 1994.

Phys. Lett. 59, 733, (1991).

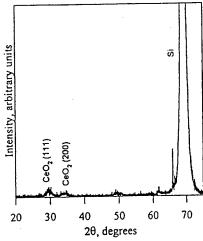


Figure 1. XRD scan of CeO<sub>2</sub> deposited on Si without IBAD.

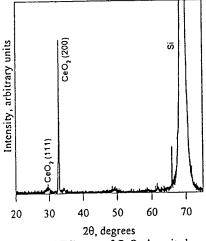


Figure 2. XRD scan of CeO<sub>2</sub> deposited on Si with IBAD.

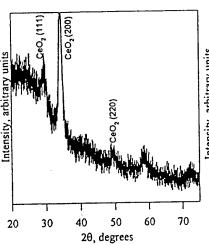


Figure 3. XRD scan of CeO<sub>2</sub> deposited on Pyrex with IBAD.

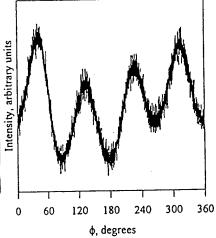


Figure 4. Phi scan of CeO2<sub>2</sub> (111) family of peaks deposited on Pyrex.

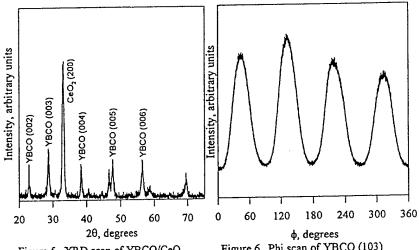
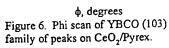


Figure 5. XRD scan of YBCO/CeO<sub>2</sub> deposited on Pyrex with IBAD.

A STATE OF THE PROPERTY OF THE PARTY OF THE

THE STATE OF THE PROPERTY OF THE PARTY OF TH



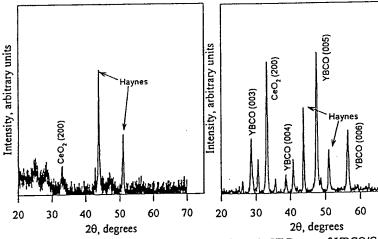


Figure 7. XRD scan of CeO<sub>2</sub> deposited on Haynes without IBAD.

Figure 8. XRD scan of YBCO/CeO<sub>2</sub> deposited on Haynes with IBAD.

70

PROCEEDINGS OF THE SYMPOSIUM ON

### LOW TEMPERATURE ELECTRONICS AND HIGH TEMPERATURE SUPERCONDUCTIVITY

#### **Editors**

Cor L. Claeys IMEC Leuven, Belgium

Stan I. Raider IBM T.J. Watson Research center Yorktown Heights, New York, USA

Randall Kirschman Mountain View, California, USA

William D. Brown University of Arkansas Fayetteville, Arkansas, USA

ENERGY TECHNOLOGY, ELECTRONICS, AND DIELECTRIC SCIENCE AND TECHNOLOGY DIVISIONS

Proceedings Volume 95-9



THE ELECTROCHEMICAL SOCIETY, INC., 10 South Main St., Pennington, NJ 08534-2896

Copyright 1995 by The Electrochemical Society, Inc.
All rights reserved.

This book has been registered with Copyright Clearance Center, Inc. For further information, please contact the Copyright Clearance Center, Salem, Massachusetts.

Published by:

The Electrochemical Society, Inc. 10 South Main Street Pennington, New Jersey 08534-2896 Telephone (609) 737-1902 Fax (609) 737-2743

Library of Congress Catalog Number: 95-60444

ISBN 1-56677-103-X

Printed in the United States of America

The firs Temper. Honolul Volume has incn

This Pi Sympo Superce Society, the Ener of the internat France, Switzer includir semicor exciting

The se contain achieve role of microw practica develor reviews the rela tunabili qualific microw the adv submic: are des  ${\tt SQUII}$ microfa unprece current perform

The fi Super superco

# Ion-beam-assisted sputter deposition of YSZ buffer layers for superconducting interconnect applications



#### Glenn Florence, Simon Ang and W D Brown

University of Arkansas, High Density Electronics Center (HiDEC) and Department of Electrical Engineering, 3217 Bell Engineering Center, Fayetteville, AR 72701, USA

Received 1 March 1995, in final form 19 April 1995

**Abstract.** Yttria-stabilized zirconia (YSZ) buffer layers have been sputter deposited onto various substrates including silicon and nickel alloy using ion-beam-assisted deposition (IBAD). This technique resulted in the formation of buffer layers which exhibit strong (100) phase growth as well as in-plane orientation as evidenced by x-ray diffraction measurements. Subsequent YBCO depositions on these films exhibit  $T_c$  values of 86 K and strong biaxial texture with the c axis normal to the surface. With further refinement, this technique may be used to fabricate the multilayer substrate structure needed for superconducting multichip modules.

#### 1. Introduction

There is widespread interest in the use of superconducting interconnects in electronics, especially in multichip modules (MCMs). Interconnects made of superconducting material have the advantage of low signal loss and very low RC propagation delays. Furthermore, due to the reduction in interconnect resistance, the linewidths can be made much smaller, allowing for higher density Superconducting MCMs require both largearea substrates and thick dielectrics in order to become technologically viable. Large area single-crystal materials such as magnesium oxide (MgO), yttria-stabilized zirconia (YSZ), and lanthanum aluminate (LaAlO<sub>3</sub>) are difficult and expensive to produce. Furthermore, these materials have very high dielectric constants, which makes them unsuitable for separating interconnect layers. In order to achieve satisfactory electrical performance and reduce parasitic capacitances at high signal speeds, these interconnects need to be separated by a thick (approximately 2-5  $\mu$ m) insulating layer with a low dielectric constant. Possible substrate and dielectric materials for these applications include silicon, silicon dioxide, or other polycrystalline materials. However, it is widely known that YBCO deposited directly onto these materials reacts with them and degrades the YBCO superconducting properties. The use of buffer layers, such as cerium dioxide (CeO<sub>2</sub>) or YSZ, reduces substrate-YBCO interaction problems, but these materials have high dielectric constants and need to exhibit a high degree of biaxial texture to reduce high-angle grain boundaries and improve the critical current density,  $J_c$ , of the YBCO layer.

One possible interconnect structure that has been proposed by researchers at the High Density Electronics Center (HiDEC) consists of two YBCO layers separated by a thick layer of SiO<sub>2</sub>, which exhibits a low dielectric constant. To prevent interdiffusion and provide for an epitaxial surface on which high-quality YBCO can be deposited, the SiO<sub>2</sub> is separated from the YBCO by a thin buffer layer of either CeO<sub>2</sub> or YSZ. Clearly, the ability to deposit aligned buffer layers on large polycrystalline or amorphous substrates would greatly improve the manufacturability and feasibility of superconducting MCMs.

Ion beams have been used previously to deposit aligned buffer layers for YBCO on polycrystalline substrates. Iijima et al [1] reported a dual-ion beam process for depositing YSZ on Hastelloy C276, a nickel-based alloy. The ion beam position with respect to the substrate normal was varied from 30° to 60°, with biaxially oriented films obtained at an angle of 45°. The energy of the ion beam was varied from 300 eV to 1000 eV, with best results obtained for energies less than 700 eV. Subsequent YBCO depositions over these films resulted in  $J_c$  values of  $2.5 \times 10^5$  A cm<sup>-2</sup> at 77 K.

Reade et al [2] also reported deposition of biaxial YSZ on nickel alloys when using ion-beam-assisted deposition (IBAD) in conjunction with laser ablation. The degree of orientation of the films was found to be strongly dependent on the incident angle of the ion beam, with

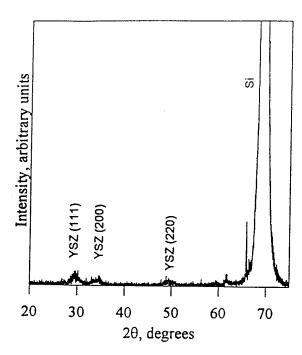


Figure 1. XRD scan of YSZ deposited on Si substrate without IBAD.

the optimal results occurring at 55° from the substrate normal. Ion beam voltage also played an important role in determining the amount of orientation of the film. They found that higher beam voltages increased film texture, whereas voltages less than 50 V resulted in films with no apparent a-b plane orientation. Changing the beam current did not enhance film texture, and currents above 50 mA reduced film deposition rates. The use of oxygen in the ion beam resulted in (100) film orientation, but no in-plane texture was observed. YBCO deposited on the oriented films exhibited  $T_c$  values of 92 K and  $J_c$  values of  $6 \times 10^5$  A cm<sup>-2</sup>.

Recently, Wu et al [3] reported  $CeO_2/YSZ$  layers deposited on flexible nickel substrates using IBAD and laser ablation. The thickness of the YSZ was 6000 to 8000 Å. A 1000 Å layer of  $CeO_2$  was then deposited over the YSZ in order to better match the lattice constants of YBCO. The full width at half-maxima (FWHM) of the (220) peaks of YSZ were found to be 14–15°. YBCO films deposited over the buffer layers exhibited  $J_c$  values of  $8 \times 10^5$  A cm<sup>-2</sup>, and the FWHM of the (103) peaks were about 10°.

Oriented YSZ growth on Pyrex substrates using IBAD in conjunction with electron beam evaporation has also been reported by Sonnenberg et al [4]. They reported detailed microstructural characterization, but did not subsequently deposit YBCO on these films.  $\phi$  scans of the films revealed strong orientation in the a-b plane. This was indicated by the presence of (111) peaks spaced 90° apart. Films were held at various angles from the ion beam, and (100) orientation was noted from 25° to 63° [4] from substrate normal, with 48° yielding the highest degree of orientation.

In the above studies, the substrate sizes were 18 mm by 10 mm, 10 mm square, or 5 mm square. The use of superconductor interconnects in MCMs will require large-area films, and these are difficult to obtain with laser ablation. This paper reports our progress to date on the

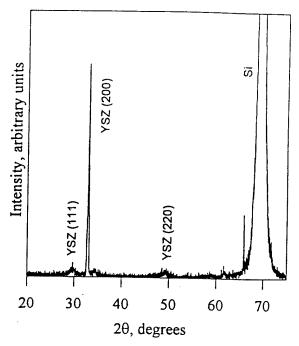


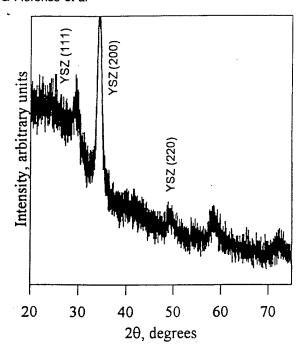
Figure 2. XRD scan of YSZ deposited on Si substrate with IBAD.

use of IBAD with magnetron sputtering, which has the advantage of being able to produce films approximately the same size as the sputtering target. However, IBAD is more difficult to implement in sputtering systems because of the low pressures (10<sup>-6</sup> to 10<sup>-4</sup> Torr) that ion beams require to operate. Furthermore, glow discharges are difficult to maintain at these pressures, especially in the presence of oxygen.

#### 2. Experimental details

All of the buffer layer films were deposited by RF magnetron sputtering in a deposition system designed at the University of Arkansas for superconductor and related dielectric research. Briefly, it is a 22" diameter side-sputtering deposition system that is pumped with two cryopumps. The deposition pressure can be precisely controlled from high vacuum to above 1 Torr, independently of the flow levels of backfill gas. This is achieved through the use of separate high- and lowconductance paths to the cryopumps. Both conductance paths utilize servo-controlled throttle valves to maintain a constant pressure regardless of the gas flow present. The chamber has multiple ports for mounting two sputter guns, an ion beam, and two substrate holders, which also serve as heaters. The chamber was pumped down to  $3 \times 10^{-7}$  Torr before each deposition to ensure adequate removal of water vapour.

The ion beam used in these experiments is an Anatech IS-3000 3" filamentless gun. It was positioned about 8 cm from the substrate and at an angle of 55° from the substrate normal. This corresponds to the angle of the [111] direction from the [100] direction for cubic YSZ, and it is believed that ions directed at this angle may suppress growth of the (111) phase while enhancing growth of the (100) phase [2]. Argon gas was flowed through the gun at a rate of 30 sccm,



**-igure 3.** XRD scan of YSZ deposited on Pyrex substrate with IBAD.

and an acceleration potential of 200-300 eV was used, with beam current of 2-5 mA.

The dielectric films were deposited from a 3" diameter YSZ target (8% by weight yttria) using a Torus 3C nagnetron sputtering gun. The target was RF sputtered n a mixture of 16 sccm Ar and 4 sccm O2 at a pressure of ).5 mTorr, and at power levels from 160-200 watts. The ow pressures were required to create a sufficiently long nean free path for the ion gun to maintain a collimated eam. According to basic vacuum theory, a mean free path of 8 cm requires a pressure lower than about 0.6 mTorr. special modifications were made to the sputtering guns o allow them to maintain plasmas at such low pressures. These modifications basically consisted of flowing the puttering gas inside the dark space shield of the sputter guns, creating a localized high pressure region. This, in conjunction with the magnetron field, confined the plasma o a region very near the surface of the target. The substrate vas not intentionally heated, but its temperature generally ncreased to about 100 °C due to radiative heating from puttering and the ion beam. The YBCO films were leposited in the same system described above, using a " magnetron sputtering gun in an off-axis geometry; the parameters are described elsewhere [5]. Briefly, substrates vere mounted onto a heater block using silver paste. The leposition temperature was held at 735 °C in 90% Ar and .0% O<sub>2</sub>. After deposition, the samples were cooled in 700 Torr of oxygen.

The following substrates were used in this experiment: pieces of  $\langle 100 \rangle$  prime silicon, 1" square Corning 7059 porosilicate glass (Pyrex), and 0.5" square Haynes alloy No 230). Haynes alloy is a nickel-based stainless steel which is a candidate substrate for YBCO films because of ts low thermal expansion coefficient mismatch with respect to YBCO. The Haynes alloy was mechanically polished using successively finer diamond paste to 0.25  $\mu$ m. The

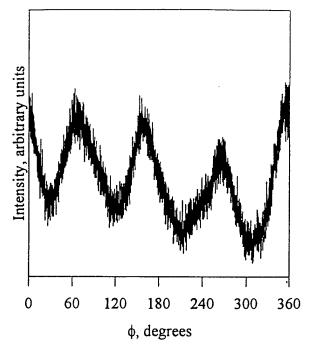


**Figure 4.**  $\phi$  scan of YSZ (111) family of peaks for the film shown in figure 3.

three different materials represent crystalline, amorphous, and polycrystalline structures, respectively, and provide a thorough test of the ability of IBAD to deposit oriented films independent of the substrate structure or orientation. YSZ films were deposited on the above substrates both with and without IBAD. All of the films in this study were grown to a thickness of about 2000 Å. The use of IBAD caused a decrease in the deposition rate, from about 40 Å min<sup>-1</sup> to 33 Å min<sup>-1</sup>. After all of the YSZ depositions were completed, the YSZ sputtering gun was removed and replaced with the YBCO sputtering gun. The YSZ films were removed for analysis, then remounted to the heater block for YBCO deposition. YBCO films of approximately 3500 Å thickness were deposited on the glass and Haynes substrates.

The thickness and index of refraction of the YSZ films deposited on bare silicon were measured using an ellipsometer. The structure and orientation of the films were analysed with a Phillips PW-1830 four-circle x-ray diffractometer (XRD) using Cu K $\alpha$  radiation, and the surface analysis was performed with a Digital Instruments atomic force microscope (AFM). Electrical characteristics were measured using a non-contact technique similar to the system described in [6]. Basically the system consists of a small coil of wire placed near the YBCO film. The coil-film assembly is cooled, and the coil is driven with a 10 kHz signal. As the film makes the transition from the normal state to the superconducting state, the inductance drops substantially due to shielding currents that are induced in the film. The  $T_c$  is obtained by noting the temperature at which a significant reduction in reflected voltage occurs. The  $J_c$  is obtained by increasing the drive current of the coil while held at 77 K. Eventually, harmonic voltages will appear in the coil, which indicate the onset of normal state resistance. The coil current at which the voltages appear is proportional to  $J_c$ .

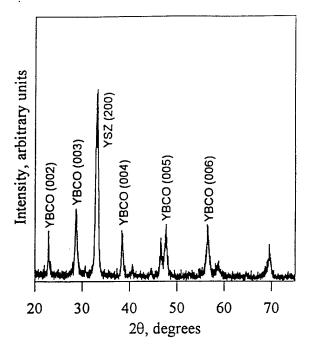


Figure 5. XRD scan of YBCO/YSZ deposited on Pyrex substrate with IBAD.

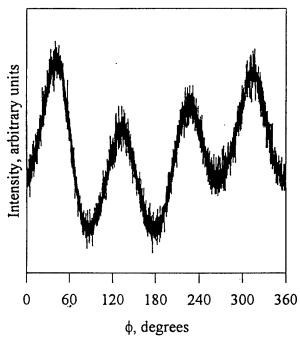


Figure 6.  $\phi$  scan of YSZ (111) family of peaks for the film shown in figure 5.

#### 3. Results and discussion

The  $\theta$ -2 $\theta$  scan of YSZ on a silicon substrate without using IBAD is shown in figure 1. The (111), (200) and the (220) peaks are present at roughly the same intensity, with the ratio of the (200) peak intensity to (111) peak intensity equal to 0.9. This indicates a polycrystalline film with no prevalent texture. The film consists of completely random oriented grains since the substrate does not provide epitaxy for the growing layers. Figure 2 shows the  $\theta$ -2 $\theta$  scan of YSZ on silicon using IBAD. As the figure indicates, IBAD causes a marked improvement in the texturing of the (h00) phase. The other phases are significantly attenuated, with

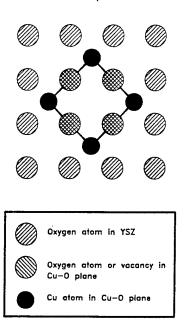


Figure 7. Illustration of the 45° (alignment of c-axis oriented YBCO on (100) oriented YSZ.

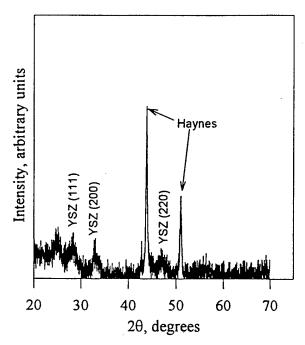


Figure 8. XRD scan of YSZ deposited on Haynes alloy substrate without IBAD.

the ratio of (200) to (111) intensities equal to 15. One reason for this dramatic improvement in texture, besides the fact that IBAD was used, is that silicon is crystalline with very nearly the same lattice constant as YSZ.

Figure 3 shows a  $\theta$ -2 $\theta$  XRD scan of IBAD deposited YSZ on Pyrex. While the (111) and (220) peaks are still visible, the (200) peak is dominant; the ratio of (200) to (111) intensities is 1.5. Figure 4 shows a  $\phi$  scan of the (111) family of YSZ peaks on Pyrex and indicates both in-plane and out-of-plane orientation, as evidenced by the four peaks spaced 90° apart. The full width at half-maximum (FWHM) for these peaks is approximately 34°. The relatively high FWHM implies that some in-plane misorientation is present. A  $\theta$ -2 $\theta$  scan of YBCO/YSZ/Pyrex is presented

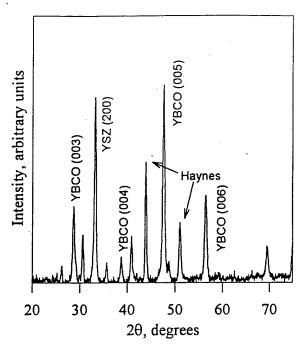


Figure 9. XRD scan of YBCO/YSZ deposited on Haynes alloy substrate with IBAD.

in figure 5. Only c-axis YBCO growth is detected, which suggests that the YSZ deposition provides a well-aligned layer upon which the YBCO can be deposited. As a further demonstration of the alignment, figure 6 shows a  $\phi$  scan of the YBCO (103) family of peaks with a FWHM of 22°. This indicates well-aligned grains in the a-b plane, which is parallel to the substrate. The presence of 45° misaligned grains would be indicated by peaks spaced 45° out of phase from the major peaks. Misaligned grains greatly reduce the  $J_c$  of the films [7], and thus, should be minimized. The (103) family of peaks are rotated 45° from the positions of the YSZ peaks shown in figure 4. This is expected since (100) orientations of YBCO tend to align with the CuO plane at a 45° rotation from the oxygen atoms in YSZ, as indicated in figure 7.

Next, data for YSZ and YBCO/YSZ structures deposited on Haynes alloy are presented. Figure 8 shows a  $\theta$ - $2\theta$  scan for YSZ deposited without IBAD. In this case, the YSZ peaks are barely discernible above the noise of the substrate, with the (111), (200) and (220) peaks at about equal intensities. The ratio of (200) to (111) intensities is equal to 0.9. Figure 9 illustrates a  $\theta$ - $2\theta$  scan of YBCO deposited on Haynes alloy with an IBAD-deposited YSZ buffer layer. As in figure 5, only c-axis YBCO growth is evident. In addition, the (200) peak of YSZ is 3.2 times more intense than the (111) peak.

YBCO was deposited on each of the three IBAD YSZ/substrate combinations and their  $T_c$  and  $J_c$  values were measured.  $T_c$  values (zero resistance) were 86 K, and  $J_c$  values ranged from  $2 \times 10^5$  A cm<sup>-2</sup> to  $7 \times 10^5$  A cm<sup>-2</sup> when measured at 77 K. Figure 10 shows the  $T_c$  plots for the films deposited on the three different substrates. These values are somewhat lower than  $T_c$  and  $J_c$  values obtained for films deposited on single-crystal YSZ substrates. The cause for the reduction in  $J_c$  is most likely due to the presence of high-angle grain boundaries, which are evident from the

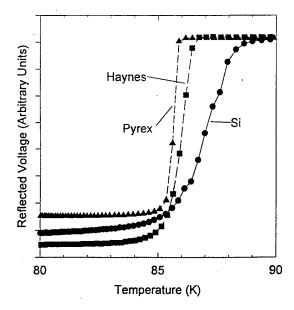


Figure 10. Transition temperature measurements for YBCO deposited on three different substrate materials.

scan shown in figure 6. These grain boundaries are known to act as weak links and reduce the critical current density [8].

It is not well understood how the ion beam provides oriented film growth, but three separate mechanisms have been postulated. First, the collimated ion beam may selectively sputter grains growing in undesirable directions. Second, the beam is believed to enhance film growth corresponding to the channelling direction of the film. As mentioned above, the [111] channelling direction is 55° away from the [100] direction. Therefore, a beam directed at this angle allows the (100) phase to become channelled to the growing film, while other phase growth is attenuated or slowly sputtered away. Finally, the ion beam imparts energy to the surface of the film, which provides increased mobility for the molecules to realign into the preferred orientation.

The average roughness  $R_a$  of the IBAD films was measured by AFM and found to be about 2.7 nm, while the  $R_a$  of the non-IBAD films was about 4.5 nm. This improvement in smoothness is most likely due to the tendency of the ion beam to etch peaked surfaces more rapidly than smooth areas, thus reducing RMS roughness [9]. This enhances superconductor quality by providing a smooth surface for YBCO nucleation. The improved surface quality, along with the stronger presence of the (100) phase, is believed to be responsible for higher YBCO film quality.

#### 4. Conclusions

Yttria-stabilized zirconia films have been sputter deposited onto several substrate materials using IBAD. These films exhibit biaxial alignment with dominant (100) phase growth, as indicated by XRD  $\theta$ -2 $\theta$  and  $\phi$  scans. The argon ion beam was positioned 55° from the substrate normal. This angle corresponds to the angle of separation of the [111] direction of cubic YSZ from the [100] direction.

High-quality YBCO was sputter deposited over the IBAD YSZ buffer layers. The YBCO exhibited  $T_{\rm c}$  values around 86 K and  $J_{\rm c}$  values ranging from  $2\times10^5$  A cm<sup>-2</sup> to  $7\times10^5$  A cm<sup>-2</sup>. IBAD has been shown to be a useful technique for depositing aligned films on crystalline, polycrystalline, and amorphous substrates. This capability allows greater flexibility in manufacturing superconductor—dielectric structures by enabling the use of low-cost substrates in place of lattice-matched single-crystal substrates, which tend to be expensive, brittle, and have high dielectric constants.

#### **Acknowledgments**

This work was supported by a grant from the Advanced Research Projects Agency and the Air Force Office of Scientific Research. The authors would also like to acknowledge John Shultz for his assistance with the XRD analysis.

#### References

- [1] Iijima Y, Tanabe N, Kohno O and Ikeno Y 1992 Appl. Phys. Lett. 60 769
- [2] Reade R P, Berdahl P, Russo R E and Garrison S M 1992 Appl. Phys. Lett. 61 2231
- [3] Sonnenberg N, Longo A S, Cima M J, Chang B P, Ressler K G, McIntyre P C and Liu Y P 1993 J. Appl. Phys. 74 1027
- [4] Wu X D, Foltyn S R, Arendt P, Townsend J, Adams C, Campbell I H, Tiwari P, Coulter Y and Peterson D E 1994 Appl. Phys. Lett. 65 1961
- [5] Florence R G, Ang S S and Brown W D 1994 Supercond. Sci. Technol. 7 741
- [6] Claassen J H, Reeves M E and Soulen R J 1991 Rev. Sci. Instrum. 62 996
- [7] Dimos D, Chaudhari P and Mannhart J 1990 Phys. Rev. B 41 4038
- [8] Char K, Colclough M S, Garrison S M, Newman N and Zaharchuk G 1991 Appl. Phys. Lett. 59 733
- [9] Scott S S 1994 MSEE Thesis University of Arkansas

mple is sample otropic tive to calcu-w t pact to neously quasi-d interbehavuit is it is es only effect,

M. Ivov, and nan for this 100 from

.oltzberg,

1991). 13,679

4 (1990) a C 177,

vashkin, nd K. V.

erg, J. R.

ev. B 45,

64&165,

68, 867

Rev. B

density, inzburg—
aniso-

Sputter-deposited yttrium-barium-copper-oxide multilayer structures incorporating a thick interlayer dielectric material

R. G. Florence, S. S. Ang, W. D. Brown, G. Salamo, L. W. Schaper, and R. K. Ulrich High Density Electronics Center, University of Arkansas, Fayetteville, Arkansas 72701

(Received 12 June 1995; accepted for publication 14 November 1995)

Physical vapor deposition technologies have been developed which allow the fabrication of multilayer structures consisting of two yttrium-barium-copper-oxide (YBa<sub>2</sub>Cu<sub>3</sub>O<sub>7-x</sub> or YBCO) layers separated by a thick ( $\sim$ 4  $\mu$ m), low dielectric constant material. The YBCO is buffered from both the substrate and the other films with ion-beam assisted deposited (IBAD) films of yttria-stabilized zirconia (YSZ). The YSZ layer provides both the texture necessary to deposit high-quality YBCO films and protection from the insulating layer material. Using these deposition processes, a variety of materials, such as Pyrex and Haynes alloy, may be used for the substrate. The critical temperature and current values obtained for the two YBCO layers of the completed structure were on the order of 85 K and  $2\times10^5$  A/cm<sup>2</sup>, respectively. © 1996 American Institute of Physics. [S0021-8979(96)06904-X]

#### I. INTRODUCTION

One of the potential applications of yttrium-bariumcopper-oxide (YBa<sub>2</sub>Cu<sub>3</sub>O<sub>7-x</sub> or YBCO) films is as the electronic interconnects on a multichip module (MCM) substrate. By using the interconnected mesh power system (IMPS) MCM topology, a superconducting MCM can be realized with two levels of superconducting interconnection.1 This is possible because the use of superconductor material for the interconnects allows for very high wiring densities. Thus, in order for this application to be realized, a large-area film of YBCO must be deposited onto a substrate, followed by a fairly thick layer of dielectric material, and finally, a second layer of YBCO. The thick layer of dielectric material is required to provide impedance control of the interconnect lines. As an additional constraint, the dielectric must have a relatively low dielectric constant in order to minimize the thickness of this layer.

Most efforts directed at the fabrication of multilayer YBCO structures have required each of the layers to maintain epitaxy of the substrate throughout the thickness of the structure. This requirement greatly constrains the choice of substrate and dielectric materials that can be used. The materials must be chemically compatible with YBCO, and their lattice constants and coefficients of thermal expansion (CTE) must closely match that of YBCO.

Ion-beam assisted deposition (IBAD) is a technique which eliminates the constraint of maintaining epitaxy throughout the entire structure. This is due to a combination of the mechanisms of preferential sputtering, ion channeling, and shadowing of misoriented grains by the ion beam. The formation of a textured microstructure results from the higher sputtering yields of all orientations other than that of the channeling direction. Thus, a textured microstructure can be formed by carefully balancing the deposition rate with the sputtering due to the ion beam. Using IBAD, epitaxial films have been grown on top of amorphous layers. IBAD has been used to deposit textured yttria-stabilized zirconia (YSZ) on Pyrex<sup>3,4</sup> and Haynes alloy<sup>4-7</sup> substrates, and cerium diox-

ide has been used as a buffer material on these and other substrate materials.8

#### II. EXPERIMENT

In this article, YSZ was first deposited onto Pyrex substrates using IBAD under the deposition conditions outlined in Ref. 4. Briefly, the ion gun was positioned at a distance of 80 mm from the substrate and at an angle of 55° from the substrate normal. Argon gas was flowed through the gun at a rate of 20 sccm and an acceleration potential of 300 eV was used, with a beam current of 7 mA and a deposition pressure of 0.7 mTorr. The thickness of the YSZ layer was about 5000 A. Next, YBCO was sputter-deposited to a thickness of 3000 A using an off-axis configuration. The substrate was heated to 735 °C at a deposition pressure of 200 mTorr in an 80% argon/20% oxygen gas mixture. The YBCO was then capped with a 2000 Å thick layer of IBAD/YSZ to prevent interdiffusion. Next, a 4  $\mu$ m thick layer of silicon dioxide (SiO<sub>2</sub>) was deposited on top of the YSZ layer by reactive sputtering of a 3 in. diameter pure silicon target. The conditions were as

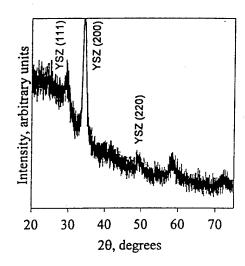


FIG. 1. Theta-two theta scan for a typical YSZ film deposited on Pyrex.

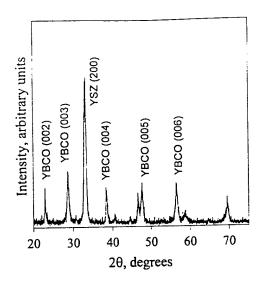


FIG. 2. Theta-two theta scan for a typical YBCO/YSZ structure deposited on Pyrex.

follows: a target-substrate distance of 50 mm, a pressure of 15 mTorr, an 80% Ar/20%  $O_2$  gas mixture, and a rf power level of 200 W. The deposition rate was  $\sim 1~\mu$ m/h, and the films were deposited at room temperature (the substrate temperature generally increased to  $\sim 120~\rm ^{\circ}C$  during deposition). The film thickness and index of refraction were measured by ellipsometry.

After the SiO<sub>2</sub> was deposited, a 5000 Å thick layer of AD/YSZ was deposited on the structure, and finally, 3000 of YBCO was deposited on top of the YSZ. All of the depositions were performed in situ; the YBCO depositions were performed with an off-axis geometry, and the SiO<sub>2</sub> and YSZ depositions were performed on-axis. During target change operations, the substrate was pulled into a load lock and pumped down to prevent reactions with the atmosphere.

#### III. RESULTS AND DISCUSSION

Figure 1 shows a theta-two theta scan for YSZ deposited on Pyrex. The (200) peak is clearly visible above the background which confirms orientation normal to the substrate surface. The phi scan of the YSZ (111) family of peaks for the same film reveals strong in-plane alignment. In Fig. 2, a theta-two theta scan for YBCO/YSZ deposited on Pyrex is presented. Only c-axis YBCO growth is visible in addition to the (200) YSZ. The phi scan of the YBCO (103) family of peaks (not shown in Fig. 2) reveals strong biaxial alignment, although grain boundaries are most likely present.

The critical temperature,  $T_c$ , curve of the YBCO film is shown in Fig. 3. This layer exhibited a  $T_c$  of 87 K and the critical current,  $J_c$ , measured using a noncontact method, was found to be  $8 \times 10^5$  A/cm<sup>2</sup> at 77 K. Degradation of the superconducting properties of the bottom YBCO layer, due to subsequent film depositions, was determined by depositing all the remaining required layers except for the second anyer of YBCO. To simulate the effects of the second YBCO deposition, the film stack was ramped to 735 °C and held at this temperature for 4 h. This approach to determining the degradation effects of subsequent depositions was necessary

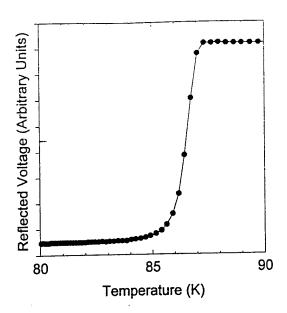


FIG. 3. The critical temperature curve of the YBCO shown in Fig. 2.

to prevent interference with  $T_c/J_c$  measurements on the bottom YBCO layer. Measurements of the superconductor properties of the bottom YBCO layer were then performed. The  $T_c$  and  $J_c$  degraded to 84 K and  $2\times10^5$  A/cm², respectively. These data were confirmed separately by transport measurements. The reasons for these reductions is most likely due to oxygen effusion from the YBCO caused by the high temperature and long dwell time.<sup>9</sup>

The thick SiO<sub>2</sub> and subsequent layers were thoroughly inspected for cracks under an optical microscope, and none were found. The stress on all of the film layers is determined by the coefficient of thermal expansion (CTE) of the Pyrex substrate, which is higher than that of the films. The substrate is also several orders of magnitude thicker than the films. This is in agreement with Yin et al. 10 who found that films

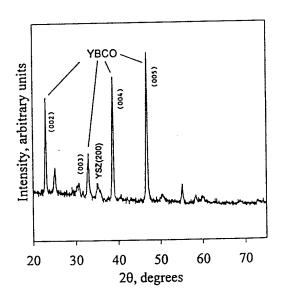


FIG. 4. Theta-two theta scan of the top YBCO layer.

with a because A t structur was det to be 8

was det to be 8 cannot YBCO the filn was for  $J_c$  than attribut ible from

Ar the str sured I as the ness of which

IV. SU

A condu μm) c beam rate tl SiO<sub>2</sub> pure YBCC respectively.

2004

. .

with a smaller CTE than that of the substrate did not crack because they are under compressive stress.

A theta-two theta scan for the top YBCO layer of the structure is shown in Fig. 4. The  $T_c$  of the top layer of YBCO was determined using a contact measurement, and was found to be 86 K. It should be noted that the noncontact method cannot be used in this case due to interference by the bottom YBCO layer on the  $T_c$  measurements. To avoid patterning of the film, the  $J_c$  was measured with a noncontact method and was found to be  $2\times10^5$  A/cm<sup>2</sup>. This slightly lower value of  $J_c$  than was obtained for the bottom layer of YBCO can be attributed to the high-angle grain boundaries which are visible from the phi scan of the (103) YBCO peaks.

Among the factors that influenced the overall quality of the structure was film roughness. The roughness, as measured by atomic force microscopy, was observed to increase as the number of layers increased. The mean surface roughness of the top-most YSZ layer was measured to be 193 nm, which can easily disrupt the YBCO lattice.

#### IV. SUMMARY AND CONCLUSIONS

A multilayer structure consisting of two layers of superconducting YBCO separated by a relatively thick layer ( $\approx 4 \mu m$ ) of SiO<sub>2</sub>, has been successfully fabricated using ion beam assisted magnetron sputtering. Buffer layers of ion beam assisted magnetron sputtered YSZ were used to separate the YBCO from the substrate material (Pyrex) and the SiO<sub>2</sub>. The SiO<sub>2</sub> was deposited by reactive sputtering of a pure silicon target. The  $T_c$  and  $J_c$  of the bottom layer of YBCO was slightly degraded to 84 K and  $2\times 10^5$  A/cm<sup>2</sup>, respectively, by the subsequent high temperature processing. The  $T_c$  and  $J_c$  of the top YBCO layer were similar to the final values of the bottom layer. These lower values for the

top layer are attributed to increasing film roughness as the number of layers of material increases. However, the results of this article indicate that multiple levels of YBCO, required for the fabrication of a superconducting multichip module, can be successfully deposited on a variety of substrate materials using ion beam assisted magnetron sputtering of YBCO and YSZ buffer layers.

#### **ACKNOWLEDGMENTS**

This work was supported by a grant from the Advanced Research Projects Agency (ARPA) and the Air Force Office of Scientific Research (AFOSR). The authors would also like to acknowledge John Shultz for his assistance with the XRD analysis.

<sup>1</sup>L. W. Schaper, S. S. Ang, Y. L. Low, and D. Oldham, IEEE Trans. Components, Hybrids, Manufacturing Technol. 18, 99 (1995).

<sup>2</sup>M. J. Burns, K. Char, B. F. Cole, W. S. Ruby, and S. A. Sachtjen, Appl. Phys. Lett. **62**, 1435 (1993).

<sup>3</sup> N. Sonnenberg, A. S. Longo, M. J. Cima, B. P. Chang, K. G. Ressler, P. C. McIntyre, and Y. P. Liu, J. Appl. Phys. 74, 1027 (1993).

<sup>4</sup>R. G. Florence, S. S. Ang, and W. D. Brown, Supercond. Sci. Technol. 8, 546 (1995).

<sup>5</sup>Y. Iijima, N. Tanabe, O. Kohno, and Y. Ikeno, Appl. Phys. Lett. 60, 769 (1992).

<sup>6</sup>R. P. Reade, P. Berdahl, R. E. Russo, and S. M. Garrison, Appl. Phys. Lett. 61, 2231 (1992).

<sup>7</sup> X. D. Wu, S. R. Foltyn, P. Arendt, J. Townsend, C. Adams, I. H. Campbell, P. Tiwari, Y. Coulter, and D. E. Peterson, Appl. Phys. Lett. 65, 1961 (1994).

<sup>8</sup>R. G. Florence, S. S. Ang, and W. D. Brown, in *Low Temperature Electronics and High Temperature Superconductivity* (Electrochemical Society, Pennington, NJ, 1995), Vol. 95-9, p. 113.

<sup>9</sup>J. D. Jorgensen, M. A. Beno, D. G. Hinks, L. Soderholm, K. J. Volin, R. L. Hitterman, J. D. Grace, and I. K. Schuller, Phys. Rev. 36, 3608 (1987).

<sup>10</sup>E. Yin, M. Rubin, and M. Dixon, J. Mater. Res. 7, 1636 (1992).

Fig. 2.

90

the botor propied. The ectively. neasurey due to gh tem-

ro y
nd none
ermined
e Pyrex
ubstrate
e films.
at films

# Magnetic field and temperature dependence of critical current densities in multilayer YBa<sub>2</sub>Cu<sub>3</sub>O<sub>7- $\delta$ </sub> films

S. Afonso, F. T. Chan, K. Y. Chen, G. J. Salamo, Y. Q. Tang, R. C. Wang, a) X. L. Xu, b) and Q. Xiong

Physics Department/High Density Electronics Center, University of Arkansas, Fayetteville, Arkansas 72701

G. Florence, S. Scott, S. Ang, W. D. Brown, and L. W. Schaper Electrical Engineering Department/High Density Electronics Center, University of Arkansas, Fayetteville, Arkansas 72701

In order to build high-temperature superconductor (HTS) multichip modules (MCMs), it is necessary to grow several epitaxial layers of YBCO that are separated by thick dielectric layers without seriously affecting the quality of the YBCO layers. In this work, we have successfully fabricated YBCO/YSZ/SiO<sub>2</sub>/YSZ/YBCO structures on single-crystal LaAlO<sub>3</sub> substrates using a combination of pulsed laser deposition for the YBCO layers and ion-beam-assisted rf sputtering to obtain biaxially aligned YSZ intermediate layers. The bottom YBCO layer had a  $T_c \sim 89$  K,  $J_c \sim 7.2 \times 10^5$  A/cm<sup>2</sup> at 77 K, whereas the top YBCO layer had a  $T_c \sim 86$  K,  $J_c \sim 6 \times 10^5$  A/cm<sup>2</sup> at 77 K. The magnetic field and temperature dependence of  $J_c$  for the YBCO films in the multilayer have been obtained. The results for each of the YBCO layers within the YBCO/YSZ/SiO<sub>2</sub>/YSZ/YBCO structure are quite similar to those for a good quality single-layer YBCO film. © 1996 American Institute of Physics. [S0021-8979(96)03308-9]

#### I. INTRODUCTION

In electronic applications of high-temperature superconductor (HTS) thin films, the critical current density  $(J_c)$  is an important characteristic. One of the potential applications of high-temperature superconducting films is as electronic interconnects on a multichip module (MCM). Since there are a minimum of two HTS thin films, separated by thick dielectric layers required, in HTS multichip modules (MCMs), it is necessary to know if the quality of the HTS layers is still maintained after the entire fabrication process is completed. In addition to the critical temperature  $(T_c)$  and critical current density at zero field, the dependence of  $J_c$  on an externally applied magnetic field and the temperature for the entire multilayer structure is crucial information for electronic applications. The YBCO/YSZ/SiO2/YSZ/YBCO multilayer structure has been fabricated by Reade et al.<sup>2</sup> They reported cracking in the top YBCO layer, which limited their investigation of the properties of the multilayered structure.

In this article, we report a study of the temperature and magnetic field dependence of  $J_c$  for both YBCO layers in a YBCO/YSZ/SiO<sub>2</sub>/YSZ/YBCO multilayer structure<sup>3</sup> performed by the magnetization method. Our results show that the temperature and magnetic field dependence of  $J_c$  of the YBCO layers of these samples are similar to those of high quality single-layer YBCO thin films.

#### II. EXPERIMENT

The YBCO/YSZ/SiO<sub>2</sub>/YSZ/YBCO multilayer samples investigated here were prepared by using a combination of pulsed laser deposition and ion-beam-assisted magnetron

under the same conditions as was used for layer 1. The orientation of the YSZ and YBCO layers was characterized by x-ray diffraction. The magnetization M(H) loop was measured using a Quantum Design Magnetometer in fields up to 4 T, applied parallel to the c-axis direction and at a fixed temperature. This was repeated for different temperatures ranging from 5 to 77 K. The values of  $J_c$  were calculated using Bean's model. The electrical resistance was measured using the standard four-lead technique.

sputtering. Details of the technique will be described elsewhere.<sup>3</sup> In short, a 200-nm-thick  $YBa_2Cu_3O_{7-\delta}$  (bottom

YBCO, layer 1) film was deposited on a single-crystal

LaAlO<sub>3</sub> substrate (100 orientation and area  $1\times1$  cm<sup>2</sup>) by

pulsed laser ablation at a substrate temperature of ~750 °C.

Ion-beam-assisted rf sputtering was used to deposit biaxially

aligned 200-nm-thick yttria-stabilized zirconia (YSZ) as a

capping layer (layer 2). Next a 1- $\mu$ m-thick, amorphous SiO<sub>2</sub>

layer (layer 3) was deposited on layer 2 at room temperature

by rf sputtering. The capping layer (YSZ) is used to prevent

diffusion of the third SiO<sub>2</sub> layer into the top YBCO layer. A

fourth layer (biaxially aligned YSZ) was then deposited on

the SiO<sub>2</sub> layer to a thickness of 200 nm using the same

method as for layer 2. This layer is very important. It not

only functions as protection against the diffusion of the third

SiO<sub>2</sub> layer into the YBCO layer, it also allows good epitaxial

YBCO growth if it has a well-aligned structure. Finally, the

top YBCO layer (layer 5) was deposited by laser ablation

#### **III. RESULTS AND DISCUSSION**

X-ray diffraction data showed that all samples investigated here were single-phase highly c-axis oriented with very good in-plane epitaxy (Fig. 1). There were no cracks observed in the top YBCO layer. The resistance R(T) and magnetization M(T) of the samples were carefully measured for each YBCO layer. Figure 2 shows the typical resistance as a function of temperature for the top YBCO layer. The

a)Permanent address: Department of Materials Science, Fudan University, Shanghai, People's Republic of China.

b)Permanent address: Ion Beam Laboratory, Shanghai Institute of Metallurgy, Chinese Academy of Sciences, Shanghai, People's Republic of China.

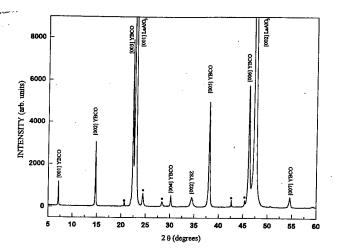


FIG. 1.  $\theta$ -2 $\theta$  x-ray diffractometer pattern for the YBCO/YSZ/SiO<sub>2</sub>/ YSZ/YBCO structure on [001] LaAlO<sub>3</sub> (\*: indicate substrate impurity peaks seen in the bare substrates of the same batch).

zero resistance temperature for this YBCO layer is about 86 K with a transition width of about 2 K. The M(T) data for a multilayer sample are shown in the inset of Fig. 2. As can be seen in the inset of Fig. 2, the onset transition of the M(T) curve is about 89 K. A second transition (indicated by the arrow in the inset of Fig. 2) is consistent with the  $T_c$  of the top YBCO layer measured by the transport method (Fig. 2). In order to verify this,  $T_c$  was remeasured again after the top layer of YBCO was etched away by using a dilute EDTA solution, and the onset transition was found to be about 89 K.

The critical current density  $J_c$  of the samples were measured by the magnetization method and calculated using Bean's model. For a rectangular single-layer film,  $J_c$  can be calculated from the following formula:<sup>4</sup>

$$J_c = 10[M_+(H) - M_-(H)]/L_1[1 - (L_1/3L_2)]V.$$
 (1)

In Eq. (1),  $M_+(H)$  and  $M_-(H)$  are the magnetization of the decreasing and increasing field branches in electromagnetic units (emu), respectively; V is the volume of the thin

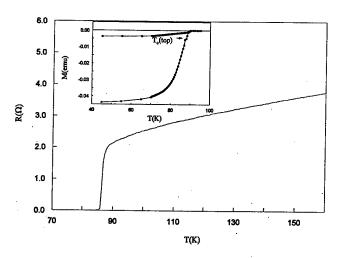


FIG. 2. Resistance vs temperature for the top YBCO layer in the YBCO/YSZ/SiO $_2$ /YSZ/YBCO/LaAlO $_3$  multilayer structure. Inset: magnetization M as a function of T for the entire multilayer structure.

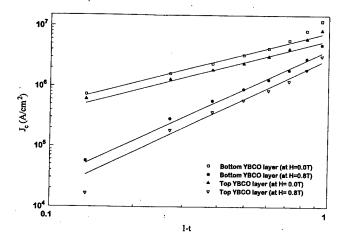


FIG. 3. Logarithmic plots of  $J_c$  vs 1-t for each of the YBCO layers within the multilayer structure. Straight lines are the curve fits to  $(1-t)^n$ , where  $n \sim 1.3$  for H = 0.0 T and  $n \sim 2.1$  for H = 0.8 T.

film in cm<sup>3</sup>,  $L_1$  and  $L_2$  are the short and long sides of the samples in cm, respectively. We have assumed that  $J_c$  is independent of the B field and excluded the anisotropic critical currents in the above calculation. In order to determine  $J_c$  of both the top and bottom YBCO layers, the magnetization  $M_+^m(H)$  and  $M_-^m(H)$  for the multilayer film was measured first, then the magnetization  $M_+^b(H)$  and  $M_-^b(H)$  for the bottom layer was measured after the top layer of YBCO was etched away. In this article we use superscript t and t for the parameters related to the top and bottom YBCO layer in the multilayer film, then t for the bottom layer should be

$$J_c^b = 10[M_+^b(H) - M_-^b(H)]/L_1^b[1 - (L_1^b/3L_2^b)]V^b,$$
 (2)

and for the top layer in the multilayer film,

$$J_c^t = 10\{[M_+^m(H) - M_+^b(H)] - [M_-^m(H) - M_-^b(H)]\}/L_1^t[1 - (L_1^t/3L_2^t)]V^t.$$

The  $J_c$  of the top YBCO layer was found to be about  $6\times10^5$  A/cm<sup>2</sup>, and a value of  $\sim7.2\times10^5$  A/cm<sup>2</sup> was obtained for the bottom layer at 77 K under zero magnetic field.  $J_c$ , as a

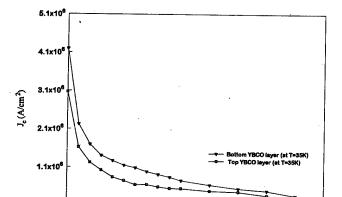


FIG. 4. Magnetic field dependence of  $J_c$  for top and bottom YBCO layers at 35 K. Field is applied perpendicular to a-b plane.

H(T)

function of (1-t), is shown in Fig. 3 for different values of the magnetic field, where  $t=T/T_c$ . It was found that, for both YBCO layers, the temperature dependence of  $J_c$  is similar to that for a good quality, single-layer YBCO film. <sup>5-7</sup> The magnetic field dependence of  $J_c$  for both YBCO layers at 35 K are shown in Fig. 4. It clearly shows that  $J_c$  for both top and bottom YBCO films essentially has the same magnetic field dependence as that for the high quality, single-layer YBCO film. <sup>5-7</sup>

#### **IV. SUMMARY**

A good quality YBCO multilayer structure has been fabricated using laser ablation and ion-beam-assisted rf sputtering. The dependence of  $J_c$  on the temperature and magnetic field for both YBCO layers in the multilayer has been determined. The results suggest that the temperature and magnetic field dependence of  $J_c$  of the YBCO layers in the multilayer structure are not altered appreciably by the multilayer growth processes.

#### **ACKNOWLEDGMENTS**

This work was supported in part by NSF DMR 9318946, the High Density Electronics Center at the University of Arkansas, DARPA (Contract No. MDA 972-90-J-1001) and through the Texas Center for Superconductivity at the University of Houston.

<sup>1</sup>M. J. Burns, K. Char, B. F. Cole, W. S. Ruby, and S. A. Sachtjen, Appl. Phys. Lett. **62**, 1435 (1993).

<sup>2</sup>R. P. Reade, P. Beardahl, R. E. Russo, and L. W. Schaper, Appl. Phys. Lett. 66, 2001 (1994).

<sup>3</sup>S. Afonso, Q. Xiong, K. Y. Chen, F. T. Chan, G. J. Salamo, Y. Q. Tang, G. Florence, S. Scott, S. Ang, W. D. Brown, and L. W. Schaper (unpublished).

E. M. Gyorgy, R. B. van Dover, K. A. Jackson, L. F. Schneemeyer, and J. V. Waszczak, Appl. Phys. Lett. 55, 283 (1989).

<sup>5</sup>Q. Xiong, W. Y. Guan, P. H. Hor, and C. W. Chu, Chin. J. Phys. 30, 851 (1992).

<sup>6</sup>D. W. Chung, I. Maartense, T. L. Peterson, and P. M. Hemenger, J. Appl. Phys. 68, 3772 (1990).

<sup>7</sup>S. B. Ogale, D. Dijkkamp, T. Venkatesan, X. D. Wu, and A. Inam, Phys. Rev. B **36**, 7210 (1987).



# FABRICATION OF HIGHLY TEXTURED SUPERCONDUCTING THIN FILMS ON POLYCRYSTALLINE SUBSTRATES USING ION BEAM ASSISTED DEPOSITION

<sup>1</sup>Q. Xiong, <sup>1</sup>S. Afonso, <sup>1</sup>F.T. Chan, <sup>1</sup>K.Y. Chen, <sup>1</sup>G.J. Salamo, <sup>2</sup>G.Florence, J. Cooksey, S. Scott, <sup>2</sup>S. Ang, <sup>2</sup>W.D. Brown and <sup>2</sup>L. Schaper, <sup>1</sup>Physics Department, <sup>2</sup>Electrical Engineering Department / High Density Electronics Center, University of Arkansas, Fayetteville, AR 72701

#### **ABSTRACT**

Tl<sub>2</sub>Ba<sub>2</sub>CaCu<sub>2</sub>O<sub>3</sub>(Tl2212) thin films on ceramic Al<sub>2</sub>O<sub>3</sub> substrates with J<sub>6</sub>(77K) of about 10<sup>5</sup> A/cm<sup>2</sup> and high quality YBCO/YSZ/SiO<sub>2</sub>/YSZ/YBCO/LaAlO<sub>3</sub> mutilayers with J<sub>6</sub>(77K) of about 6×10<sup>5</sup> A/cm<sup>2</sup> in the top YBCO layer have been successful deposited for the first time. These Mirror-like, highly c-axis oriented films were grown on highly textured YSZ buffer layers, which were deposited through Ion Beam-Assisted Laser Ablation. The zero resistance temperature is 95-108K for the Tl2212 films, and 85-90K for the multilayer YBCO films. The results suggest that using cheap non-single crystal substrates to fabricate good HTS films is possible.

#### 1. Introduction

Since the discovery of high temperature superconductors(HTS), many possible applications of HTS thin films have been design and demonstrated, from very useful fault current limiters to the electronic interconnects on multichip module (MCM) substrates. All of these applications would benefit from the use of HTS thin films. One of the major problems for the application of HTS's is that HTS's can carry only a limited amount of current without resistance. This problem is related to their two dimensional layered structure. According to earlier studies 1-2, if the layers do not line up properly, the critical current density will decrease dramatically in the misaligned region. One way to overcome this problem is to grow micron-thin layers of the material on well organized substrates, epitaxally. The process has the effect of lining up the superconducting layers more accurately. HTS thin films grown on single crystal substrates of LaAlO, or SrTiO, have good lattice match between the HTS and substrate, and have critical current densities of about ~10<sup>6</sup> A/cm<sup>2</sup>, which is large enough for most HTS thin film applications. While this effort is impressive, it is far from useful, since the films so developed are much too expensive because the single crystal substrates are very expensive and available only in relatively small sizes. Moreover, for some electronic applications such as HTS multi-chip modules(MCM's),



there are at least two HTS thin films that are separated by thick dielectric layers. Useful dielectric layers such as SiO<sub>2</sub> have noncrystalline structures. For this reason, HTS thin film layers cannot be grown on the dielectric layer with good alignment by conventional methods. Recent studies<sup>3-7</sup> have shown that highly biaxially aligned YSZ layers can be grown on non-crystalline substrates, which are cheaper and easy to get in any size needed by Ion beam-assisted laser deposition(IBAD). Using this method, high quality YBa<sub>2</sub>Cu<sub>3</sub>O<sub>y</sub> (YBCO) films have been deposited on biaxially aligned YSZ layers grown on non-crystalline substrates with J<sub>e</sub>'s of up to 8×10<sup>5</sup>A/cm<sup>2</sup> at 75K.

Here, we report the results from Tl2212 films fabricated on polycrystalline Al<sub>2</sub>O<sub>3</sub> substrates with an IBAD deposited YSZ buffer layer and YBCO/YSZ/SiO<sub>2</sub>/YSZ/YBCO/LaAlO<sub>3</sub> mutilayers.

#### II Experimental

Fine polished Al<sub>2</sub>O<sub>3</sub> was used for the substrates of the Tl2212 films. Ion-beam assisted pulsed laser deposition was used to prepare highly biaxial aligned YSZ buffer layers at room temperature. While YSZ was deposited by pulse laser deposition, an Ion-beam (argon ion source) bombarded the substrates at an angle of 55° from the substrate normal. The laser used here was an ArF excimer laser (wavelength = 193 nm, shot frequency = 5 Hz). The energy density of the laser beam, which was focused on the YSZ target, was set to about 2 - 3 J/cm<sup>2</sup>. The ion beam energy was typically set at about 250 eV, and the beam current density was about 120 µA/cm<sup>2</sup>. The oxygen partial pressure was maintained at  $3x10^{-1}$  Torr, and with the ion beam the total pressure in the vacuum chamber was about 8x10<sup>-4</sup> Torr during the deposition of the YSZ layers. The substrate temperature increased to about 100 °C due to the assisting ion beam. The growth rate was about 0.5 Å/S. The thickness of the YSZ buffer layers in our experiment was about 5000 Å. For the YBCO multilayer structure, 2000 Å thick YBCO layers were deposited by pulsed laser ablation at ~750 °C. A 4-5 micron thick amorphous SiO<sub>2</sub> layer was deposited as a dielectric layer at room temperature by rf sputtering. For the Tl2212 films, 2000~3000Å Ba<sub>2</sub>CaCu<sub>2</sub>O<sub>v</sub> precursor films were deposited on the YSZ-buffer layer at a temperature of 400°C using pulsed laser ablation. The films were then treated in a thallination process at 810°C.

The structures of deposited films were characterized by x-ray diffraction.  $T_c$  and  $J_c$  of HTS layers were measured by both transport method using the standard four-lead technique and the magnetization method using a Quantum Design Magnetometer.

#### III. Results and Discussion

All YSZ films deposited on the polycrystalline  $Al_2O_3$  substrates for Tl2212 or on first YBCO layer, or on amorphous  $SiO_2$  layer were (001) oriented with the <001> axis normal to the substrate plane. A typical X-ray  $\theta$ -2 $\theta$  diffraction pattern for a YSZ film deposited on a polycrystalline  $Al_2O_3$  substrate is shown in Fig.1. Observation of only the YSZ(002) peak in the

# 8 8 8

X-ray  $\theta$ -2 $\theta$  diffraction pattern indicates that the YSZ was highly (001) oriented. The  $\phi$  scan width of the {111} peaks is about 25° (FWHM).

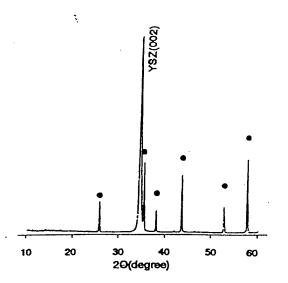


Fig. 1. X-ray diffraction θ-2θ scan of YSZ on Al<sub>2</sub>O<sub>3</sub> (● Λl<sub>2</sub>O<sub>3</sub> peak)

**Typical** resistance versus temperature data for TI2212 is shown in Fig.2. The zero resistance temperature  $T_c$  is 105.6K which is comparable with the results from the high quality films grown on LaAlO, or SrTiO3 substrates. The critical current densities of these films are about 8×104 A/cm² by transport method. Fig.3 shows the typical resistance as a function of temperature for the top YBCO layer in the multilayer structures. The zero resistance temperature for this YBCO layer is about 86K with a transition width of about 2 K. The Messier effect M(T) for the same mutilayer sample is shown in the inset of Fig.3. As in the inset of Fig.3, the onset

transition of the M(T) curve is at about 89 K, a second transition (indicated by the arrow) in the inset of Fig.3 is consistent with the T<sub>c</sub> of the top YBCO layer measured by the transport method (Fig.3). In order to verify this, T<sub>c</sub> was remeasured again after the top layer of YBCO was etched

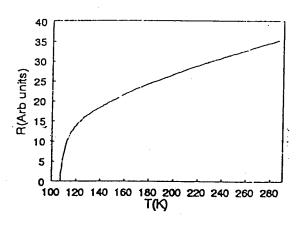


Fig. 2. Resistance vs. Temperature for the Tl<sub>2</sub>Ba<sub>2</sub>CaCu <sub>2</sub>O<sub>4</sub> on YSZ/Al<sub>2</sub>O<sub>3</sub>.

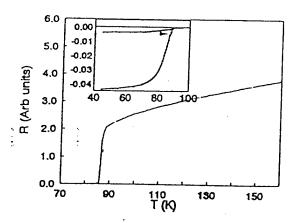


Fig. 3. Resistance vs.temperature for the top YBCO layer in the YBCO/YSZ/SiO<sub>2</sub>/YSZ/YBCO/LaAlO<sub>3</sub> multilayer. Inset: Magnetization M as a function of temperature for the entire multilayer.

away by using a dilute EDTA solution, and the onset transition was found to be at about 89 K without the second transition. The critical current density, J<sub>c</sub> of the samples were measured by the

£ ...

magnetization method and calculated using Bean's model before and after the top layer of YBCO was etched away. The  $J_c$  of the bottom YBCO layer is about  $7.2\times10^5$  A/cm² at 77 K, and of the top YBCO layer is about  $6\times10^5$  A/cm² at 77 K, For comparison, we deposited both YBCO and Tl2212 on ceramic  $Al_2O_3$  substrates. Even though the  $T_c$  of these films were about the same,  $J_c$  is  $<10^4$  A/cm². Which is about two orders of magnitude lower than that of the film on the biaxially aligned YSZ layer

#### IV. SUMMARY

Tl2212 films on ceramic Al<sub>2</sub>O<sub>3</sub> substrates have been grown for the first time and good quality YBCO multilayer structures have been prepared using laser ablation and ion beam assisted rf sputtering. Our results demonstrate that good quality HTS films can be grown on cheap nonsingle crystal substrates though the Ion Beam-assisted deposition technique.

#### **ACKNOWLEDGMENTS**

This work is supported in part by NSF DMR 9318946, DARPA (Contract No. MDA 972-90-J-1001) through Texas Center for Superconductivity at the University of Houston.

#### REFRENCE

- D. Dimos, P. Chaudhari, J. Mannhart, and F. K.LeGoues, Phys. Rev. Lett.61(1988)219.
   D. Dimos, P. Chaudhari, J. Mannhart, Phys. Rev. B 41(1990) 4038.
- 2. "Effect of Pressure on the Critical Current Density of YBa2Cu3O7-d Thin Films,"
  - Q. Xiong, Y. Y. Xue, Y. Y. Sun, P. H. Hor, C. W. Chu, M. F. Davis, J. C. Wolfe, S. C.Deshmukh and D. J. Economou, Physica C 205, 307 (1993).
- 3. R. P. Reade, P. Berdahl, R. E. Russo, and S. M. Garrison, Appl. Phys. Lett. 61, 2231 (1992).
- .4. 2. Y. Iijima, N. Tanabe, O. Kohno, and Y. Ikeno, Appl. Phys. Lett. 60, 769 (1992).
- X. D. Wu, S. R. Foltyn, P. Arendt, J. Townsend, C. Adams, I. H. Campbell, P. Tiwari, Y. Coulter, and D. E. Peterson, Appl. Phys. Lett. 65, 1961 (1994).
- 6. F. Yang, E. Narumi, S. Patel, and D. T. Shaw, Physica, C 244, 299 (1995).
- X. D. Wu, S. R. Foltyn, P. N. Arendt, W. R. Blumenthal, I. H. Campbell, J. D. Cotton, J. Y. Coulter, W. L. Hults, M. P. Maley, H. F. Safar, and J. L. Smith, Appl. Phys. Lett. 67, 2397(1995).

# PROCEDINGS of the ANNIVERSARY HTS WORKSHOP

on Physics, Materials and Applications

Edited by

B. Batlogg
Lucent Technologies, USA

C. W. Chu
Texas Center for Superconductivity
University of Houston, USA

W. K. Chu
Texas Center for Superconductivity
University of Houston, USA

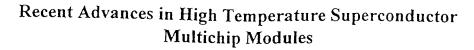
**D. U. Gubser**Naval Research Laboratory, USA

K. A. Müller
IBM Zürich, Switzerland



March 12-16, 1996 Doubletree Hotel at Allen Center Houston, Texas, USA







J. W. Cooksey, S. S. Scott, W. D. Brown, S. S. Ang and R. G. Florence
 High Density Electronics Center/Department of Electrical Engineering
 University of Arkansas, Fayetteville, AR 72701
 Phone: 501-575-8603 Fax: 501-575-2719 E-mail: jwc1@engr.uark.edu

S. Afonso
High Density Electronics Center/Department of Physics
University of Arkansas, Fayetteville, AR 72701

#### Abstract

Two different techniques for fabricating high temperature superconducting (HTS) MCM-D substrates have been developed and tested. The first unit consists of two digital gallium arsenide bare die connected by  $YBa_2Cu_3O_{7.0}$  (YBCO) HTS interconnects to form two ring oscillators on a 2.25 cm² MCM-D substrate. The interconnections consist of two wiring layers of YBCO separated by a 4-5  $\mu$ m silicon dioxide interlevel dielectric. The signal lines are routed between power and ground lines which form an interconnected mesh power system (IMPS) and, thereby, the module avoids the necessity of having two additional layers for power and ground planes. Connection between the two YBCO layers is accomplished with low contact resistance 40  $\mu$ m gold vias through the interlevel dielectric layer. The signal interconnects have 50  $\mu$ m linewidths and 75  $\mu$ m spacings. Electrical connections between the die and the MCM substrate and between the substrate and the PC board were made using ultrasonic Al wire bonds to low contact resistance gold/YBCO bond pads on the MCM substrate.

The second module, known as the Flip-Mesh superconducting MCM, provides an alternative to the multilayer MCM-D substrate described above. It involves using flip chip bonding techniques to connect multiple single-layer substrates, thereby reducing the processing complexity of fabricating multiple layers. X-plane and Y-plane interconnects are fabricated on separate substrates and interconnected using solder bumps. The IMPS topology is also utilized in this structure so that power, ground, and signals can be fabricated on two planes. The initial Flip-Mesh design incorporates 100 µm (4 mil) solder bump vias with similar spacings, which results in a low packing density for MCM-D technology, but a high density for I/O technology.

Key words: High temperature superconductors, MCM-D, Interconnected Mesh Power System (IMPS), YBCO

#### Introduction

Unlike that of VLSI technologies where smaller feature sizes in successive generations allow interconnect lengths and power dissipation to be reduced, multichip modules (MCMs) will not have that same luxury. As the complexity of ICs advances, pinout count per IC increases, and operating frequencies increase, MCM normal metal interconnections will have to grow in length and will not be allowed to reduce in cross-sectional area. On MCM-D substrates, typical copper or aluminum interconnection dimensions are about 2 to 5 µm in thickness and between 15 and 30  $\mu m$  wide. The resistivity of copper or aluminum decreases by at least a factor of 7 when decreasing the temperature from 300 K to 77 K (liquid nitrogen temperature), which allows smaller cross-section interconnections to be fabricated

on cryo-cooled MCMs. In order to increase the wiring density in MCMs beyond that of cryo-cooled MCMs and improve the chip-to-chip bottleneck at high frequencies, alternatives to conventional metal interconnects must be considered [1].

High temperature superconductor (HTS) interconnections, with negligible resistivity at operating frequencies of several tens of GHz and lower, have great potential to reduce the interconnection line cross-section even further with typical thicknesses being less than 1  $\mu$ m and widths could be reduced to less than 2  $\mu$ m for MCM applications. The critical current density of HTS interconnects, which limits the line's minimum cross-section, is similar in value to the maximum current density allowed in Al interconnects to inhibit electromigration. These small, low resistance

ENTERED 194

0-7803-3787-5/97 \$5.00 @1997 IEEE

1997 International Conference on Multichip Modules

# Proceedings

1997

# International Conference on Multichip Modules

April 2-4, 1997 The Adam's Mark Hotel Denver, Colorado

Sponsored by:











interconnects offer significant performance advantages over normal metal interconnects for MCM-D technology using CMOS or GaAs integrated circuits which have enhanced chip level performance at liquid nitrogen temperatures (77 K). An added benefit of HTS lines is the reduced capacitive coupling between adjacent interconnections (due to their reduced thickness) which allows the lines to be spaced more closely together. The reduced cross-section of HTS interconnects should allow a significant increase in packing density and a corresponding decrease in the number of interconnect layers required to achieve the same functionality with normal metal interconnects.

We have been developing two separate HTS MCM prototypes. One is to be the first planar HTS MCM utilizing a thick layer of silicon dioxide as an interlevel dielectric and is based on MCM-D technology. The second prototype is based on interconnecting two layers of HTS interconnects on separate substrates via solder bumps and flip chip techniques. Our development has centered around the HTS material YBa<sub>2</sub>Cu<sub>3</sub>O<sub>7-4</sub> (YBCO) which has a transition temperature of about 91 K (well above the boiling point of liquid nitrogen, 77 K) and critical current densities typically greater than 5 x 10<sup>5</sup> A/cm<sup>2</sup>.

#### I. HTS MCM-D Prototype

A cross-section of our proposed HTS MCM is shown in Figure 1.

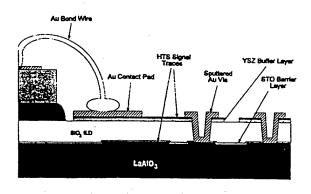


Figure 1. HTS MCM cross-section.

This novel structure has several key features that provide advantages over previously demonstrated HTS MCMs [2,3]. These advantages are:

 the utilization of an Interconnected Mesh Power System (IMPS) topology that is ideal for HTS multilayer fabrication because it allows an MCM to be constructed with only two layers of interconnects as opposed to the four that are traditionally used: x-signal, ysignal, and ground and power planes;

(2) a thick (~ 5 μm) layer of SiO<sub>2</sub> that is sandwiched between a thin buffer layer dielectric and a thin diffusion barrier layer dielectric to form a composite interlevel dielectric that is compatible with multilayer YBCO processing while allowing controlled impedance (Z<sub>o</sub> = 50 Ω) lines to be fabricated, which are necessary for high speed signal propagation;

(3) chemical-mechanical polishing to create a planar SiO<sub>2</sub> surface for deposition of a high quality top level superconductor/buffer layer;

high-aspect ratio, low contact resistance vias that utilize noble metals to form contacts between the two layers of YBCO interconnects, as opposed to large area, low-aspect ratio superconducting vias that have been fabricated with marginal success previously.

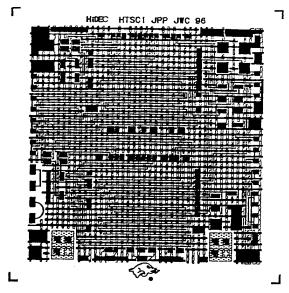
Due to the grain boundary problems associated with making very wide, sloping superconducting vias through a thick dielectric layer, alternative methods have to be explored to create the compact, high-aspect ratio vias necessary for fast, high density HTS MCMs.

Yttria stabilized zirconia (YSZ) was chosen as the material for providing a diffusion barrier/buffer layer between the superconductor and the interlevel dielectric material, silicon dioxide, because of its diffusion barrier properties as well as having a close lattice spacing and coefficient of thermal expansion (CTE) match to YBCO. Silicon dioxide was chosen as the interlevel dielectric material because of its low dielectric constant and well developed deposition and etching processes.

#### **Experimental Details**

Our MCM-D substrate was constructed of two layers of laser-ablated YBCO interconnects separated by a multilayer dielectric consisting of  $SrTiO_3/SiO_2/YSZ$ . We are able to attain critical current densities >  $5 \times 10^5 \text{ A/cm}^2$  in both YBCO layers. The laser-ablated  $SrTiO_3$  (STO) and ion beam assisted laser-ablation deposited (IBAD) YSZ (yttria-stabilized zirconia) layers were ~0.5  $\mu$ m thick while the reactively-sputtered  $SiO_2$  ranges between 4 and 5  $\mu$ m thick. The multilayered thin film structure is fabricated on 15 mm x 15 mm LaAlO3 and YSZ substrates.

The HTS MCM was layed out as shown in Figure 2 on the following page.



7

.

ä.

Figure 2. Layout of a 2 layer 15 mm x 15 mm HTS MCM-D substrate.

The 2.25 cm<sup>2</sup> substrate consists of two separate ring oscillators built using YBCO interconnects between two digital GaAs bare die (4.4 mm x 3.5 mm). The first ring oscillator is connected using the smallest possible interconnection, whereas, the second is connected by a much longer interconnect. performance comparison between the two oscillators is planned for future work. There are also bond pads on the substrate for mounting various sizes of surface mount decoupling capacitors and terminating resistors. A prototype of our ring oscillator using one of the GaAs bare die wirebonded to 20 mil wide copper traces on a PC board was tested at liquid nitrogen temperature and was found to oscillate at ~250 MHz. Based on this result, our HTS MCM ring oscillator is estimated to operate at about the same frequency.

The via fabrication process is shown in Figure 3. The etching involves a 500 eV ion mill through the top YSZ buffer layer, which is followed by a reactive ion etch (RIE) through the SiO<sub>2</sub> interlevel dielectric selectively stopping at the barrier layer of STO. To complete the etching process, a 500 eV ion mill is done to etch through the STO and into the underlying YBCO. The final milling is very nonselective and requires close observation to keep from overetching through the bottom layer of YBCO. When depositing the top layer of YBCO at ~700° C, whatever material is deposited on the via sidewalls is presumably corroded due to interdiffusion of Si from SiO2 into the YBCO but, presumably, does not affect the quality of the via. The subsequent in situ deposition of ~2000 Å of Au by laser ablation creates low resistance contacts without having to do a high temperature anneal in oxygen as

was described by Ekin et al. [4]. This Au capping layer also acts as a passivation layer for the YBCO. In similar structures, contact resistivities of less than  $10^{-7}$   $\Omega$ -cm² have consistently been attained. An additional 1.5-2.0  $\mu$ m of Au is deposited over the existing YBCO/Au and then patterned using ion milling and photoresist as a mask.

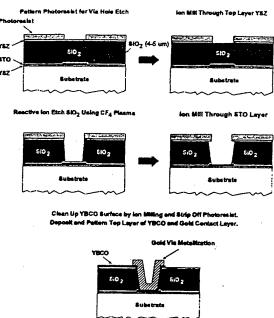


Figure 3. HTS via fabrication process.

This type of via structure has several advantages over previously demonstrated superconducting vias for use in HTS MCMs [2,3]. Since HTS thin films have to be deposited on planar surfaces or gradual slopes to maintain a reasonable current density, due to grain boundary problems, they require gradually sloped via holes that take up a wide area. By using a noble metal, compact, high-aspect ratio vias can be fabricated reliably.

Ultrasonic Al wire bonds were then made between YBCO/Au bond pads on the substrate and a wire bondable PC board. Via chain resistance was measured using a conventional 4-point contact configuration and measuring the voltage drop across the vias while passing DC current through it. The resistance vs. temperature of a ~0.5 cm long via chain structure with ten 40 µm square vias interconnecting 50 μm wide YBCO lines is shown in Figure 4. The room temperature resistance was measured to be about 515 Ω, and upon cooling to 78.5 K, the resistance dropped to about 87  $\Omega$ . As is shown in this figure, there are two separate superconducting transitions occurring at about 89 K and 80 K, which correspond to the top and bottom layer YBCO transitions. At 78.5 K, the interconnects had not yet become fully superconducting.

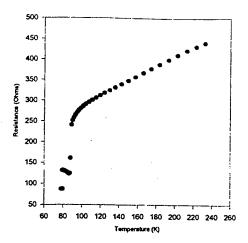


Figure 4. Temperature transition of a chain of ten 40 μm wide vias.

#### II. Flip-Mesh HTS MCM

The Flip-Mesh Superconducting Multi Chip Module (MCM) is an alternative to the conventional multi-layer superconducting MCM. It is desired that a superconducting MCM be fabricated using High-Temperature Superconductor (HTS) materials, with which such an MCM can be cooled using liquid nitrogen. However, many difficulties arise in the formation of multiple superconducting planes separated by dielectric layers on a single substrate. The crystalline nature of HTS materials such as Yttrium-Barium-Copper-Oxide (YBCO) requires that the deposition surface be closely matched to the HTS material in crystalline structure.

The high temperatures needed to form HTS materials requires that the other HTS MCM materials be matched with the superconductor in coefficient of thermal expansion (CTE), and not crack or delaminate at such high temperatures. These requirements lead to a complex stack of materials in order to create a multiple-superconducting-plane MCM interconnect structure. This combination of materials also complicates selective patterning processes with respect to the HTS material.

#### Flip-Mesh Basics

The fundamental concept of Flip-Mesh is that instead of depositing multiple HTS layers on a single substrate and connecting the layers by vias, single HTS layers are deposited on multiple substrates, and opposing superconducting layers on separate substrates

are connected by flip-chip technology. This reduces the number of high-temperature processing steps to one, eliminating most of the difficulties in the multilayer structure. However, the use of I/O technology to form vias limits the ultimate density of the Flip-Mesh Superconducting MCM.

In the multilayer MCM, Ion Beam Assisted Deposition (IBAD) [5] is used to form an oriented buffer layer so that an HTS film can be grown on an amorphous surface. This also allows the use of an amorphous substrate. Since Flip-Mesh requires only one superconducting plane per substrate, it is an ideal application for depositing HTS films on amorphous substrates. Amorphous substrates are considerably less costly than single-crystal substrates.

#### Flip-Mesh Substrate Arrangement

There are three substrates in a Flip-Mesh module. The main substrate contains x-plane interconnect and bonding sites for chips. Two smaller secondary substrates contain y-plane interconnect, and are "flipped" onto the main substrate. The chip bonding sites are between the secondary substrates. I/O pads are located on the outside edges of the main substrate. The Flip-Mesh substrate configuration is shown in Figure 5. As with the multilayer MCM, the Interconnected Mesh Power System (IMPS) topology [6] allows complete power, ground, and signals to be formed in two conducting planes. The term "Flip-Mesh" is derived from the flipping of IMPS-mesh interconnect planes to form an MCM interconnect structure.

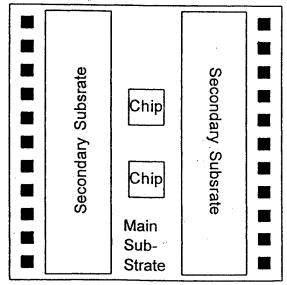


Figure 5. Flip-Mesh substrate configuration.

YBCO films are formed by laser ablation [7] on 1/2" or 1" square single-crystal yttria-stabilized zirconia (YSZ) or IBAD YSZ-buffered alumina substrates. The YBCO films are then patterned by argon ion milling [8] using conventional photoresist as a mask. The fact that ion milling is non-selective is not important in Flip-Mesh, since the underlying layer is always the substrate, which can be over-etched. The ion milling system is equipped with a water cooled sample stage to prevent YBCO or photoresist damage due to excessive heating from the ion milling.

Gold pads are then formed where electrical contact to YBCO is desired. A lift-off process is employed in which 2  $\mu$ m of gold is sputter deposited onto a patterned photoresist layer. The Flip-Mesh substrates are exposed to a brief low-energy ion milling, which serves to prime the exposed YBCO surface for the gold deposition. After deposition, the photoresist layer is lifted off in an ultrasonic bath of acetone, leaving the gold pads on the YBCO. The lift-off process again avoids selective etching with respect to the YBCO. The Flip-Mesh substrates are then annealed at 600 °C for I hour in 500 Torr of oxygen to form a sturdy low-resistance contact.

The critical element of Flip-Mesh is the material used for the vias and the method used to form the interconnection. Figure 6 shows a cross-section of a Flip-Mesh via bump.

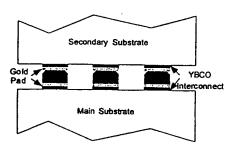


Figure 6. Flip-Mesh via cross-section.

The initial approach was to form gold balls using a ball bonding machine, and then press the substrates together while heating. Ball placement was found to be tedious, but workable. It was discovered, however, that the ball bonding process would often damage the underlying YBCO. This was not obvious unless the gold ball detached from the bonding pad. Ball detachment can be avoided by attaching to a bonding pad that is at least 1.5 times the size of the ball, but it is believed that this only disguises the damage.

Typical gold ball sizes range from 70  $\mu m$  to 100  $\mu m$  in diameter. The size of the Flip-Mesh bonding pad is 100  $\mu m$ . Since density is already a limiting factor in the Flip-Mesh approach, increasing the via size is not desirable. It was also found that the extreme heat and pressure required to make an acceptable contact between the Flip-Mesh substrates caused the YBCO to become non-superconducting. The YBCO could be repaired by annealing, but the substrates would detach in the process.

The second assembly method attempted was to individually place preformed indium spheres. Indium was chosen because of its decent conductivity and low melting point. It was quickly discovered, however, that indium is far too soft to be handled mechanically, and no modules could be formed using this method. Stencil printing was then determined to be the ideal method for placing Flip-Mesh via bumps. A batch process would certainly be desirable, but the small via size (4 mil) and pitch (8 mil) puts severe limitations on this technology.

The first material to be screen printed was conductive epoxy, but this material was unable to meet the density requirement. The epoxy bumps would flatten and create shorts. Further work with the viscosity of the epoxy may lead to a useful application.

The next stencil printing material used was tin/lead solder. A special high-density solder was acquired, and worked nicely, but standard tin/lead solder has a leaching problem with the gold contact pads. Modules fabricated in this process detached within hours due to the leaching. Another solder paste was then acquired, which contained an additional 2% silver to prevent gold leaching.

After screen printing solder pads to the main substrate, the secondary substrates are aligned to the main substrate, and the solder is reflowed. The current Flip-Mesh material components are laser-ablated YBCO on single-crystal YSZ substrates with gold contact pads interconnected by screen printed tin/lead/silver solder bumps.

#### Initial Flip-Mesh Circuit

The initial Flip-Mesh circuit is a ring oscillator formed from 2 quad-XOR HCMOS chips. The first XOR gate has one input tied high, which turns it into an inverter. The other gates have one input tied low, which makes them buffers. This arrangement permits the number of gates in the loop to be adjusted from 2 to 8, allowing different speeds of oscillation.

The IMPS power and ground stripes are 250  $\mu$ m wide, the signals are 50  $\mu$ m wide, and the spacing between the two is 50  $\mu$ m. The main substrate is 10

mm x 10 mm, and the secondary substrates are 2.5 mm x 10 mm. As was discussed previously, the contact pads are 100  $\mu$ m x 100  $\mu$ m. The XOR chips are approximately 1mm x 1mm each.

#### Flip-Mesh Assembly and Testing

After a Flip-Mesh substrate module is completed, the XOR chips are attached using thermoplastic tape. The leads of the chips are then aluminum wire bonded to the main substrate. The number of gates in the oscillator loop is selected by a wire bond in the center of the main substrate. The assembled Flip-Mesh module is then attached to a test board using thermoplastic tape. The I/O pads of the module are then aluminum wire bonded to the test board.

When complete, the test board is attached to an oscilloscope and power supply, measuring the output signal of the first XOR gate. The module is then slowly immersed in a small dewar of liquid nitrogen.

#### Conclusions

In summary, 40 µm YBCO/Au via chain structures have been characterized for use in an MCM-D substrate. The preliminary work shown here is to be improved upon by improving the quality of the YBCO layers, lowering the contact resistances, and possibly improving the step coverage of Au through the via by increasing its thickness. We are hoping to have an HTS MCM-D substrate fabricated in the near future. The performance of this MCM will be compared to that of a nearly identical Al interconnect module operating at liquid nitrogen temperature.

Thus far, functional Flip-Mesh modules have been fabricated only with metal interconnects. These modules were built on glass substrates with gold/titanium-tungsten metallization, and the substrates were interconnected with gold balls formed by a ball bonder. These units were tested both at room temperature and while immersed in liquid nitrogen with 2 to 8 gates in the oscillator loop. As would be expected, the modules ran faster at cryogenic temperature. While the gold ball vias worked adequately for a metal module, they were found to be

incompatible with YBCO due to damage caused by the attachment process. The stencil printing processes discussed are under investigation to find a YBCO-compatible process. It will be interesting to compare the performance of the HTS Flip-Mesh to the cryogenic metal Flip-Mesh.

Despite the great processing complexity involved with fabricating an HTS MCM, great progress is being made toward achieving practical MCM substrates utilizing these novel materials.

#### References

- [1] S. K. Tewksbury, L. A. Hornak, L. A. Tewksbury, and L. Chen, "A System-Level Evaluation of HTS Interconnections on MCMs for High Performance VLSI Systems", Journal of Microelectronic Systems Integration, Vol. 4, No. 2, (1996).
- [2] M. J. Burns, K. Char, B. F. Cole, W. S. Ruby, and S. A. Sachtjen, "Multichip module using multilayer YBa<sub>2</sub>Cu<sub>3</sub>O<sub>7-8</sub> interconnects", Appl. Phys. Lett., 62 1435 (1993).
- [3] B. Santo, "Superconducting MCM demo'd", Electronic Engineering Times, August 10 (1992).
- [4] J. W. Ekin, S. E. Russek, C. C. Clickner, and B. Jeanneret, "In situ noble metal YBa<sub>2</sub>Cu<sub>3</sub>O<sub>7.4</sub> thin-film contacts", Appl. Phys. Lett., 62 369 (1993).
- [5] G. Florence, "Fabrication and Characterization of Superconducting Yttrium Barium Copper Oxide Multilayer Structures", Ph.D. Dissertation, University of Arkansas, (1995).
- [6] L.W. Schaper, S. Ang, Y.L. Low, and D. Oldham, "Electrical Characterization of the Interconnected Mesh Power System (IMPS) MCM Topology", Proceedings of the 44th Electronic Components & Technology Conference, Washington, D.C., May 1-4, pp. 791-795, (1994).
- [7] S. Afonso et al., "Magnetic Field and Temperature Dependence of Critical Current Densities in Multilayer YBa<sub>2</sub>Cu<sub>3</sub>O<sub>7-a\_</sub>Films", Journal of Applied Physics, Vol. 79, No. 8, pp. 6593-6595, (1996).
- [8] S. Scott, "Ion Milling of Yttrium-Barium-Copper-Oxide for Interconnects in a Superconducting Multichip Module", M.S.E.E. Thesis, University of Arkansas, (1994).

# Fabrication and characterization of vias for contacting YBa2Cu3O7-x multilayers

J. W. Cooksey, S. Afonso, W. D. Brown, L. W. Schaper, S. S. Ang, R. K. Ulrich, G. J. Salamo, and F. T. Chan

High Density Electronics Center, University of Arkansas, 600 W. 20th Street, Fayetteville, AR 72701 USA

In order to connect multiple layers of high temperature superconductor (HTS) interconnects, low contact resistance vias must be used to maintain high signal propagation speeds and to minimize signal losses. In this work,  $40~\mu m~via~contacts~through~YBa_2Cu_3O_{7.x}/SrTiO_3/SiO_2/YSZ/YBa_2Cu_3O_{7.x}~multilayers~utilizing~dry~etching~techniques$ and sputter deposited Au for contacting through the vias have been successfully fabricated and characterized. The vias connect two laser ablated YBa<sub>2</sub>Cu<sub>3</sub>O<sub>7-x</sub> (YBCO) signal lines through thick (4-5 μm) SiO<sub>2</sub> insulating layers. This approach to making multilayer superconductor vias provides a low resistance contact between the YBCO layers while maintaining space efficiency and fabrication compatibility with the superconductor.

#### 1. INTRODUCTION

0 - 13

r. if

hed-

juest

a A.

tered

pt to

ired:

adia,

stan.

SA.

nths

ırt

rth

32.

17-

orf 1.

1 and

clands

Since the discovery of high temperature superconductivity (HTS), researchers have utilized their low resistance behavior in many applications. One such application is that of multichip modules (MCMs.) Unlike that of VLSI technologies where smaller feature sizes in successive generations allow interconnect lengths and power dissipation to be reduced, MCMs will not have that same luxury. As the complexity of ICs advances, pinout count per IC increases, and operating frequencies increase, MCM normal metal interconnections will have to grow in length and will not be allowed to reduce in crosssectional area. On MCM-D substrates, typical copper or aluminum interconnection dimensions are about 2 to 5  $\mu m$  in thickness and between 15 and 30  $\mu m$  wide with corresponding via sizes. By cooling the metal to 77 K (liquid nitrogen temperature), the resistivity of copper decreases by a factor of about 7 which allows a corresponding decrease in the interconnect's crosssectional area. In order to increase the wiring density beyond that of cryo-cooled MCMs and improve the chip-to-chip bottleneck at high frequencies, alternatives to conventional metal interconnects must be considered [1].

HTS interconnections, with negligible resistivity at operating frequencies of several tens of GHz and lower, have great potential to reduce an interconnect's cross-sectional area with typical thicknesses of less than 1  $\mu m$  and widths of less than 2  $\mu m$  for MCM applications with similar spacings. The main

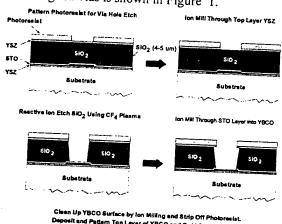
0921-4534/97/\$17.00 © Elsevier Science B.V. All rights reserved. PII S0921-4534(97)00495-4

challenge for attaining multiple layers of high density, high performance HTS interconnects appears to be in fabricating compact, low resistance vias.

The work presented here focuses on this problem and describes a method of fabricating noble metal vias for use in an HTS MCM prototype.

#### 2. EXPERIMENTAL DETAILS AND RESULTS

A cross-section of our multilayer YBCO structure utilizing Au vias is shown in Figure 1.



and Pattern Top Layer of YBCO and Gold Contact Lay

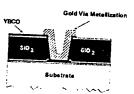


Figure 1. HTS via process.

đ ١ľ

of

le

ιic be oa-

/ou

the na-

1 of . (on arti-

2) to rsion t the

Id be

mpliree of Hisher

fled to

bei tha Ty Ph len the me ten erl M: Αl coj wi. tro Ste Aτ C¢: Ca ph

sha

PA

CU

Re

ถน

the cx

Ш

Ш

an-

Our research has centered around two layers of laser ablated YBa2Cu3O7-x (YBCO) interconnects separated dielectric consisting multilayer SrTiO<sub>3</sub>/SiO<sub>2</sub>/YSZ. We are able to attain critical current densities > 5 x 10<sup>5</sup> A/cm<sup>2</sup> in both YBCO layers. The SrTiO<sub>3</sub> (STO) and YSZ (yttria-stabilized zirconia) layers being ~0.5 μm thick while the SiO<sub>2</sub> ranges between 4 and 5 µm.

The via fabrication process is as shown in Figure 1. The etching involves a 500 eV ion mill through the top YSZ buffer layer, which is followed by a reactive ion etch through the SiO<sub>2</sub> interlevel dielectric selectively stopping at the barrier layer of STO. To complete the etching process, a 500 eV ion mill is done to etch through the STO. The final milling is very nonselective and requires close observation to keep from overetching through the bottom layer of YBCO. When depositing the top layer of YBCO at ~700° C, whatever material is deposited on the via sidewalls is presumably corroded due to interdiffusion of Si from SiO2 into the YBCO but, presumably, does not effect the quality of the via. The subsequent in situ deposition of ~2000 Å of Au by laser ablation creates low resistance contacts without having to do a high temperature anneal in oxygen as was described by Ekin et al. [2]. In similar structures, contact resistivities of less than  $10^{-7} \Omega$ -cm<sup>2</sup> have consistently been attained. An additional 1.5-2.0 µm of Au is deposited over the existing YBCO/Au and then patterned using ion milling and photoresist as a mask.

This type of via structure has several advantages over previously demonstrated superconducting vias for use in HTS MCMs [3,4]. Since HTS thin films need to be deposited on planar surfaces or gradual slopes to maintain a reasonable current density, due to grain boundary problems, they require gradually sloped via holes that take up a wide area. By using a noble metal, compact, high-aspect ratio vias can be fabricated reliably.

Ultrasonic Al wire bonds were then made between YBCO/Au bond pads on the substrate and a wire bondable PC board. Via chain resistance was measured using a conventional 4-point contact configuration and measuring the voltage drop across the vias while passing DC current through it. The resistance vs. temperature of a ~0.5 cm long via chain structure with ten 40 µm square vias interconnecting 50 µm wide YBCO lines is shown in Figure 2. The room temperature resistance was measured to be about 515  $\Omega$ , and upon cooling to 78.5 K, the resistance

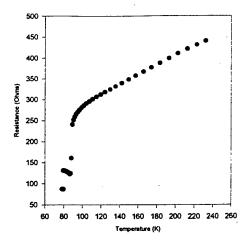


Figure 2. Temperature transition of a chain of ten 40 µm wide vias.

dropped to about 87  $\Omega$ . As is shown in Figure 2, there are two separate superconducting transitions occurring at about 89 K and 80 K which correspond to the top and bottom layer YBCO transitions. At 78.5 K, the interconnects had not yet become fully superconducting.

In summary, 40 µm YBCO/Au via chain structures have been characterized. The preliminary work shown here is to be improved upon by improving the quality of the YBCO layers, lowering the contact resistances, and possibly improving the step coverage of Au through the via by increasing its thickness.

#### **ACKNOWLEDGEMENT**

This work was supported in part by NSF (DMR 9318946), U.S. Army Research Office (DAAH04-96-1-0455), and DARPA (MDA 972-93-I-0036).

#### REFERENCES

- 1. S. K. Tewksbury, L. A. Hornak, L. A. Tewksbury, and L. Chen, Journal of Microelectronic Systems Integration, Vol. 4, No. 2, (1996).
- 2. J. W. Ekin, S. E. Russek, C. C. Clickner, and B. Jeanneret, Appl. Phys. Lett., 62 369 (1993).
- 3. M. J. Burns, K. Char, B. F. Cole, W. S. Ruby, and S. A. Sachtjen, Appl. Phys. Lett., 62 1435 (1993).
- 4. B. Santo, Electronic Engineering Times, August 10 (1992).





Fabrication techniques and electrical properties of YBa<sub>2</sub>Cu<sub>3</sub>O<sub>7-x</sub> multilayers with rf sputtered amorphous SiO<sub>2</sub> interlayers

\*S. Afonso, \*K. Y. Chen, \*Q. Xiong, \*F. T. Chan, \*G. J. Salamo, \*J. W. Cooksey, \*S. Scott, \*S. Ang, \*W. D. Brown, and \*L. W. Schaper.

\*Department of Physics and Department of Electrical Enginneering/High Density Electronics Center, University of Arkansas, Fayetteville, AR 72701, USA

We have successfully fabricated YBa<sub>2</sub>Cu<sub>3</sub>O<sub>7-x</sub>/YSZ/SiO<sub>2</sub>/YSZ/YBa<sub>2</sub>Cu<sub>3</sub>O<sub>7-x</sub> multilayer structures on single crystal LaAlO<sub>3</sub> (100), substrates. The YBa<sub>2</sub>Cu<sub>3</sub>O<sub>7-x</sub>(YBCO) layers were deposited using pulsed laser ablation (PLD), the biaxially aligned YSZ (250 nm thick) layers were deposited using ion beam assisted PLD (IBAD-PLD), and an amorphous SiO<sub>2</sub> (1-2μm) layer fabricated via rf sputtering was sandwiched between the YSZ layers. Fabrication techniques and characterization results are reported for patterned layers in this work.

#### 1. INTRODUCTION

For high temperature superconductor multichip module(HTS-MCM) applications the basic building block is the HTS/Insulator (thickness > 1 \( \mu \) /HTS structure. A HTS-MCM can be defined as a miniaturized version of a multilayered printed wiring board with superconducting interconnects. Previously such a HTS-MCM prototype using a YBCO/SrTiOs(500nm)/YBCO has been successfully fabricated by Burns et al [1]. Recently the use of ion beam assisted deposition to deposit biaxially aligned YSZ buffer layers on polycrystalline amorphous substrates allowed for good quality YBCO films on these substrates [2-5]. Reade et al [6] were able to demonstrate ion beam assisted pulsed the using deposition (IBAD-PLD) technique that it was possible to fabricate the YBCO/YSZ-/amorphousYSZ(5µm)/YSZ/YBCO multilayers on oriented YSZ substrates with the top YBCO Tc ~ 87 K. They also fabricated the same structure using amorphous SiO2, but cracks in the top YBCO layer did not permit electrical measurements of the top layer. The main advantage of SiO2 is its low dielectric constant (~ 3.89), which makes it an ideal insulator material for MCMs.

In this paper we briefly describe the method to fabricate and the results obtained

from the characterization of the YBCO/YSZ-/SiO<sub>2</sub>/YSZ/YBCO multilayers.

#### 2. EXPERIMENTS

The first YBCO layer (300nm thick) was fabricated by pulsed laser deposition using standard conditions. After patterning, part of the pads were masked to allow for transport measurements later. Next a 250 nm thick YSZ layer was deposited via IBAD PLD using conditions described in [5]. After this a 1-2 µm thick SiO2 layer was deposited by reactively sputtering a Si target in oxygen ambient (the details of this process are described in [4]). Following the SiO<sub>2</sub> deposition another 250 nm thick biaxially aligned YSZ buffer/capping layer was deposited via IBAD PLD. Finally the masks were taken off and the top YBCO was deposited using the same conditions as the first YBCO except that the deposition temperature was kept ~ 20-30° lower. For the first set of multilayers the top YBCO layer was patterned into bridges over the underlying bridge patterns but shifted a little to the side so that the top bridge goes over step edges. The patterning was carried out by using photolithography and ion milling. For the second set of multilayers the top YBCO layer was patterned into

so mesentation



bridges whereas the bottom YBCO layer was not patterned. Finally in the third set the top YBCO layer was patterned into serpentine (meander) lines crossing over the patterned bottom YBCO serpentine lines

#### 3. RESULTS

The X-ray diffraction pattern for an unpatterned multilayer in Fig. 1. shows that the films have good c-axis orientation. We also measured the top YBCO  $\phi$  scan full width at half maximum (FWHM) ~ 26° (for the (103) peaks), while for YSZ (111) peaks the FWHM was ~ 2-3° greater than that of the top YBCO.

For the first set, the bottom 40  $\mu m$  wide bridge the  $T_c \sim 90$  K and  $J_c \sim 2\times10^6$  A/cm² whereas for the top YBCO bridge 60  $\mu m$  wide (with step edges), the  $T_c \sim 86\text{-}87$  K and  $J_c \sim 3\times10^4$  A/cm². In the second set, the top YBCO bridge patterns of the same width without step edges the  $J_c \sim 10^5$  A/cm² with  $T_c \sim 87\text{-}88$  K. Finally in Fig. 2(A) is shown the resistance versus temperature plot for 20  $\mu m$  serpentine bottom YBCO line 19 cm long the  $T_c \sim 87$  K and  $J_c \sim 2\times10^5$  A/cm², whereas the same width serpentine line on the top layer showed semiconducting behavior as seen in Fig.2(B).

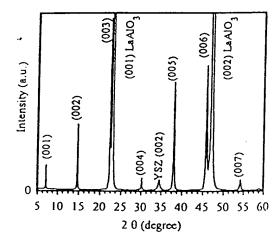


Fig. 1. X-ray diffraction pattern for a multilayer YBCO/YSZ/SiO<sub>2</sub>/YSZ/YBCO sample

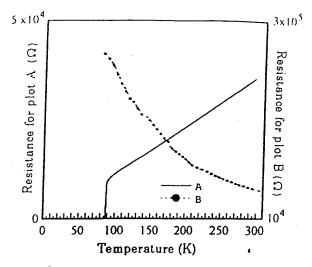


Fig. 2 Resistance versus temperature curves for (A) 20 µm wide bottom YBCO serpentine line.

#### (B) 20 $\mu m$ wide top YBCO serpentine line

#### 4. CONCLUSIONS

Good quality YBCO layers separated by an amorphous SiO<sub>2</sub> interlayer have been fabricated by using biaxially aligned YSZ layers. However if the bottom YBCO is densely patterned then planarization is necessary to prevent degradation of superconducting properties at the step edges.

#### ACKNOWLEDGEMENT

This work was supported in part by NSF (DMR 9318946), U.S. Army Research Office (DAAH04-96-1-0455), and DARPA (MDA 972-93-1-0036).

#### REFERENCES

- M. J. Burns et al., Appl. Phys. Lett. 62,(1993) 1435
- 2. Y. lijima et al., J. Appl. Phys. 74 (1993) 1905
- 3. X. Wu et al., Appl. Phys. Lett. 65.(1994) D1961
- R. G. Florence et al., Supercond. Sci. Technol 8, (1995) 546.
- 5. K.Y. Chen et al., Physica C 267 (1996) 355.
- R. P. Reade, et al., Appl. Phys. Lett. 66, (1995) 2001.



## Y<sub>1</sub>Ba<sub>2</sub>Cu<sub>3</sub>O<sub>7-x</sub> multilayer structures with a thick SiO<sub>2</sub> interlayer for multichip modules

S. Afonso, K. Y. Chen, Q. Xiong, Y. Q. Tang, G. J. Salamo, and F. T. Chan Department of Physics/HiDEC, University of Arkansas, Fayetteville, Arkansas 72701

J. Cooksey, S. Scott, Y. J. Shi, S. Ang, W. D. Brown, and L. W. Schaper Department of Electrical Engineering/HiDEC, University of Arkansas, Fayetteville, Arkansas 72701

(Received 14 April 1997; accepted 17 July 1997)

For high temperature superconducting multichip modules and other related electronic applications, it is necessary to be able to fabricate several Y<sub>1</sub>Ba<sub>2</sub>Cu<sub>3</sub>O<sub>7-r</sub> (YBCO) layers separated by thick low dielectric constant dielectric layers. In this work, we report the successful fabrication of YBCO/YSZ/SiO<sub>2</sub> (1-2 μm)/YSZ/YBCO multilayer structures on single crystal yttria stabilized zirconia (YSZ) substrates. In contrast to previously reported work, the top YBCO layer did not show any cracking. This is due to a technique that allows for stress relief in the SiO<sub>2</sub> layer before the second YBCO layer is deposited. The top YBCO layer in our multilayer structure had  $T_c = 87 \text{ K}$  and  $J_c = 10^5 \text{ A/cm}^2$ (at 77 K), whereas the bottom YBCO layer had  $T_c = 90$  K and  $J_c = 1.2 \times 10^6 \text{ A/cm}^2$  (at 77 K). We also showed that the quality of the bottom YBCO layer was preserved during the fabrication of the multilayer due to the annealing process during which O2 diffused into the YBCO, replacing the O<sub>2</sub> lost during the deposition of the top YBCO layer.

#### I. INTRODUCTION

In high temperature superconducting (HTS) multichip modules (MCM's) the basic building block is a multilayer structure consisting of several superconductive layers separated by thick dielectric layers. The HTSC layers are patterned into interconnects for electrically connecting the different chips on a layer, and vias are used for interconnecting the various YBCO layers. In order to keep the distributed capacitance low, 1 the thickness of the interlevel dielectric layer should be of the order of the HTSC interconnect line width and have a low dielectric constant (ideally <5). Such a multilayer structure would have a power plane, a ground plane, and two or more wiring layers. However, by using the Interconnected Mesh Power System (IMPS) topology,<sup>2</sup> a superconducting MCM (IMPS-MCM) can be realized using only two layers of superconducting interconnects. Switching from a four-layered structure to one with only two layers greatly reduces the technological difficulties as well as cost. Previously reported work on multilayer structures used sputtering or pulsed laser deposition (PLD) at high temperatures (700-800 °C) in order to achieve epitaxial growth of the dielectric layer.<sup>3-7</sup> The main drawback with this process is the loss of O<sub>2</sub> from the underlying Y<sub>1</sub>Ba<sub>2</sub>Cu<sub>3</sub>O<sub>7-r</sub> (YBCO) layer due to the long deposition time required in the case of thick dielectric layers. The loss of oxygen in the underlying YBC layer results in severe degradation of its superconducting properties.

Previously YSZ has been successfully used as an epitaxial buffer layer for depositing high quality YBCO films on technologically important substrates, such as SOS (Silicon on Sapphire) and Si.8.9 In recent years the other major use of YSZ has been in the deposition of biaxially aligned YSZ buffer layers on amorphous or polycrystalline substrates, such as pyrex, Haynes alloy, and nickel. 10-15 The biaxially aligned YSZ layers are deposited at room temperature using the ion beam assisted deposition (IBAD) method.<sup>12</sup> These results therefore indicate that IBAD YSZ could be used for fabricating multilayers with amorphous isolation layer materials that have lower dielectric constants suitable for MCM applications. For example, YBCO/YSZ/SiO<sub>2</sub>/ YSZ/YBCO/YSZ (substrate) multilayer structures fabricated using the plasma enhanced chemical vapor deposition (PECVD) method for depositing the amorphous SiO2 layer, and ion-beam assisted PLD for the biaxially aligned YSZ dielectric layers on single crystal YSZ substrates have previously been reported. 16 SiO2 was chosen as the insulating layer because of its low dielectric constant ( $\epsilon \sim 3.8$ ). Unfortunately, cracks in the top YBCO layer did not allow for transport measurements and prevented applications of the multilayered structure, as reported in Ref. 16. In this paper, we describe a technique to produce two high quality YBCO layers and present results of transport  $T_c$  and  $J_c$  measurements for both YBCO layers in a YBCO/YSZ/SiO<sub>2</sub>/YSZ/YBCO/YSZ (substrate) multilayer structure which make the possibility of a HTS-MCM a realizable goal.

#### II. EXPERIMENTAL

In our experiments the first 2500 Å thick YBCO layer was deposited on a  $0.5'' \times 0.5''$  YSZ single crystal substrate using an ArF excimer laser (wavelength = 193 nm, frequency = 5 Hz). The beam was focused to an energy density of  $\sim 3-4$  J/cm<sup>2</sup>. Substrate temperature of 750 °C and an O<sub>2</sub> pressure of 200 mTorr were maintained in the deposition chamber. We used three YBCO targets mounted on a carousel. The targets were exposed alternately for 2 min, and the deposition rate was  $\sim 150$  Å/min. We have found that this technique results in higher yield of good quality YBCO films as compared to the yield of good quality films using a single YBCO target. After deposition the chamber was backfilled with 500 Torr of O2, and bottom YBCO film was cooled to room temperature in about 70 min. After this the YBCO film was polished in a slurry of isopropanol and CeO<sub>2</sub> polishing powder. This is an important step that reduces the average surface roughness of the YBCO film (from 16 nm to 3 nm) and the number of boulders on the surface. 17,18 A bridge (40  $\mu$ m wide) was patterned using photolithography and ion milling. Part of the pads to the bridge were masked during the deposition of the next insulating layer so as to allow for transport measurements at the end of the multilayer fabrication.

The second layer of 2500 Å thick YSZ was then deposited using ion-beam assisted PLD. <sup>16</sup> This layer serves as a capping layer to prevent diffusion of the (to be deposited) amorphous SiO<sub>2</sub> layer (3rd layer) into the YBCO layer. Diffusion of SiO<sub>2</sub> into the YBCO layer has been observed to have an adverse effect on the YBCO film properties. <sup>19-23</sup> We used a biaxially aligned YSZ layer because some samples fabricated with an amorphous YSZ layer resulted in poor quality bottom YBCO layers. This could be due to the less dense structure of amorphous YSZ, allowing for diffusion of SiO<sub>2</sub> through the YSZ capping layer and into the underlying YBCO layer.

The samples were then transferred to a PECVD system for deposition of a  $1-2 \mu m$  thick  $SiO_2$  layer. Our first attempts at depositing PECVD  $SiO_2$  at 250 °C and an rf power of 55 W resulted in cracking of the multilayers during the deposition of the top YBCO layer, as reported by Reade *et al.*<sup>16</sup> In order to determine at which step in the process of making the multilayered

structure cracking occurs, we stopped before adding the SiO<sub>2</sub> layer. Next the YSZ/YBCO/YSZ (substrate) structures were heated to 450 °C for 10 min in 500 Torr of O<sub>2</sub>. Parts of these test samples were heated to 450 °C in vacuum. Most of the samples did not crack except for very few cases where cracks would appear in the YSZ layer, especially if prior to YSZ deposition the patterned YBCO samples were left exposed to ambient conditions (relative humidity ~50%) for long periods of time.

Next, to determine whether cracking was due to stress in the PECVD deposited SiO<sub>2</sub>, we heated SiO<sub>2</sub>/ YSZ/YBCO/YSZ (substrate) structure in vacuum soon after depositing the PECVD SiO2. Here we found that small islands of all three layers begin to peel off the substrate at about 300 °C, thus suggesting that the stress which leads to cracking originates from the SiO<sub>2</sub> film. In order to overcome the cracking problem in the case of PECVD deposited SiO2, we followed procedures based on earlier work done on PECVD and CVD SiO2 layers deposited on silicon substrates.<sup>24-30</sup> Evidence offered in previous work indicates that PECVD SiO, is in tensile stress before annealing. Annealing the SiO<sub>2</sub> in a N<sub>2</sub> ambient at high temperatures (>700 °C) reduced the water and silanol content, increased the density, and decreased the tensile stress. Instead of annealing in a N<sub>2</sub> ambient, we observed that if the SiO<sub>2</sub> layers were heated (ramp up ~10 °C/min) in 500 Torr of O<sub>2</sub> and annealed for ~8 min at 650 °C, no cracks were present during the later stages in the multilayer fabrication. This success is likely to be due to the reduced tensile stress in the SiO<sub>2</sub> after annealing. As a result after annealing, heating of the SiO<sub>2</sub> layer during the deposition of the top YBCO will no longer increase the tensile stress beyond the cracking point. The above annealing step allowed for successful fabrication of the entire multilayer. Samples annealed at temperatures below 650 °C still exhibited cracks as before.

After annealing, the SiO<sub>2</sub> layer was again capped with a 2500 A thick biaxially aligned YSZ layer (4th layer), which also serves as an epitaxial template for the topmost YBCO layer. Finally, the 2000-2500 Å thick top YBCO layer (5th layer) was deposited under the same conditions as the first YBCO layer except that after pumping the chamber down to a base pressure of  $5 \times 10^{-5}$  Torr, it was immediately back-filled with 500 Torr of O<sub>2</sub>, and then the substrate was heated to ~630 °C. As soon as the substrate temperature reached 630 °C the chamber was again pumped down to 200 mTorr for the YBCO deposition at 720 °C. This approach minimizes the degradation of the bottom YBCO layer. This is indicated by the fact that in the case of samples where the top YBCO layer was fabricated under the same conditions as that of the bottom layer, we observed a degradation in both the  $T_c$  values and  $J_c$ values of the bottom YBCO layer.

#### III. RESULTS AND DISCUSSION

The orientation of the YSZ and YBCO layers was characterized by x-ray diffraction. The x-ray diffraction pattern for the multilayer structure shown in Fig. 1 indicates good c-axis orientation. The  $\phi$  scan widths (FWHM) for the top layer YBCO (103) were  $26^{\circ}-28^{\circ}$ . For both the top and bottom 2500 Å thick IBAD-YSZ layer the  $\phi$  scan widths (FWHM) obtained is  $\sim$ 32°. The in-plane alignment achieved using IBAD is independent of the template used. Better in-plane alignment of the top IBAD YSZ layer can be achieved by increasing its thickness. For example, a 5000 Å thick YSZ layer has a  $\phi$  scan width of 24°, as reported in Ref. 31.

A schematic of the patterned layers used for the transport measurements is shown in Fig. 2. The bottom layer consists of a 40  $\mu$ m wide bridge [Fig. 2(a)], as well as an unpatterned part of the bottom layer [Fig. 2(b)] to provide a comparison between the  $T_c$  and  $J_c$  values of the top layer bridges with and without step edges [Figs. 2(c) and 2(d), respectively]. All the transport measurements were obtained using the four-probe method.

Figure 3 A shows the resistance versus temperature curve for the 40  $\mu$ m wide bottom YBCO bridge. Its  $T_c$  was 90 K and its  $J_c = 1.2 \times 10^6$  A/cm². The top layer 60  $\mu$ m wide bridge with step edges had  $T_c = 87$  K (Fig. 3 B) and  $J_c = 4.5 \times 10^4$  A/cm². The 30  $\mu$ m bridge without step edges had the same  $T_c$  value (Fig. 3 C), but its  $J_c$  was  $1 \times 10^5$  A/cm². The reduced critical current for the 60  $\mu$ m bridge with step edges could be attributed to disruption of epitaxial growth at the step edges and large-angle grain boundaries. No shorts were detected between the top and bottom YBCO layers from electrical resistance measurements. In addition, our experiments on YBCO/YSZ/SiO<sub>2</sub>/YSZ/YBCO/YSZ (substrate) multilayered structure have consistently shown that the magnetic field dependence of

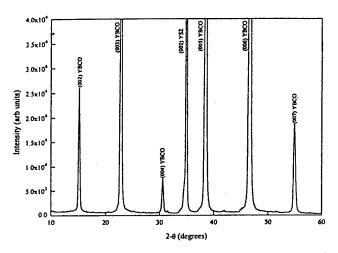


FIG. 1.  $\theta$ -2 $\theta$  x-ray diffractometer pattern for the YBCO/YSZ/SiO<sub>2</sub>/YSZ/YBCO structure on (001)YSZ.

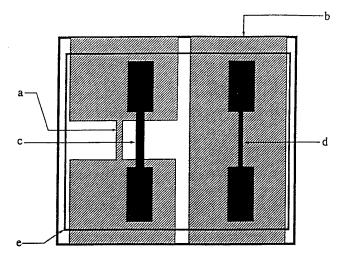


FIG. 2. Schematic of the patterned multilayer structure. (a) 40  $\mu$ m wide bridge in the bottom YBCO layer. (b) Unpatterned bottom YBCO layer. (c) 60  $\mu$ m wide bridge with step edges on the top YBCO layer. (d) 30  $\mu$ m wide bridge without step edges on the top YBCO layer. (e) YSZ/SiO<sub>2</sub>/YSZ insulator layers.

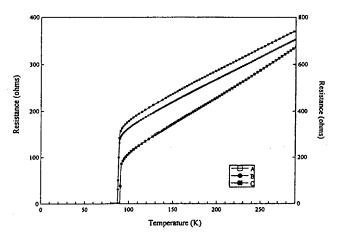


FIG. 3. Resistance versus temperature for the (A) 40  $\mu$ m wide bridge in the bottom YBCO layer. (B) 60  $\mu$ m wide bridge in the top YBCO layer with step edges. (C) 30  $\mu$ m wide bridge in the top YBCO without step edges. Left y-axis used for plots A and C and right y-axis for plot B.

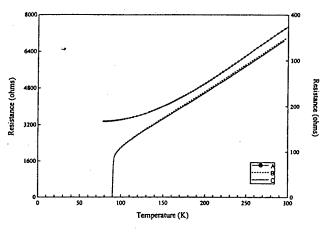
 $J_c$  is not appreciably altered over that of a single layer YBCO film. For example, we have found that for the multilayered structures, the  $J_c$  of the top layer was  $1 \times 10^4$  A/cm<sup>2</sup>, measured using the magnetization method at 77 K in a field of 1 T (magnetic field applied parallel to the c-axis). This number is consistent with what others have reported for a single layer on a polycrystalline substrate with an IBAD YSZ buffer layer.<sup>12</sup> For the bottom layer the  $J_c$  was  $5 \times 10^4$  A/cm<sup>2</sup> at 77 K in a field of 1 T (magnetic field applied parallel to the c-axis).

Studies carried out on YBCO/epitaxial insulator bilayers<sup>3</sup> showed a significant decrease in the O<sub>2</sub> diffusion rate due to the presence of the epitaxial insulating layer.

In order to investigate the effect of YSZ/SiO<sub>2</sub>/YSZ layers and the effect of the top YBCO layer deposition on the underlying YBCO layer, we patterned a 40  $\mu$ m wide bridge on the bottom YBCO. Next, we deposited the YSZ/SiO<sub>2</sub>/YSZ layers; measurements performed after this step were  $T_c \sim 90$  K (Fig. 4 C) and  $J_c \sim 1.0 \times$ 106 A/cm<sup>2</sup>. Thereafter we simulated the top YBCO layer deposition, except that no top layer was deposited and the YSZ/SiO<sub>2</sub>/YSZ/YBCO structure was cooled down immediately (~15 min) in 200 mTorr of O<sub>2</sub>. The resistance versus temperature curve (Fig. 4 A) shows a twentyfold increase in the bridge resistance at room temperature and the bridge is no longer superconducting. After these measurements the structure was annealed at 450 °C in 500 Torr of  $O_2$  for 30 min. The results of  $T_c$ (Fig. 4 B) and  $J_c$  measurements showed no appreciable change as compared to the original values, indicating that the superconducting properties were entirely recovered. Thus we have demonstrated that during the top YBCO layer deposition, O2 diffuses out of the underlying YBCO layer resulting in a tetragonal YBCO, while annealing in 500 Torr of O2 results in rediffusion of O2 which returns it back to the orthorhombic structure. The above results indicate that O<sub>2</sub> readily diffuses through the thick YSZ/SiO<sub>2</sub>/YSZ interlevel dielectric. Efforts are currently underway to estimate the diffusion constant for O<sub>2</sub> through the YSZ/SiO<sub>2</sub>/YSZ structure.

#### IV. CONCLUSION

We have reported on an investigation of the development of a structure that has potential to lead to a HTS MCM. Our results demonstrate that stress relief in PECVD deposited SiO<sub>2</sub> via an annealing process can avoid cracking in this multilayer structure. We have also demonstrated that YSZ/SiO<sub>2</sub>/YSZ multilayer structure



• FIG. 4. Resistance versus temperature for the 40  $\mu$ m wide bridge in the bottom YBCO. (A) After simulation of top YBCO deposition. (B) After annealing at 450 °C in 500 Torr of O<sub>2</sub> for 30 min. Left y-axis used for plot A and right y-axis used for plots B and C. (C) Before simulation of top YBCO deposition.

is a good  $O_2$  diffuser. Although the total thickness of the YSZ/SiO<sub>2</sub>/YSZ multilayer structure is ~2-3  $\mu$ m, a sufficient amount of  $O_2$  can still diffuse into the bottom YBCO layer in a relatively short time. By achieving better in-plane alignment for the IBAD YSZ layer, the top layer  $J_c$  can be further improved. Also, lower  $J_c$  values obtained in the case of a top layer bridge with step edges clearly indicates the need for planarization. We are currently working on improving the top YBCO layer  $J_c$  and are developing a planarization process.

#### **ACKNOWLEDGMENTS**

The authors would like to thank J. Schultz for assistance with x-ray diffraction measurements and Y. Nishath and E. Porter for assistance with the PECVD depositions. This work was supported in part by NSF DMR 9318946, DARPA (Contract No. MDA 972-93-I-0036) through High Density Electronics Center at the University of Arkansas, and U.S. Army Research Office DAAH04-96-1-0455.

#### REFERENCES

- M. J. Burns, K. Char, B. F. Cole, W. S. Ruby, and S. A. Satchen, Appl. Phys. Lett. 62, 1435 (1993).
- L. W. Schaper, S. S. Ang, Y. L. Low, and D. Oldham, IEEE Trans. Components, Hybrids, Manufacturing Technol. 18, 99 (1995).
- J. Talvacchio, M. G. Forrester, and J. R. Gavalier, "Properties of passive structures for multilayer HTS digital circuits," IEEE Trans. Appl. Supercond. (1995).
- E. Olsson, G. Brorsson, P. A. Nilsson, and T. Claeson, Appl. Phys. Lett. 63, 1567 (1993).
- G. L. Waytena, H. A. Hoff, R. R. Wolcott, Jr., P. R. Broussard, C. L. Vold, and C. Lee, J. Electron. Mater. 3, 24, 189 (1995).
- A. Findikoglu, C. Doughty, S. Bhattacharya, Q. Li, X. X., T. Venkatesan, R. E. Fahey, A. J. Strauss, and J. M. Phillips, Appl. Phys. Lett. 61, 1718 (1995).
- J. J. Kingston, F. C. Wellstood, P. Lerch, A. H. Miklich, and J. Clarke, Appl. Phys. Lett. 56, 189 (1990).
- D. K. Fork, F. A. Ponce, J. Tramontana, N. Newman, J. M. Phillips, and T. H. Geballe, Appl. Phys. Lett. 58, 2432 (1991).
- D. K. Fork, D. B. Fenner, R. W. Barton, J. M. Phillips, G. A. N. Connel, J. B. Boyce, and T. H. Geballe, Appl. Phys. Lett. 57, 1161 (1990).
- K. Y. Chen, G. J. Salamo, S. Afonso, X. L. Xu, Y. Q. Tang, Q. Xiong, F. T. Chan, and L. W. Schaper, Physica C 267, 355 (1996).
- R.G. Florence, S.S. Ang, and W.D. Brown, Supercond. Sci. Technol. 8, 546 (1995).
- Y. Ijima, N. Tanabe, O. Kohno, and Y. Ikeno, Appl. Phys. Lett. 60, 769 (1992).
- R. P. Reade, P. Beardahl, R. E. Russo, and S. M. Garrison, Appl. Phys. Lett. 61, 2231 (1992).
- X. D. Wu, S. R. Foltyn, P. Arendt, J. Townsend, C. Adams, I. H. Campbell, P. Tiwari, Y. Coulter, and D. E. Peterson, Appl. Phys. Lett. 65, 1961 (1994).
- R. G. Florence, S. S. Ang, and W. D. Brown, Proc. Low Temperature Electronics and High Temperature Superconductivity, Vol. 95-9. Electrochemical Society, 113 (1995).
- R. P. Reade, P. Beardahl, R. E. Russo, and L. W. Schaper, Appl. Phys. Lett. 66, 2001 (1995).

- 17. J.M. Phillips, J. Appl. Phys. 79 (4), 1829 (1996).
- S. Afonso, Ph.D. Thesis, Department of Physics, University of Arkansas, Fayetteville, AR, Chap. IV (1997).
- D. B. Fenner, A. M. Viano, D. K. Fork, G. A. N. Connel, J. B. Boyce, F. A. Ponce, and J. C. Tramontana, J. Appl. Phys. 69, 2176 (1991).
- S. Chromik, J. Sith, V. Strbik, J. Schilder, V. Smatko, S. Benacka, V. Kliment, and J. Levarsky, J. Appl. Phys. 66, 1477 (1988).
- Y. K. Fang, K. H. Chen, S. B. Hwang, S. J. Wu, C. R. Liu, W. T. Lin, and J. R. Chen, Thin Solid Films 208, 228 (1992).
- T. Komatsu. O. Tanaka, K. Matusita, M. Takata, and T. Yamashita, Jpn. J. Appl. Phys. 27, L1025 (1988).
- G. Florence. Ph.D. Thesis, Department of Electrical Engineering, University of Arkansas, Fayetteville, AR, Chap. 5, pp. 155-156, May 1995.

- 24. H.M. Dauplaise, K. Vacarro, B.R. Bennett, and J.P. Lorenzo, J. Electrochem. Soc. 139, 1684 (1992).
- A. K. Sinha, H. J. Levenstein, and T. E. Smith, J. Appl. Phys. 49, 2423 (1978).
- 26. I. Blech and U. Cohen, J. Appl. Phys. 53, 4202 (1982).
- 27. C. Blaauw, J. Appl. Phys. 54, 5064 (1983).
- 28. M. S. Haque, H. A. Naseem, and W. D. Brown, IEEE International Reliability Physics Proceedings, May 1996, p. 274.
- M. S. Haque, H. A. Naseem, and W. D. Brown, J. Electrochem. Soc. 142, 3864 (1995).
- 30. H. Sunami, Y. Itoh, and K. Sato, J. Appl. Phys. 41, 5115 (1970).
- 31. K. Y. Chen, S. Afonso, Q. Xiong, G. J. Salamo, and F. T. Chan, Physica C (in press).
- F. C. Wellstood, J. J. Kingston, and J. Clarke, J. Appl. Phys. 75, 683 (1994).

# Presentation

# A Comparison of High-Temperature Superconductors in Multi-Chip Module Applications

D.E. Ford, S.S. Scott, S.S. Ang and W.D. Brown High-Density Electronics Center (HiDEC) Department of Electrical Engineering University of Arkansas Fayetteville, AR 72701

### Abstract

In the application of high-temperature superconductors (HTSCs) in multi-chip module (MCM) technology, it is first necessary to investigate the advantages and disadvantages of the various HTSC compounds. The standard criteria for comparing the suitability of HTSCs in electronics applications has been critical temperature ( $T_c$ ) and critical current density ( $J_c$ ). It is also necessary to consider the physical properties of HTSCs in relation to the various processing techniques required in fabrication of MCMs. These techniques can be grouped into four main areas: deposition, patterning, packaging, and characterization. The four main HTSC materials, Y-Ba-Cu-O, Bi-Sr-Ca-Cu-O, Tl,Ba-Ca-Cu-O and Hg-Ba-Ca-Cu-O, will be compared to determine which is most suitable for MCM application.

### Introduction

In the decades since the popular advent of the transistor in the 1960s, there has been continual and steady improvement in both the performance and cost of electronics equipment through miniaturization. This effort has given us the multi-chip module (MCM) as the latest and most promising technique to be introduced. MCM technology improves the speed at which devices can operate and decreases the power lost by eliminating as much length as possible from the interconnection between the individual devices. With this new technology some new barriers to increased speed and performance have arisen. By concentrating all of the devices in one area, the problems due to Joulean heating (I2R losses) and electromigration are increased. Also, the lack of recent improvements may indicate that the upper limit of the speeds that can be expected from current semiconductor devices using conventional interconnects have been reached.

All of these problems can be addressed by combining high-temperature superconductors (HTSCs) with MCMs. Some of the interconnecting lines may typically carry 50-100 mA of current. Therefore, they account for a major portion of the heat generated (Burns et al., 1993). Replacing the lines with zero resistance HTSCs eliminates these I<sup>2</sup>R losses. This means less heat and less power consumed. The refrigeration required for HTSC operation further limits the overall heat production to less than that produced by the individual devices. All of this allows for an even greater decrease in the interconnection lengths which, in turn, maximizes the operating speed of the MCM.

HTSC devices have been shown to be more than 2.5

times faster than their semiconductor counterparts, use three orders of magnitude less power, and do not suffer from electromigration problems (Van Duzer and Tuner, 1981). Their use in MCMs should produce the next quantum jump in performance. A cross-sectional schematic of an MCM is shown in Figure 1.

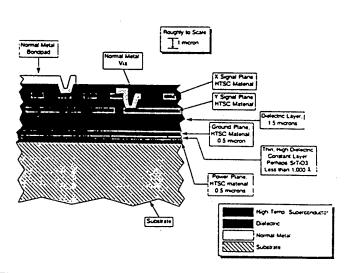


Fig. 1. Cross-sectional Schematic of a Superconducting Multi-Chip Module.

But, which HTSC offers the best overall prospects for MCM applications? This is the first question to be answered in the search for a viable superconducting MCM. When comparing HTSCs, the standard for suitability in electronics applications has been the materials critical temperature,  $(T_c)$ , and critical current density,  $(J_c)$ . It is

78th ANNUAL MEETING of the ARKANSAS ACADEMY of SCIENCE DONESBORD, AZ
APRIL-8-9,1994

### Gamma-ray and Fast Neutron Radiation Effects on Thin Film Superconductors\*

J. W. Cooksey, W. D. Brown, S. S. Ang, H. A. Naseem, and R. K. Ulrich High Density Electronics Center (HiDEC) University of Arkansas, Fayetteville, AR 72701

and

L. West

Department of Mechanical Engineering University of Arkansas, Fayetteville, AR 72701

Abstract

II. EXPERIMENTAL PROCEDURES

The gamma-ray and neutron radiation hardness of YBa<sub>2</sub>Cu<sub>3</sub>O<sub>7-x</sub>, Tl<sub>2</sub>Ba<sub>2</sub>CaCu<sub>2</sub>O<sub>8+x</sub>, and Tl<sub>2</sub>Ba<sub>2</sub>Ca<sub>2</sub>Cu<sub>3</sub>O<sub>10+x</sub> superconducting thin films deposited by off-axis sputtering and laser-ablation deposition techniques on substrates of MgO and LaAlO<sub>3</sub> was investigated. The unbiased samples were irradiated with 662 keV gamma-rays up to a cumulative dose of 1.5 Mrad(Si) and with neutron fluences up to 1 x 10<sup>14</sup> neutrons/cm<sup>2</sup>.

It was determined through nondestructive critical temperature transition,  $T_{\rm c}$ , and critical current density,  $J_{\rm c}$ , measurements and x-ray diffraction analysis that the thin film superconductors were radiation hard up to moderate levels of neutrons and gamma-rays. It was also determined that extended exposure to moderately humid air degraded the critical current density of all the films.

### I. INTRODUCTION

Space applications of multichip modules (MCMs) appear to be part of the driving force for their development. In the future, thin film superconductors (TFSCs) will potentially be used as interconnects for MCMs. As a result of this application of TFSCs, their response to a radiation environment is of great interest. In the past, studies of radiation effects on superconductor materials have been restricted to the bulk form [1-5], but if superconducting interconnects are to be used in future MCMs, the impact of exposure to gamma-rays and fast neutrons on the properties of TFSC materials must be examined. In addition to the effects of radiation on the superconductor material, the substrate material on which the superconductor is deposited, as well as the dielectric material used to separate the multiple levels of interconnects, must also be examined for sensitivity to radiation exposure.

\*We would like to acknowledge the assistance of Tim Welty of the Southwest Radiation Calibration Center in the radiation experiments. We would also like to acknowledge Conductus, Inc. and Superconductor Technologies Inc. for their donation of superconductor samples. This research was funded by E-Systems, Inc. and the Advanced Research Projects Agency.

In the work reported here, YBa<sub>2</sub>Cu<sub>3</sub>O<sub>7-x</sub> (YBCO), Tl<sub>2</sub>Ba<sub>2</sub>Ca<sub>2</sub>Cu<sub>2</sub>O<sub>8+x</sub> (Tl-2212), and Tl<sub>2</sub>Ba<sub>2</sub>Ca<sub>2</sub>Cu<sub>3</sub>O<sub>10+x</sub> (Tl-2223) thin films on substrates of MgO and LaAlO<sub>3</sub>, some of the more common superconductor/substrate combinations, were subjected to both gamma-ray and neutron radiation in an electrically unbiased state. Although radiation without bias does not fully explore the impact on dielectric substrates, it does examine the impact on high temperature superconductors. The samples were deposited using laserablation and off-axis sputtering techniques, and were of varying quality and thickness in order to determine if their radiation hardness varied accordingly. The thin film thicknesses ranged from about 200 to 1000 nm.

The superconductors were characterized by their critical temperature transition, T, and critical current density, J, measured using a nondestructive inductance method as described by Claassen et al. [6]. This measurement technique involves placing a thin, multiturn copper coil next to the film surface and driving the coil with a low distortion audiofrequency sine-wave current. In turn, the driving current induces shielding currents in the film. The nonlinearity in the coil-film system increases abruptly when the induced current in the film reaches its critical level. A schematic of the measurement system used is shown in Figure 1. The resulting voltage across the coil is filtered by a passive twintee notch filter with a center frequency the same as the drive current frequency, 1 kHz, and analyzed by the lock-in amplifier for third harmonics. Either a single or double coil can be used. A single coil acts as "both the drive and pickup coil." We have used a single coil setup in our measurements since it functions as well as a two coil setup according to Claassen et al. The samples were measured down to liquid nitrogen temperature (77 K). This type of measurement was chosen over the four point contact method because the samples had to be measured after each irradiation. Any probe technique would destroy a large surface area of the film after each subsequent measurement since we were dealing with samples less than 1 cm<sup>2</sup>. A Philips x-ray diffractometer was also used in an attempt to detect any atomic disorder in the superconductor films resulting from neutron bombardment.

The superconductor/substrate structures were irradiated with gamma-rays up to a cumulative dose of 1.5 Mrad(Si)



31ST ANNUAL INTOENTATIONAL NUCLEAR AND SPACE RADIATION EXFECTS CONFERENCE

TUCSON, AZ

JULY 18-22, 1994

Presentation: Poster

1875 Meeting of the ELECNOCHEMICAL. SUCLETY

### The Electrochemical Society, Inc.

# **ABSTRACT FORM**

Reno, Nevada, May 21-26, 1995

ENTERED 152

Submit to: The Electrochemical Society  Abstract No
10 South Main Street, Pennington, NJ 08534-2896 (To be assigned by the Society)
With a copy to the Symposium Organizer(s)—by December 1, 1994
Title of Symposium: General Society Student Poster Session
Sponsoring Division(s)/Group(s) All Divisions and Groups
Title of Paper: Development of vias for use in high temperature
superconductor multichip modules
Author(s) with complete mailing address(es) - (List presenting author first and include contact author's Telephone and Fax numbers).
1 <u>Mr. J. W. Cooksey, University of Arkansas, BELL 3217, Fayettevi</u> lle <u>AR 72701</u> Phone: (501)575-3005 Fax: (501)575-7967
2 Dr. W. D. Brown, University of Arkansas, BELL 3217, Fayetteville, AR 72701
3 Dr. L. W. Schaper, University of Arkansas, Engineering Research Center, rm. 373, Fayetteville, AR 72701
4 Dr. S. S. Ang, University of Arkansas, BELL 3217, Fayetteville, AR 72701
5 Dr. R. K. Ulrich, University of Arkansas, BELL 3202, Fayetteville, AR 72701
Type abstract in area below - double spaced. If more space is needed, use an additional sheet of paper.
In the development of high speed multichip modules, high
temperature superconducting interconnects are viewed as a viable
alternative to copper interconnects to improve the overall speed
of the module. Vias that provide low contact resistivity
connections to the superconducting layers while maintaining space
efficiency and fabrication compatibility are necessary for eff-
icient utilization of the superconductors. Our research involves
the fabrication and characterization of noble metal (primarily
Au and Ag) vias to connect multiple layers of YBCO interconnects.
Do you plan to present more than one paper at this Meeting?
Do you require any audio-risual equipment?  3Smm (2x2") slide projector  Overhead projector  Please indicate other equipment at author's expense and subject to availability  Check here if you are interested in becoming a member of The Electrochemical Society, Inc. A membership brochure containing an Application for Membership will be sent to author(s) #

Presentation: paper



Ion Beam Assisted Sputter Deposition of CeO<sub>2</sub> Buffer Layers for Superconducting Multichip Module (MCM) Applications

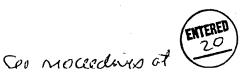
Glenn Florence, Simon Ang, and W. D. Brown High Density Electronics Center (HiDEC) and Department of Electrical Engineering, University of Arkansas 3217 Bell Engineering Center, Fayetteville, AR 72701

Cerium dioxide (CeO<sub>2</sub>) buffer layers have been sputter deposited onto various substrates including silicon and nickel alloy using ion beam assisted deposition (IBAD). This technique has resulted in the formation of CeO<sub>2</sub> which exhibits strong (100) phase growth as well as in-plane orientation as evidenced by X-ray diffraction. Subsequent YBCO depositions on these films exhibit T<sub>c</sub>'s of 86 K and biaxial texture with the c-axis normal to the surface. With further refinement, this technique may be used to fabricate the multilayer structure needed for superconducting multichip modules.

### INTRODUCTION

There is widespread interest in the use of superconducting interconnects in electronics, especially in multichip modules (MCMs). Superconductor interconnects have advantages of low signal loss and very low RC propagation delays. Furthermore, due to the reduction in interconnect resistance, the linewidths can be made much smaller. allowing for a reduction in the number of signal layers. One proposed structure for the superconducting MCM is the interconnected mesh power system (IMPS), which requires only two interconnect layers, thereby reducing the complexity of the manufacturing process (1). In order to achieve satisfactory electrical performance and reduce parasitic capacitances, these interconnects need to be separated by a thick (~2-5 µm) insulating layer with a low dielectric constant. Possible substrate and dielectric materials for these applications include silicon, silicon dioxide, or other polycrystalline materials. However, it has been shown that YBCO deposited directly onto these materials reacts with them and degrades the YBCO superconducting properties. The use of buffer layers such as cerium dioxide (CeO<sub>2</sub>) or yttria-stabilized zirconia (YSZ) can mitigate these problems, but they have high dielectric constants and need to exhibit a high degree of biaxial texture to reduce high-angle grain boundaries and improve the critical current density, Jc, of the YBCO layer.

One possible interconnect structure that has been proposed by researchers at the High Density Electronics Center (HiDEC) consists of two YBCO layers separated by a thick layer of SiO<sub>2</sub>, which exhibits a low dielectric constant. To prevent interdiffusion and provide for an epitaxial surface on which high quality YBCO can be deposited, the SiO<sub>2</sub> is



separated from the YBCO by a thin buffer layer of either cerium dioxide or yttriastabilized zirconia. Clearly, the ability to deposit aligned buffer layers on polycrystalline or amorphous substrates would greatly improve the manufacturability of superconducting MCMs.

Ion beams have been used previously to deposit aligned buffer layers for YBCO on polycrystalline substrates. Iijima et al. (2) reported a dual-ion beam process for depositing YSZ on Hastelloy C276, a nickel-based alloy. The ion beam position with respect to the substrate normal was varied from 30° to 60°, with bi-axially oriented films obtained at an angle of 45°. Reade et al. (3) also reported biaxial deposition of YSZ on nickel alloys when using ion beam assisted deposition in conjunction with laser ablation. The degree of orientation of the films was found to be strongly dependent on the incident angle of the ion beam, with the optimal results occurring at 55° from the substrate normal. Ion beam voltage and current also played important roles in determining the amount of orientation of the film. Oriented YSZ growth on Pyrex substrates using IBAD has also been reported by Sonnenberg et al (4). They reported detailed microstructural characterization, but did not subsequently deposit YBCO on these films. This paper reports our progress to date in the use of IBAD with magnetron sputtering, which has the advantage of producing larger area films than laser ablation.

### EXPERIMENTAL DETAILS

All of the buffer layer films were deposited by RF magnetron sputtering in a deposition system designed at the University of Arkansas for superconductor and related dielectric research. Briefly, it is a 22" diameter side-sputtering deposition system that is pumped with two cryopumps. The deposition pressure can be precisely controlled from high vacuum to above 1 Torr, independently of the amount of backfill gas present. This is achieved through the use of separate high- and low-conductance paths to the cryopumps. Both conductance paths utilize servo-controlled throttle valves to maintain a constant pressure regardless of the gas flow present. The chamber has multiple ports for mounting two sputter guns, an ion beam, and two substrate holders, which also serve as heaters. The chamber was pumped down to  $4 \times 10^{-7}$  Torr before each deposition.

The ion beam used in these experiments is an Anatech IS-3000 3" filamentless gun. It was positioned about 8 cm from the substrate and at an angle of 55° from the substrate normal. This corresponds to the angle of the [111] direction from the [100] direction for cubic CeO<sub>2</sub>, and it is believed that ions directed at this angle may suppress growth of the (111) phase while enhancing growth of the (100) phase (3). Argon gas was flowed through the gun and an acceleration potential of 200-300 eV was used, with a beam current of 2-5 mA.

The dielectric films were deposited from a stoichiometric 2" diameter CeO<sub>2</sub> target which was RF sputtered in 80% Ar and 20% O<sub>2</sub> at pressures ranging from 0.2 mTorr to 1 mTorr, and at power levels from 60-80 watts. The low pressures were required to create

a long enough mean free path for the ion gun to maintain a collimated beam. According to basic vacuum theory, a mean free path of 8 cm requires a pressure lower than 0.61 mTorr. Special modifications were made to the sputtering guns to allow them to maintain plasmas at such low pressures. These modifications basically consisted of flowing the sputtering gas inside the dark space shield of the sputter guns, creating a localized high pressure region. The substrate was unheated, but its temperature generally increased to about 50 °C due to radiative heating from sputtering and the ion beam.

The YBCO films were deposited in the same system described above, using a 2" magnetron sputtering gun in an off-axis geometry; the parameters are described elsewhere (5). Briefly, substrates were mounted onto a heater block using silver paste. The deposition temperature was held at 735 °C in 80% Ar and 20% O<sub>2</sub>. After deposition, the samples were cooled in 700 Torr of oxygen.

The following substrates were used in this experiment: pieces of <100> prime silicon, 1" square Corning 7059 borosilicate glass (Pyrex), and 0.5" square Haynes alloy (#230). Haynes alloy is a nickel-based stainless steel which is a candidate substrate for YBCO films because of its low thermal expansion coefficient mismatch with YBCO. The Haynes alloy was mechanically polished using successively finer diamond paste to 0.25 µm. The three different materials represent crystalline, amorphous, and polycrystalline structures, respectively, and provide a thorough test of the ability of IBAD to deposit oriented films independently of the substrate structure or orientation.

Cerium dioxide films were deposited on the above substrates both with and without IBAD. All of the films in this study were grown to a thickness of about 2000 Å. The use of IBAD caused a decrease in the deposition rate, from about 16 Å/min to 13 Å/min. After all of the CeO<sub>2</sub> depositions were completed, the CeO<sub>2</sub> sputtering gun was removed and replaced with the YBCO sputtering gun. The CeO<sub>2</sub> films were removed for analysis, then remounted to the heater block for YBCO deposition. YBCO films of approximately 3500 Å thickness were deposited on the glass and Haynes substrates.

The thickness and index of refraction of the CeO<sub>2</sub> films deposited on bare silicon were measured using an ellipsometer. The structure of the films was analyzed with a Phillips PW-1830 four-circle x-ray diffractometer (XRD) using copper kα radiation, and the surface analysis was performed with a Digital Instruments atomic force microscope (AFM). Electrical characteristics were measured using a non-contact technique similar to the system described in (6).

### RESULTS AND DISCUSSION

The index of refraction of both the IBAD and non-IBAD films was around 2.3, compared to 2.2 for bulk CeO<sub>2</sub>. This indicates that the films are slightly oxygen deficient (7), but theta-two theta XRD scans show only evidence of the CeO<sub>2</sub> phase. The theta-two theta scan of CeO<sub>2</sub> on a silicon substrate without using IBAD is shown in figure 1. The presence of the (111), (200), and the (220) peaks are present at roughly the same

intensity, with the ratio of the (200) peak intensity to (111) peak intensity equal to 0.95. This suggests a polycrystalline film with no prevalent texture. The film consists of completely random oriented grains since the substrate does not provide epitaxy for the growing layers. Figure 2 shows the theta-two theta scan of CeO<sub>2</sub> on silicon using IBAD. As the figure indicates, IBAD causes a marked improvement in the texturing of the (100) phase. The other phases are significantly attenuated, with the ratio of (200) to (111) intensities equal to 14.5. One reason for this dramatic improvement in texture, besides the fact that IBAD was used, is that silicon is crystalline with very nearly the same lattice constant as CeO<sub>2</sub>.

Figure 3 shows a theta-two theta XRD scan of IBAD deposited CeO<sub>2</sub> on Pyrex. While the (111) and (220) peaks are still visible, the (200) peak is dominant; the ratio of (200) to (111) intensities is 1.4. Figure 4 shows a phi scan of the (111) family of CeO<sub>2</sub> peaks on Pyrex and indicates both in-plane and out-of-plane orientation, as evidenced by the four peaks spaced 90° apart. The full-width-at-half-maximum (FWHM) for these peaks is approximately 34°. The relatively high FWHM implies that some in-plane misorientation is present. A theta-two theta scan of YBCO/CeO<sub>2</sub>/Pyrex is presented in figure 5. Only c-axis YBCO growth is detected, which suggests that the CeO<sub>2</sub> deposition provides a well-aligned layer upon which the YBCO can be deposited. As a further demonstration of the alignment, figure 6 shows a phi scan of the YBCO (103) family of peaks with a FWHM of 22°. This indicates well-aligned grains in the a-b plane, which is parallel to the substrate. The presence of 45° misaligned grains would be indicated by peaks spaced 45° out of phase from the major peaks. Misaligned grains greatly reduce the J<sub>c</sub> of the films.

Next, data for CeO<sub>2</sub> and YBCO/CeO<sub>2</sub> structures deposited on Haynes alloy are presented. Figure 7 shows a theta-two theta scan for CeO<sub>2</sub> deposited without IBAD. In this case, the CeO<sub>2</sub> peaks are barely discernible above the noise of the substrate, with the (111), (200), and (220) peaks at about equal intensity. The ratio of (200) to (111) intensities is equal to 0.9. Figure 8 illustrates a theta-two theta scan of YBCO deposited on Haynes alloy with an IBAD-deposited CeO<sub>2</sub> buffer layer. As in figure 5, only c-axis YBCO growth is evident. In addition, the (200) peak of CeO<sub>2</sub> is 3.2 times more intense than the (111) peak.

YBCO was deposited on the three  $CeO_2$ /substrate structures and their  $T_es$  and  $J_es$  were measured.  $T_es$  (zero resistance) were 86 K, and  $J_es$  ranged from  $1 \times 10^5$  A/cm<sup>2</sup> to  $5 \times 10^5$  A/cm<sup>2</sup> when measured at 77 K. These values are somewhat lower than  $T_es$  and  $J_es$  obtained for films deposited on single crystal substrates, such as yttria stabilized zirconia. The cause for the reduction in  $J_e$  is most likely due to the presence of high-angle grain boundaries, which are evident from the scan shown in figure 6. These grain boundaries are known to act as weak links and reduce the critical current density (8).

It is not well understood how the ion beam provides oriented film growth, but three separate mechanisms have been postulated. First, the collimated ion beam may selectively sputter grains growing in undesirable directions. Second, the beam is believed to enhance film growth corresponding to the channeling direction of the film. As mentioned above, the [111] channeling direction is 55° away from the [100] direction. Therefore, a beam directed at this angle allows the (100) phase to become channeled to the growing film, while other phase growth is attenuated or slowly sputtered away. Finally, the ion beam imparts energy to the surface of the film, which provides increased mobility for the molecules to realign into the preferred orientation.

The average roughness R, of the IBAD films was measured by AFM and found to be about 2.6 nm, while the R, of the non-IBAD films was about 3.8 nm. This improvement in smoothness is most likely due to the tendency of the ion beam to etch peaked surfaces more rapidly than smooth areas (9). This enhances superconductor quality by providing a smooth surface for YBCO nucleation. The improved surface quality, along with the stronger presence of the (100) phase, is believed to be responsible for higher YBCO film quality.

### **CONCLUSIONS**

Cerium dioxide films have been sputter deposited onto several substrate materials using IBAD. These films exhibit bi-axial alignment with dominant (100) phase growth, as indicated by XRD theta-two theta and phi scans. The argon ion beam was positioned 55° from the substrate normal. This angle corresponds to the angle of separation of the [111] direction of cubic CeO<sub>2</sub> from the [100] direction.

High quality YBCO was deposited over the IBAD buffer layers. The YBCO exhibited T<sub>c</sub>s around 86 K and J<sub>c</sub>s ranging from 1 × 10<sup>5</sup> A/cm<sup>2</sup> to 5 × 10<sup>5</sup> A/cm<sup>2</sup>. IBAD has been shown to be a useful technique for depositing aligned films on crystalline, polycrystalline, and amorphous substrates. This capability allows greater flexibility in manufacturing superconductor-dielectric structures by enabling the use of low-cost substrates in place of lattice-matched single crystal substrates, which tend to be expensive, brittle, and have high dielectric constants.

### REFERENCES

- 1. L. W. Schaper, S. S. Ang, Y. L. Low, and D. Oldham, to appear in IEEE Trans. on Comp., Hyb., and Man. Tech.
- 2. Y. Iijima, N. Tanabe, O. Kohno, and Y. Ikeno, Appl. Phys. Lett., 60, 769 (1992).
- 3. R. P. Reade, P. Berdahl, R. E. Russo, and S. M. Garrison, Appl. Phys. Lett., 61, 2231 (1992).
- 4. N. Sonnenberg, A. S. Longo, M. J. Cima, B. P. Chang, K. G. Ressler, P. C. McIntyre, and Y. P. Liu, J. Appl. Phys., 74, 1027 (1993).
- 5. R. G. Florence, S. S. Ang, and W. D. Brown, Supercond. Sci. Technol., 7, 741, (1994).

- 6. J. H. Claassen, M. E. Reeves, and R. J. Soulen, Rev. Sci. Instrum., 62, 996 (1991).
- 7. S. Yaegashi, T. Kurihara, H. Hoshi, H. Segawa, Jpn. J. Appl. Phys. 33, 270 (1994).
- 8. K. Char, M. S. Colclough, S. M. Garrison, N. Newman, and G. Zaharchuk, Appl. Phys. Lett. 59, 733, (1991).
- 9. S. S. Scott, M.S. EE thesis, University of Arkansas, 1994.

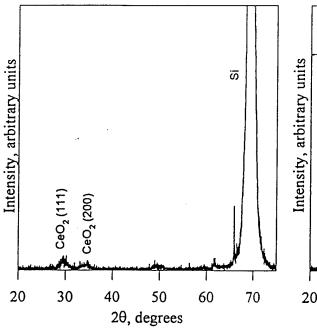


Figure 1. XRD scan of CeO<sub>2</sub> deposited on Si without IBAD.

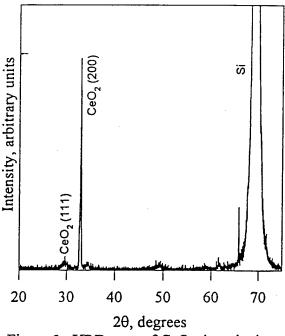


Figure 2. XRD scan of CeO<sub>2</sub> deposited on Si with IBAD.

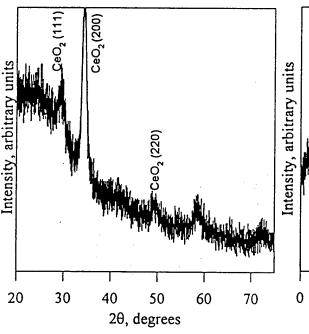


Figure 3. XRD scan of CeO<sub>2</sub> deposited on Pyrex with IBAD.

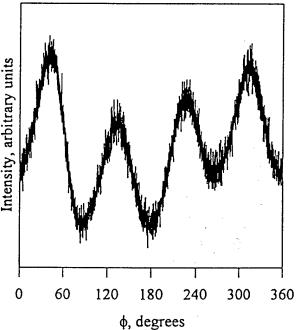


Figure 4. Phi scan of CeO2<sub>2</sub> (111) family of peaks deposited on Pyrex.

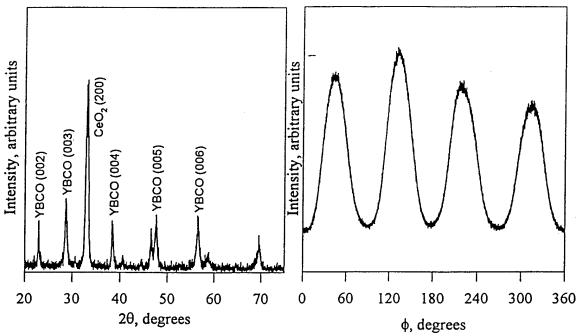


Figure 5. XRD scan of YBCO/CeO<sub>2</sub> deposited on Pyrex with IBAD.

Figure 6. Phi scan of YBCO (103) family of peaks on CeO<sub>2</sub>/Pyrex.

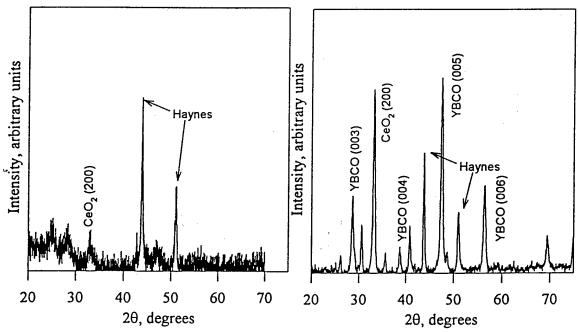


Figure 7. XRD scan of CeO<sub>2</sub> deposited on Haynes without IBAD.

Figure 8. XRD scan of YBCO/CeO<sub>2</sub> deposited on Haynes with IBAD.

# Ion Beam Assisted Sputter Deposition of CeO<sub>2</sub> Buffer Layers for Superconducting Multichip Module (MCM) Applications

List of Keywords

cerium dioxide
multichip modules (MCMs)
buffer layers
ion beam assisted deposition (IBAD)
sputtering
YBCO thin films
x-ray diffraction

# Presentation: paper



# THE EFFECTS OF LOW-ENERGY BLANKET ION MILLING ON THE PROPERTIES OF SUPERCONDUCTING YBCO FILMS

S. S. Scott, S. S. Ang, and W. D. Brown High-Density Electronics Center (HiDEC) Department of Electrical Engineering University of Arkansas 3217 Bell Engineering Center Fayetteville, AR 72701

### **ABSTRACT**

The effects of low-energy blanket ion milling on the electrical and structural properties of superconducting yttrium-barium-copper-oxide (YBa<sub>2</sub>Cu<sub>3</sub>O<sub>7-x</sub>, or YBCO) were investigated. This process has proven not to have a detrimental effect on the electrical or structural properties of high-quality YBCO films. In fact, it has been found that, in many cases, the critical current density ( $J_c$ ) improves as a result of a brief exposure to a low-energy ion beam. Also, milling of high-quality films results in a reduction in RMS surface roughness. Lower-quality films are typically degraded by the same process.

### INTRODUCTION

The High-Density Electronics Center (HiDEC) at the University of Arkansas is conducting research directed at the fabrication of superconducting multi-chip modules (MCMs). These modules will consist of semiconducting ICs on a superconducting interconnect structure. The superconductor material of choice is YBCO. Due to the reactivity of YBCO with air and water, its surface develops a non-superconducting layer through processing and handling. It is desired that this layer be removed prior to metallization (preferably in-situ) to produce a low-resistance contact. Ion milling is under consideration to serve this purpose. Consequently, the effects of ion bombardment on the electrical and structural properties of YBCO must be investigated to determine the effectiveness of this process.

The proposed superconducting MCM interconnect structure consists of two superconducting planes separated by dielectric layers which are deposited on a substrate. This two-layer structure is based on the interconnected mesh power system (IMPS) MCM topology [1], in which the power, ground, and signal components are combined into two planes. Due to the high dependence on the crystallographic properties when interfacing ceramic materials, minimization of layers is critical in this structure.

The four-sided problem of lattice matching, coefficient of thermal expansion (CTE), interdiffusion, and dielectric constant prevent the use of a single material for the

See publication



dielectric layer in this structure. The currently proposed dielectric layer for the HiDEC superconducting MCM consists of silicon oxide  $(Si_xO_y)$  buffered by layers of cerium dioxide  $(CeO_2)$  grown either by an ion beam-assisted sputtering or laser ablation technique.  $Si_xO_y$  has been chosen due to its low dielectric constant, and its extensive application in electronics. The  $Si_xO_y$  will be tailored by sputter deposition for the best trade-off between its dielectric constant and CTE.  $CeO_2$  has been chosen to buffer between  $Si_xO_y$  and YBCO because of its lattice parameter and CTE match with YBCO.

The superconductor planes are to be connected by metal vias. Previous publications have illustrated the severe degradation of the critical current density  $(J_c)$  of a superconducting YBCO via [2]. This reduction in  $J_c$  is due to the anisotropic nature of current flow in YBCO [3]. In order to keep the YBCO layers planar, the  $Si_xO_y$  will be planarized prior to the second YBCO deposition, and the YBCO layers will be connected by reach-through vias. The ideal metal for low-resistance contact to YBCO is gold (Au). Other options are silver (Ag), platinum (Pt), or a multi-layer metal. A cross-sectional representation of the superconducting MCM interconnect structure is shown in Figure 1.

An item of extreme importance, not considered in the previous section, is that of the reactivity of YBCO with its surroundings. YBCO has been shown to be reactive with many of its environmental components, especially air and water [4-6]. This results in the formation of a non-superconducting surface layer on YBCO films upon exposure to air and conventional wet processing steps, such as photolithography. This reacted layer results in higher-resistance contacts and defeats the purpose of lattice matching at the interface of a dielectric and a reacted YBCO surface. Avoidance of these reactions by shielding YBCO from a reactive atmosphere would be very time consuming as well as expensive. Figure 2 shows the interconnect structure of Figure 1 taking into account a non-superconducting surface on the YBCO planes of the superconducting MCM interconnect structure.

### EXPERIMENTAL PROCEDURES

Removal of the non-superconducting surface of YBCO is the most feasible solution to the reactivity problem. It is desirable for this removal process to be performed in the same chamber as the subsequent deposition step, so that the superconducting surface of the YBCO is not exposed to air. In the fabrication of the HiDEC module, where the CeO<sub>2</sub> layers are deposited by ion-beam assisted sputtering in the same chamber in which metallization is performed, the ion source may be used to etch the YBCO films until the superconducting bulk is exposed. This arrangement then allows for the deposition of the dielectric layer or metal following the in-situ milling process.

The use of inert ions to bombard a surface in order to remove material is called ion milling. Ion milling has been applied extensively to the patterning of YBCO films [7,8]. However, it has also been reported that it degrades the electrical properties of YBCO [9]. Since the surface preparatory process exposes the entire surface of the film

(this is where the term "blanket" comes from), a major concern is damage to the remaining film. In order to minimize the damage to the underlying superconducting YBCO, caused by exposure to ion milling, the process is performed at an energy lower than that common to bulk etching processes.

In order to evaluate the effects of low-energy blanket ion milling on YBCO films, the electrical properties of critical current density  $(J_c)$  and critical temperature  $(T_c)$  were measured prior to processing and after repeated exposures. The effects on the structural properties of YBCO were determined using atomic force microscopy (AFM) by which the surface structure was observed for changes and the surface roughness was calculated for a 100  $\mu m^2$  area.

Each milling step was performed at a beam energy of 500 eV and a beam current density of 0.3 mA/cm² for 2-minute intervals. The ion source was oriented normal to the sample surface at a distance of 15 cm. Argon gas was used to create the inert ions. The background pressure during milling was 1x10<sup>-4</sup> Torr. Typically, bulk etching is performed at energies greater than 1000 eV and a current density of approximately 1 mA/cm². In order to minimize residual damage from ion bombardment, an energy of 500 eV and a current density of 0.3 mA/cm² was chosen for the work described here. The etch rate of YBCO for these etching parameters is approximately 100 Å/min, so about 200 Å were removed per exposure. The initial thickness of the films was approximately 3000 Å-4000 Å.

YBCO films were deposited by sputtering or laser ablation on yttria-stabilized zirconia (YSZ), lanthanum aluminate (LaAlO<sub>3</sub>, or LAO), or strontium titanate (SrTiO<sub>3</sub>, or STO) substrates. Measurements of J<sub>c</sub> and T<sub>c</sub> were performed using a non-contact system that employs a current induction technique [10]. AFM data was obtained with a Digital Instruments Dimension 3000 Scanning Probe Microscope. The ion milling was performed with an Ion Tech model FC3000 filament-type 3 cm ion source.

### EXPERIMENTAL RESULTS

As previously noted, the intent of the surface preparation process is to remove the non-superconducting surface from YBCO without degrading its electrical or structural properties. However, what has been discovered is an improvement of  $J_c$  in some cases and typically a degradation of  $T_c$ . Figure 3 shows the plot of  $T_c$  for a YBCO film deposited by laser ablation onto a LAO substrate. As can be seen, the onset temperature remains the same while the zero temperature has degraded from 88 K to 83 K after one exposure to the blanket ion milling. Figure 4 shows a plot of critical current ( $I_c$ ) for the same sample. For a crossover criterion of 20 V,  $I_c$  has increased from 11 mA to 25 mA, which corresponds to a  $I_c$  increase from  $3.77 \times 10^5$  A/cm<sup>2</sup> to  $8.57 \times 10^5$  A/cm<sup>2</sup>.

Figures 5 and 6 show the  $T_c$  and  $I_c$ , respectively, of a YBCO film deposited by sputtering onto a YSZ substrate. After one exposure to blanket ion milling,  $T_c$  remained

unchanged at 88 K while  $I_c$  increased from 30 mA to 36 mA, which corresponds to a  $J_c$  increase from  $1.029 \times 10^6$  A/cm² to  $1.234 \times 10^6$  A/cm². Figures 7 and 8 show the  $T_c$  and  $I_c$ , respectively, of another YBCO film deposited by-sputtering on YSZ. After milling, the  $T_c$  remained unchanged at 87 K while the  $I_c$  increased from 32 mA to 52 mA, which corresponds to a  $I_c$  increase from  $1.097 \times 10^6$  A/cm² to  $1.783 \times 10^6$  A/cm².

Not all samples exposed to blanket ion milling behaved in this manner. Figure 9 plots the variation in  $I_c$  after each blanket mill for six samples. After one exposure to blanket ion milling, three of the films showed an increase in  $J_c$ , two showed a decrease, while one remained unchanged. After the second exposure, one film showed an increase in  $J_c$ , three showed a decrease, while one remained unchanged. One sample was milled three times and showed a continous decrease in  $J_c$ .

In addition to the electrical properties of YBCO, it is desirable that the surface roughness of the films not be degraded by the in-situ processing to promote epitaxy and planarity. Figure 10 plots the variation in RMS surface roughness ( $R_q$ ) after each blanket mill for six samples. After one exposure to the blanket ion milling, three of the films showed a decrease in  $R_q$ , while three showed an increase. The films consistently showed an increase in  $R_q$  after subsequent exposures.

### **CONCLUSIONS**

As discussed previously, the intent of the in-situ surface conditioning process described in this paper is to remove a non-superconducting surface without degrading the electrical or structural properties of YBCO. It has been shown that, in many cases, the  $J_c$  of YBCO films can be increased by a 2-minute exposure to an argon ion beam at 500 eV and 0.3 mA/cm². The increase in  $J_c$  is believed to be due to damage caused by the argon ions which creates flux pinning centers on the surface of the YBCO [11,12].

The effect on surface roughness of low-energy blanket ion milling are intriguing. While the films studied here showed some increase in surface roughness, the amount of the increase is acceptable considering that these films initially are sufficiently smooth for patterning of lines as small as 5  $\mu$ m. It has also been found that films with poor initial roughness (>30 nm RMS) are consistently smoothed by low-energy blanket ion milling. The films that did show an increase in roughness initially contained many pits on the surface which were progressively worsened by the milling. Films which were initially pit-free were shown to decrease in roughness after milling, even for films which were initially very smooth (<10 nm RMS).

The effects of ion milling on the electrical properties of YBCO films correlate well with changes in roughness. Films which exhibited high quality initially were more likely to be improved by low-energy blanket ion milling. On the other hand, poorer quality films typically degraded with ion milling. However, the results of these experiments show that YBCO films can be exposed to low-energy blanket ion milling

with relatively little detrimental effect on their electrical or structural properties. In fact, it may be reasonable to perform ion milling with the intent of increasing the  $J_c$  of YBCO films.

### REFERENCES

- 1. Schaper, L., S. Ang, Y. Low, and D. Oldham, To be published in IEEE Trans. Comp., Hybrids, and Manuf. Tech.
- 2. Burns, M., K. Char, B. Cole, W. Ruby, and S. Sachtjen, Appl. Phys. Lett., 62, 1435 (1993).
- 3. Braginski, A., Physica C, 153-155, 1598 (1988).
- 4. Bansal, N. and A. Sandkuhl, Appl. Phys. Lett., 52, 323 (1988).
- 5. Behner, H., K. Rührnschopf, G. Wedler, and W. Rauch, Physica C, 208, 419 (1993).
- 6. Büyüklimanli, T. and J. Simmons, Phys. Rev. B, 44, 727 (1991).
- 7. Alff, L., G. Fischer, R. Gross, F. Kober, A. Beck, K. Husemann, and T. Nissel, Physica C, 200, 277 (1992).
- 8. Ivanov, Z., P. Nilsson, E. Andersson, and T. Claeson, Supercond. Sci. Technol., 4, S112 (1991).
- 9. Xavier, P., T. Fournier, J. Chaussy, J. Richard, and M. Charalambous, J. Appl. Phys., 75, 1219 (1994).
- 10. Pena, O., Meas. Sci. Technol., 2, 470 (1991).
- Liu, J., Kulik, J., Zhao, Y., Chu, W., Nucl. Instrum. Methods Phys. Res. Sect. B, 80-81, 1255 (1993).
- 12. Abdullah, M., Shiraishi, K., Solid State Commun., 86, 109 (1993).

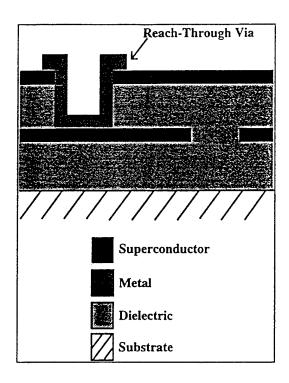


Figure 1: Interconnect Structure

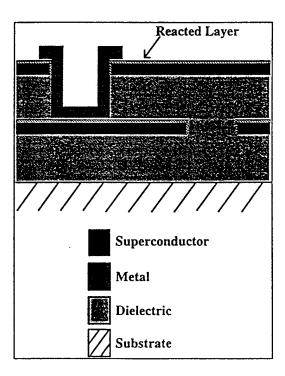


Figure 2: Reactivity of YBCO

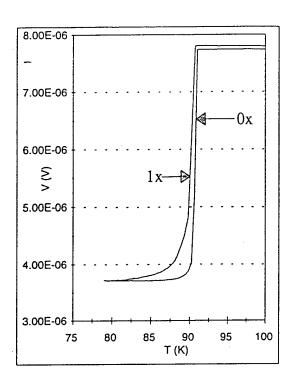


Figure 3: T<sub>c</sub> of laser-deposited YBCO on LAO

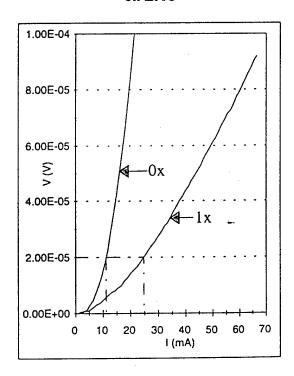


Figure 4: I<sub>C</sub> of laser-deposited YBCO on LAO

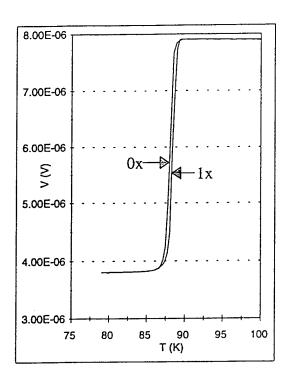


Figure 5:  $T_c$  of sputtered YBCO on YSZ

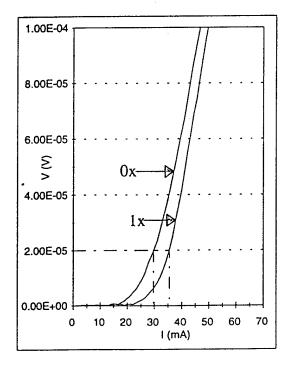


Figure 6:  $I_{\text{C}}$  of sputtered YBCO on YSZ

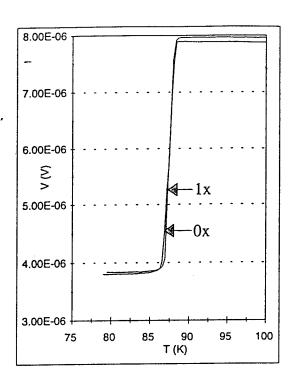


Figure 7:  $T_c$  of sputtered YBCO on YSZ

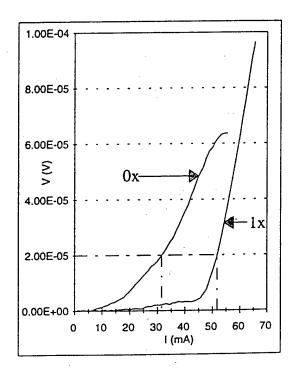


Figure 8:  $I_c$  of sputtered YBCO on YSZ

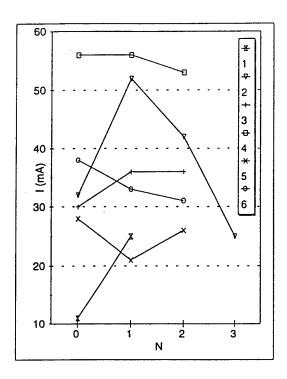


Figure 9:  $I_c$  vs. number of mills

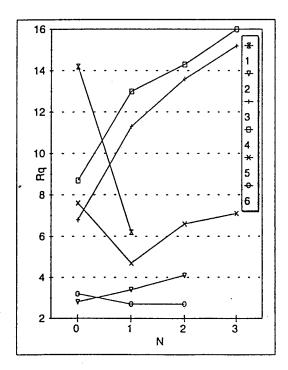


Figure 10: RMS roughness vs. number of mills

PROCEEDINGS OF THE SYMPOSIUM ON

# LOW TEMPERATURE ELECTRONICS AND HIGH TEMPERATURE SUPERCONDUCTIVITY

M4721-26,1595

RONO, NV

et the 187th Meeting of the ELECTRO CHENICAL Editors

Cor L. Claeys IMEC Leuven, Belgium

Stan I. Raider IBM T.J. Watson Research center Yorktown Heights, New York, USA

Randall Kirschman Mountain View, California, USA

William D. Brown University of Arkansas Fayetteville, Arkansas, USA

ENERGY TECHNOLOGY, ELECTRONICS, AND DIELECTRIC SCIENCE AND TECHNOLOGY DIVISIONS

Proceedings Volume 95-9



THE ELECTROCHEMICAL SOCIETY, INC., 10 South Main St., Pennington, NJ 08534-2896

### FRSENTOTION: POSTU

# Magnetic field and temperature dependence of critical current densities in multilayer YBa<sub>2</sub>Cu<sub>3</sub>O<sub>7- $\delta$ </sub> films

S. Afonso, F. T. Chan, K. Y. Chen, G. J. Salamo, Y. Q. Tang, R. C. Wang, a) X. L. Xu, b) and Q. Xiong

Physics Department/High Density Electronics Center, University of Arkansas, Fayetteville, Arkansas 72701

G. Florence, S. Scott, S. Ang, W. D. Brown, and L. W. Schaper Electrical Engineering Department/High Density Electronics Center, University of Arkansas, Fayetteville, Arkansas 72701

In order to build high-temperature superconductor (HTS) multichip modules (MCMs), it is necessary to grow several epitaxial layers of YBCO that are separated by thick dielectric layers without seriously affecting the quality of the YBCO layers. In this work, we have successfully fabricated YBCO/YSZ/SiO<sub>2</sub>/YSZ/YBCO structures on single-crystal LaAlO<sub>3</sub> substrates using a combination of pulsed laser deposition for the YBCO layers and ion-beam-assisted rf sputtering to obtain biaxially aligned YSZ intermediate layers. The bottom YBCO layer had a  $T_c \sim 89$  K,  $J_c \sim 7.2 \times 10^5$  A/cm<sup>2</sup> at 77 K, whereas the top YBCO layer had a  $T_c \sim 86$  K,  $J_c \sim 6 \times 10^5$  A/cm<sup>2</sup> at 77 K. The magnetic field and temperature dependence of  $J_c$  for the YBCO films in the multilayer have been obtained. The results for each of the YBCO layers within the YBCO/YSZ/SiO<sub>2</sub>/YSZ/YBCO structure are quite similar to those for a good quality single-layer YBCO film. © 1996 American Institute of Physics. [S0021-8979(96)03308-9]

### I. INTRODUCTION

In electronic applications of high-temperature superconductor (HTS) thin films, the critical current density  $(J_c)$  is an important characteristic. One of the potential applications of high-temperature superconducting films is as electronic interconnects on a multichip module (MCM). Since there are a minimum of two HTS thin films, separated by thick dielectric layers required, in HTS multichip modules (MCMs), it is necessary to know if the quality of the HTS layers is still maintained after the entire fabrication process is completed. In addition to the critical temperature  $(T_c)$  and critical current density at zero field, the dependence of  $J_c$  on an externally applied magnetic field and the temperature for the entire multilayer structure is crucial information for electronic applications. The YBCO/YSZ/SiO2/YSZ/YBCO multilayer structure has been fabricated by Reade et al.2 They reported cracking in the top YBCO layer, which limited their investigation of the properties of the multilayered structure.

In this article, we report a study of the temperature and magnetic field dependence of  $J_c$  for both YBCO layers in a YBCO/YSZ/SiO<sub>2</sub>/YSZ/YBCO multilayer structure<sup>3</sup> performed by the magnetization method. Our results show that the temperature and magnetic field dependence of  $J_c$  of the YBCO layers of these samples are similar to those of high quality single-layer YBCO thin films.

### II. EXPERIMENT

The YBCO/YSZ/SiO<sub>2</sub>/YSZ/YBCO multilayer samples investigated here were prepared by using a combination of pulsed laser deposition and ion-beam-assisted magnetron

sputtering. Details of the technique will be described elsewhere.<sup>3</sup> In short, a 200-nm-thick YBa<sub>2</sub>Cu<sub>3</sub>O<sub>7-8</sub> (bottom YBCO, layer 1) film was deposited on a single-crystal LaAlO<sub>3</sub> substrate (100 orientation and area  $1 \times 1$  cm<sup>2</sup>) by pulsed laser ablation at a substrate temperature of ~750 °C. Ion-beam-assisted rf sputtering was used to deposit biaxially aligned 200-nm-thick yttria-stabilized zirconia (YSZ) as a capping layer (layer 2). Next a 1-µm-thick, amorphous SiO<sub>2</sub> layer (layer 3) was deposited on layer 2 at room temperature by rf sputtering. The capping layer (YSZ) is used to prevent diffusion of the third SiO<sub>2</sub> layer into the top YBCO layer. A fourth layer (biaxially aligned YSZ) was then deposited on the SiO<sub>2</sub> layer to a thickness of 200 nm using the same method as for layer 2. This layer is very important. It not only functions as protection against the diffusion of the third SiO<sub>2</sub> layer into the YBCO layer, it also allows good epitaxial YBCO growth if it has a well-aligned structure. Finally, the top YBCO layer (layer 5) was deposited by laser ablation under the same conditions as was used for layer 1.

The orientation of the YSZ and YBCO layers was characterized by x-ray diffraction. The magnetization M(H) loop was measured using a Quantum Design Magnetometer in fields up to 4 T, applied parallel to the c-axis direction and at a fixed temperature. This was repeated for different temperatures ranging from 5 to 77 K. The values of  $J_c$  were calculated using Bean's model. The electrical resistance was measured using the standard four-lead technique.

### III. RESULTS AND DISCUSSION

X-ray diffraction data showed that all samples investigated here were single-phase highly c-axis oriented with very good in-plane epitaxy (Fig. 1). There were no cracks observed in the top YBCO layer. The resistance R(T) and magnetization M(T) of the samples were carefully measured for each YBCO layer. Figure 2 shows the typical resistance as a function of temperature for the top YBCO layer. The



a)Permanent address: Department of Materials Science, Fudan University, Shanghai, People's Republic of China.

b)Permanent address: Ion Beam Laboratory, Shanghai Institute of Metallurgy, Chinese Academy of Sciences, Shanghai, People's Republic of China.



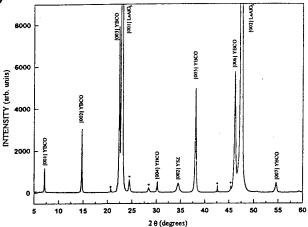


FIG. 1.  $\theta$ -2 $\theta$  x-ray diffractometer pattern for the YBCO/YSZ/SiO<sub>2</sub>/ YSZ/YBCO structure on [001] LaAlO<sub>3</sub> (\*: indicate substrate impurity peaks seen in the bare substrates of the same batch).

zero resistance temperature for this YBCO layer is about 86 K with a transition width of about 2 K. The M(T) data for a multilayer sample are shown in the inset of Fig. 2. As can be seen in the inset of Fig. 2, the onset transition of the M(T) curve is about 89 K. A second transition (indicated by the arrow in the inset of Fig. 2) is consistent with the  $T_c$  of the top YBCO layer measured by the transport method (Fig. 2). In order to verify this,  $T_c$  was remeasured again after the top layer of YBCO was etched away by using a dilute EDTA solution, and the onset transition was found to be about 89 K.

The critical current density  $J_c$  of the samples were measured by the magnetization method and calculated using Bean's model. For a rectangular single-layer film,  $J_c$  can be calculated from the following formula:<sup>4</sup>

$$J_c = 10[M_+(H) - M_-(H)]/L_1[1 - (L_1/3L_2)]V.$$
 (1)

In Eq. (1),  $M_+(H)$  and  $M_-(H)$  are the magnetization of the decreasing and increasing field branches in electromagnetic units (emu), respectively; V is the volume of the thin

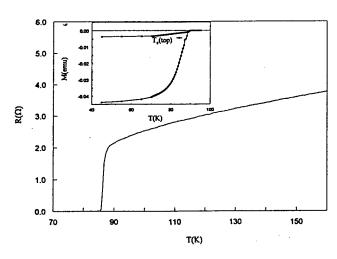


FIG. 2. Resistance vs temperature for the top YBCO layer in the YBCO/ $YSZ/SiO_2/YSZ/YBCO/LaAIO_3$  multilayer structure. Inset: magnetization M as a function of T for the entire multilayer structure.

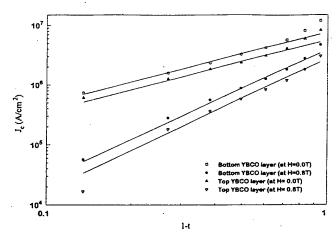


FIG. 3. Logarithmic plots of  $J_c$  vs 1-t for each of the YBCO layers within the multilayer structure. Straight lines are the curve fits to  $(1-t)^n$ , where  $n \sim 1.3$  for H = 0.0 T and  $n \sim 2.1$  for H = 0.8 T.

film in cm<sup>3</sup>;  $L_1$  and  $L_2$  are the short and long sides of the samples in cm, respectively. We have assumed that  $J_c$  is independent of the B field and excluded the anisotropic critical currents in the above calculation. In order to determine  $J_c$  of both the top and bottom YBCO layers, the magnetization  $M_-^m(H)$  and  $M_-^m(H)$  for the multilayer film was measured first, then the magnetization  $M_+^b(H)$  and  $M_-^b(H)$  for the bottom layer was measured after the top layer of YBCO was etched away. In this article we use superscript t and t for the parameters related to the top and bottom YBCO layer in the multilayer film, then t for the bottom layer should be

$$J_c^b = 10[M_+^b(H) - M_-^b(H)]/L_1^b[1 - (L_1^b/3L_2^b)]V^b,$$
 (2)

and for the top layer in the multilayer film,

$$J_c^t = 10\{ [M_+^m(H) - M_+^b(H)] - [M_-^m(H) - M_-^b(H)] \} / L_1^t [1 - (L_1^t/3L_2^t)] V^t.$$
 (3)

The  $J_c$  of the top YBCO layer was found to be about  $6 \times 10^5$  A/cm<sup>2</sup>, and a value of  $\sim 7.2 \times 10^5$  A/cm<sup>2</sup> was obtained for the bottom layer at 77 K under zero magnetic field.  $J_c$ , as a

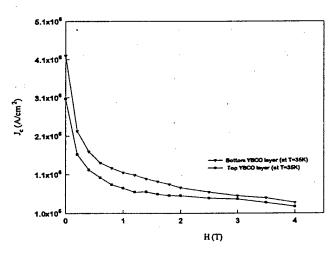


FIG. 4. Magnetic field dependence of  $J_c$  for top and bottom YBCO layers at 35 K. Field is applied perpendicular to a-b plane.

function of (1-t), is shown in Fig. 3 for different values of the magnetic field, where  $t=T/T_c$ . It was found that, for both YBCO layers, the temperature dependence of  $J_c$  is similar to that for a good quality, single-layer YBCO film. <sup>5-7</sup> The magnetic field dependence of  $J_c$  for both YBCO layers at 35 K are shown in Fig. 4. It clearly shows that  $J_c$  for both top and bottom YBCO films essentially has the same magnetic field dependence as that for the high quality, single-layer YBCO film. <sup>5-7</sup>

### IV. SUMMARY

A good quality YBCO multilayer structure has been fabricated using laser ablation and ion-beam-assisted rf sputtering. The dependence of  $J_c$  on the temperature and magnetic field for both YBCO layers in the multilayer has been determined. The results suggest that the temperature and magnetic field dependence of  $J_c$  of the YBCO layers in the multilayer structure are not altered appreciably by the multilayer growth processes.

### **ACKNOWLEDGMENTS**

This work was supported in part by NSF DMR 9318946, the High Density Electronics Center at the University of Arkansas, DARPA (Contract No. MDA 972-90-J-1001) and through the Texas Center for Superconductivity at the University of Houston.

- <sup>1</sup>M. J. Burns, K. Char, B. F. Cole, W. S. Ruby, and S. A. Sachtjen, Appl. Phys. Lett. **62**, 1435 (1993).
- <sup>2</sup>R. P. Reade, P. Beardahl, R. E. Russo, and L. W. Schaper, Appl. Phys. Lett. 66, 2001 (1994).
- <sup>3</sup>S. Afonso, Q. Xiong, K. Y. Chen, F. T. Chan, G. J. Salamo, Y. Q. Tang, G. Florence, S. Scott, S. Ang, W. D. Brown, and L. W. Schaper (unpublished).
- <sup>4</sup>E. M. Gyorgy, R. B. van Dover, K. A. Jackson, L. F. Schneemeyer, and J. V. Waszczak, Appl. Phys. Lett. 55, 283 (1989).
- <sup>5</sup>Q. Xiong, W. Y. Guan, P. H. Hor, and C. W. Chu, Chin. J. Phys. 30, 851 (1992).
- <sup>6</sup>D. W. Chung, I. Maartense, T. L. Peterson, and P. M. Hemenger, J. Appl. Phys. 68, 3772 (1990).
- <sup>7</sup>S. B. Ogale, D. Dijkkamp, T. Venkatesan, X. D. Wu, and A. Inam, Phys. Rev. B 36, 7210 (1987).

### 494

### THURSDAY AFTERNOON



HQ-15

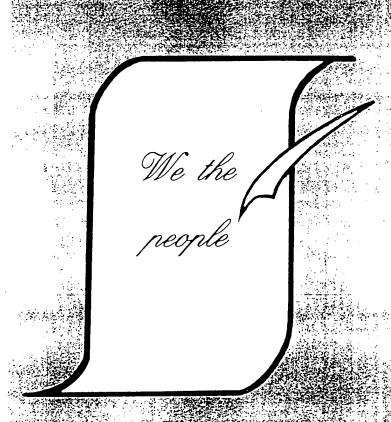
THE MAGNETIC FEILD AND TEMPERATURE DEPENDENCE OF CRITICAL CURRENT DENSITIES IN MULTILAYER Y<sub>1</sub>Ba<sub>2</sub>Cu<sub>2</sub>O<sub>1</sub>, FILMS

- S Afonso, F.T. Chan, K.Y. Chen, G.J. Salamo, Y.Q. Tang, R.C Wang\* and Q. Xiong Physics Department / High Density Electronics Center, University of Arkansas, Fayetteville, AR 72701
- G. Florence, S. Ang, W.D. Brown and L. Schaper, Electrical Engineering Department / High Density Electronics Center, University of Arkansas, Fayetteville, AR 72701

In order to build high temperature superconductor (HTSC) multichip modules (MCM's), it is necessary to grow several epitaxial layers of YBCO that are separated by dielectric layers without seriously effecting the quality of the YBCO layers. In this work, we have successfully fabricated YBCO/YSZ/SiO\_YSZ/YBCO on single crystal LaAlO<sub>1</sub> substrates using a combination of pulsed laser deposition for the YBCO layers and ion beam assisted sputtering to obtain biaxially aligned YSZ intermediate layers. The bottom YBCO liver had a T<sub>c</sub>-89K, J<sub>c</sub> 10<sup>3</sup> A/cm<sup>2</sup> at 77K, whereas the top YBCO layer had a T<sub>c</sub>-86K, J<sub>c</sub> 10<sup>3</sup> A/cm<sup>2</sup> at 77K. The magnetic field and temperature dependence of J<sub>c</sub> in these multilayer YBCO films has been obtained. The results from YBCO/YSZ/SiO\_YSZ/YBCO and YBCO/YSZ/SiO\_YSZ are quite similar to that from a single layer YBCO film.

<sup>\*</sup> Permanent address Department of materials Science, Fudan University, Shanghai, P. R. China.

<sup>\*\*</sup>This work has been supported in part by NSF DMR 9318946, the Texas Center for Superconductivity at the University of Houston under prime grant MDA972-90-J-1001 to the University of Houston from Defense Advanced Research Projects Agency.



# PRESENTATION: Paper



# FABRICATION OF HIGHLY TEXTURED SUPERCONDUCTING THIN FILMS ON POLYCRYSTALLINE SUBSTRATES USING ION BEAM ASSISTED DEPOSITION

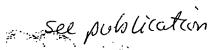
<sup>1</sup>Q. Xiong, <sup>1</sup>S. Afonso, <sup>1</sup>F.T. Chan, <sup>1</sup>K.Y. Chen, <sup>1</sup>G.J. Salamo, <sup>2</sup>G.Florence, J. Cooksey, S. Scott, <sup>2</sup>S. Ang, <sup>2</sup>W.D. Brown and <sup>2</sup>L. Schaper, <sup>1</sup>Physics Department, <sup>2</sup>Electrical Engineering Department / High Density Electronics Center, University of Arkansas, Fayetteville, AR 72701

### **ABSTRACT**

Tl<sub>2</sub>Ba<sub>2</sub>CaCu<sub>2</sub>O<sub>2</sub>(Tl2212) thin films on ceramic Al<sub>2</sub>O<sub>3</sub> substrates with J<sub>c</sub>(77K) of about 10<sup>5</sup> A/cm<sup>2</sup> and high quality YBCO/YSZ/SiO<sub>2</sub>/YSZ/YBCO/LaAlO<sub>3</sub> mutilayers with J<sub>c</sub>(77K) of about 6×10<sup>5</sup> A/cm<sup>2</sup> in the top YBCO layer have been successful deposited for the first time. These Mirror-like, highly o-axis oriented films were grown on highly textured YSZ buffer layers, which were deposited through Ion Beam-Assisted Laser Ablation. The zero resistance temperature is 95-108K for the Tl2212 films, and 85-90K for the multilayer YBCO films. The results suggest that using cheap non-single crystal substrates to fabricate good HTS films is possible.

### 1. Introduction

Since the discovery of high temperature superconductors(HTS), many possible applications of HTS thin films have been design and demonstrated, from very useful fault current limiters to the electronic interconnects on multichip module (MCM) substrates. All of these applications would benefit from the use of HTS thin films. One of the major problems for the application of HTS's is that HTS's can carry only a limited amount of current without resistance. This problem is related to their two dimensional layered structure. According to earlier studies<sup>1-2</sup>, if the layers do not line up properly, the critical current density will decrease dramatically in the misaligned region. One way to overcome this problem is to grow micron-thin layers of the material on well organized substrates, epitaxally. The process has the effect of lining up the superconducting layers more accurately. HTS thin films grown on single crystal substrates of LaAlO<sub>3</sub> or SrTiO<sub>3</sub> have good lattice match between the HTS and substrate, and have critical current densities of about ~10<sup>6</sup> A/cm<sup>2</sup>, which is large enough for most HTS thin film applications. While this effort is impressive, it is far from useful, since the films so developed are much too expensive because the single crystal substrates are very expensive and available only in relatively small sizes. Moreover, for some electronic applications such as HTS multi-chip modules(MCM's),



there are at least two HTS thin films that are separated by thick dielectric layers. Useful dielectric layers such as SiO<sub>2</sub> have noncrystalline structures. For this reason, HTS thin film layers cannot be grown on the dielectric layer with good alignment by conventional methods. Recent studies<sup>3-7</sup> have shown that highly biaxially aligned YSZ layers can be grown on non-crystalline substrates, which are cheaper and easy to get in any size needed by Ion beam-assisted laser deposition(IBAD). Using this method, high quality YBa<sub>2</sub>Cu<sub>3</sub>O<sub>y</sub> (YBCO) films have been deposited on biaxially aligned YSZ layers grown on non-crystalline substrates with J<sub>c</sub>'s of up to 8×10<sup>5</sup>A/cm<sup>2</sup> at 75K.

Here, we report the results from Tl2212 films fabricated on polycrystalline Al<sub>2</sub>O<sub>3</sub> substrates with an IBAD deposited YSZ buffer layer and YBCO/YSZ/SiO<sub>2</sub>/YSZ/YBCO/LaAlO<sub>3</sub> mutilayers.

### II Experimental

Fine polished Al<sub>2</sub>O<sub>3</sub> was used for the substrates of the Tl2212 films. Ion-beam assisted pulsed laser deposition was used to prepare highly biaxial aligned YSZ buffer layers at room temperature. While YSZ was deposited by pulse laser deposition, an Ion-beam (argon ion source) bombarded the substrates at an angle of 55° from the substrate normal. The laser used here was an ArF excimer laser (wavelength = 193 nm, shot frequency = 5 Hz). The energy density of the laser beam, which was focused on the YSZ target, was set to about 2 - 3 J/cm<sup>2</sup>. The ion beam energy was typically set at about 250 eV, and the beam current density was about 120 μA/cm². The oxygen partial pressure was maintained at  $3x10^4$  Torr, and with the ion beam the total pressure in the vacuum chamber was about  $8x10^4$  Torr during the deposition of the YSZ layers. The substrate temperature increased to about 100 °C due to the assisting ion beam. The growth rate was about 0.5 Å/S. The thickness of the YSZ buffer layers in our experiment was about 5000 Å. For the YBCO multilayer structure, 2000 Å thick YBCO layers were deposited by pulsed laser ablation at ~ 750 °C. A 4-5 micron thick amorphous SiO<sub>2</sub> layer was deposited as a dielectric layer at room temperature by rf sputtering. For the Tl2212 films, 2000-3000Å Ba<sub>2</sub>CaCu<sub>2</sub>O<sub>y</sub> precursor films were deposited on the YSZ-buffer layer at a temperature of 400°C using pulsed laser ablation. The films were then treated in a thallination process at 810°C.

The structures of deposited films were characterized by x-ray diffraction. T<sub>e</sub> and J<sub>e</sub> of HTS layers were measured by both transport method using the standard four-lead technique and the magnetization method using a Quantum Design Magnetometer.

### III. Results and Discussion

All YSZ films deposited on the polycrystalline  $Al_2O_3$  substrates for Tl2212 or on first YBCO layer, or on amorphous  $SiO_2$  layer were (001) oriented with the <001> axis normal to the substrate plane. A typical X-ray  $\theta$ -2 $\theta$  diffraction pattern for a YSZ film deposited on a polycrystalline  $Al_2O_3$  substrate is shown in Fig.1. Observation of only the YSZ(002) peak in the

A Company

X-ray  $\theta$ -2 $\theta$  diffraction pattern indicates that the YSZ was highly (001) oriented. The  $\phi$  scan width of the {111} peaks is about 25° (FWHM).

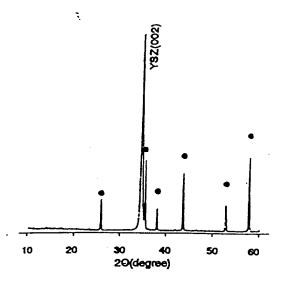


Fig. 1. X-ray diffraction θ-2θ scan of YSZ on Al<sub>2</sub>O<sub>3</sub> (Φ Al<sub>2</sub>O<sub>3</sub> peak)

Typical resistance versus temperature data for Tl2212 is shown in Fig.2. The zero resistance temperature T<sub>e</sub> is 105.6K which is comparable with the results from the high quality films grown on LaAlO, or SrTiO<sub>3</sub> substrates. The critical current densities of these films are about 8x104 A/cm<sup>2</sup> by transport method. Fig.3 shows the typical resistance as a function of temperature for the top YBCO layer in the multilayer structures. The zero resistance temperature for this YBCO layer is about 86K with a transition width of about 2 K. The Messier effect M(T) for the same mutilayer sample is shown in the inset of Fig.3. As in the inset of Fig.3, the onset

transition of the M(T) curve is at about 89 K, a second transition (indicated by the arrow) in the inset of Fig.3 is consistent with the T<sub>c</sub> of the top YBCO layer measured by the transport method (Fig.3). In order to verify this, T<sub>c</sub> was remeasured again after the top layer of YBCO was excluded

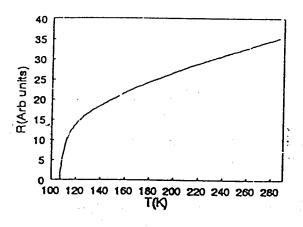


Fig. 2. Resistance vs. Temperature for the Tl<sub>2</sub>Ba<sub>2</sub>CaCu <sub>2</sub>O<sub>2</sub> on YSZ/Al<sub>2</sub>O<sub>3</sub>.

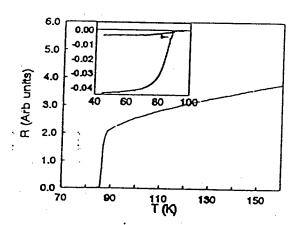


Fig. 3. Resistance vs temperature for the top YBCO layer in the YBCO/YSZ/SiO<sub>2</sub>/YSZ/YBCO/LaAlO<sub>3</sub> multilayer. Inset: Magnetization M as a function of temperature for the entire multilayer.

away by using a dilute EDTA solution, and the onset transition was found to be at about 89 K without the second transition. The critical current density, J<sub>c</sub> of the samples were measured by the

magnetization method and calculated using Bean's model before and after the top layer of YBCO was etched away. The  $J_c$  of the bottom YBCO layer is about  $7.2\times10^5$  A/cm² at 77 K, and of the top YBCO layer is about  $6\times10^5$  A/cm² at 77 K, For comparison, we deposited both YBCO and Tl2212 on ceramic  $Al_2O_3$  substrates. Even though the  $T_c$  of these films were about the same,  $J_c$  is  $<10^4$  A/cm². Which is about two orders of magnitude lower than that of the film on the biaxially aligned YSZ layer

### IV. SUMMARY

T12212 films on ceramic Al<sub>2</sub>O<sub>3</sub> substrates have been grown for the first time and good quality YBCO multilayer structures have been prepared using laser ablation and ion beam assisted rf sputtering. Our results demonstrate that good quality HTS films can be grown on cheap nonsingle crystal substrates though the Ion Beam-assisted deposition technique.

### **ACKNOWLEDGMENTS**

This work is supported in part by NSF DMR 9318946, DARPA (Contract No. MDA 972-90-J-1001) through Texas Center for Superconductivity at the University of Houston.

### REFRENCE

- D. Dimos, P. Chaudhari, J. Mannhart, and F. K.LeGoues, Phys. Rev. Lett.61(1988)219.
   D. Dimos, P. Chaudhari, J. Mannhart, Phys. Rev. B 41(1990) 4038.
- "Effect of Pressure on the Critical Current Density of YBa2Cu3O7-d Thin Films,"
   Q. Xiong, Y. Y. Xue, Y. Y. Sun, P. H. Hor, C. W. Chu, M. F. Davis, J. C. Wolfe, S. C.Deshmukh and D. J. Economou, Physica C 205, 307 (1993).
- 3. R. P. Reade, P. Berdahl, R. E. Russo, and S. M. Garrison, Appl. Phys. Lett. 61, 2231 (1992).
- 4. 2. Y. Iijima, N. Tanabe, O, Kohno, and Y. Ikeno, Appl. Phys. Lett. 60, 769 (1992).
- 5. X. D. Wu, S. R. Foltyn, P. Arendt, J. Townsend, C. Adams, I. H. Campbell, P. Tiwari, Y. Coulter, and D. E. Peterson, Appl. Phys. Lett. 65, 1961 (1994).
- 6. F. Yang, E. Narumi, S. Patel, and D. T. Shaw, Physica, C 244, 299 (1995).
- X. D. Wu, S. R. Foltyn, P. N. Arendt, W. R. Blumenthal, I. H. Campbell, J. D. Cotton, J. Y. Coulter, W. L. Hults, M. P. Maley, H. F. Safar, and J. L. Smith, Appl. Phys. Lett. 67, 2397(1995).

# PROCEEDINGS of the ANNIVERSARY HTS WORKSHOP

on Physics, Materials and Applications

Edited by

B. Batlogg
Lucent Technologies, USA

C. W. Chu
Texas Center for Superconductivity
University of Houston, USA

W. K. Chu
Texas Center for Superconductivity
University of Houston, USA

D. U. Gubser Naval Research Laboratory, USA

K. A. Müller IBM Zürich, Switzerland



March 12-16, 1996 Doubletree Hotel at Allen Center Houston, Texas, USA



PRESENTATION: Paper



### Fabrication and characterization of vias for contacting YBa<sub>2</sub>Cu<sub>3</sub>O<sub>7-x</sub> multilayers

J. W. Cooksey, S. Afonso, W. D. Brown, L. W. Schaper, S. S. Ang, R. K. Ulrich, G. J. Salamo, and F. T. Chan

High Density Electronics Center, University of Arkansas, 600 W. 20th Street, Fayetteville, AR 72701 USA

In order to connect multiple layers of high temperature superconductor (HTS) interconnects, low contact resistance vias must be used to maintain high signal propagation speeds and to minimize signal losses. In this work, 40 µm via contacts through YBa<sub>2</sub>Cu<sub>3</sub>O<sub>7-x</sub>/SrTiO<sub>3</sub>/SiO<sub>2</sub>/YSZ/YBa<sub>2</sub>Cu<sub>3</sub>O<sub>7-x</sub> multilayers utilizing dry etching techniques and sputter deposited Au for contacting through the vias have been successfully fabricated and characterized. The vias connect two laser ablated YBa<sub>2</sub>Cu<sub>3</sub>O<sub>7-x</sub> (YBCO) signal lines through thick (4-5 µm) SiO<sub>2</sub> insulating layers. This approach to making multilayer superconductor vias provides a low resistance contact between the YBCO layers while maintaining space efficiency and fabrication compatibility with the superconductor.

### 1. INTRODUCTION

Since the discovery of high temperature superconductivity (HTS), researchers have utilized their low resistance behavior in many applications. One such application is that of multichip modules (MCMs.) Unlike that of VLSI technologies where smaller feature sizes in successive generations allow interconnect lengths and power dissipation to be reduced, MCMs will not have that same luxury. As the complexity of ICs advances, pinout count per IC increases, and operating frequencies increase, MCM normal metal interconnections will have to grow in length and will not be allowed to reduce in crosssectional area. On MCM-D substrates, typical copper or aluminum interconnection dimensions are about 2 to 5 µm in thickness and between 15 and 30 µm wide with corresponding via sizes. By cooling the metal to 77 K (liquid nitrogen temperature), the resistivity of copper decreases by a factor of about 7 which allows a corresponding decrease in the interconnect's crosssectional area. In order to increase the wiring density beyond that of cryo-cooled MCMs and improve the chip-to-chip bottleneck at high frequencies. alternatives to conventional metal interconnects must be considered [1].

HTS interconnections, with negligible resistivity at operating frequencies of several tens of GHz and lower, have great potential to reduce an interconnect's cross-sectional area with typical thicknesses of less than 1 µm and widths of less than 2 µm for MCM applications with similar spacings. The main

challenge for attaining multiple layers of high density, high performance HTS interconnects appears to be in fabricating compact, low resistance vias.

The work presented here focuses on this problem and describes a method of fabricating noble metal vias for use in an HTS MCM prototype.

### 2. EXPERIMENTAL DETAILS AND RESULTS

A cross-section of our multilayer YBCO structure utilizing Au vias is shown in Figure 1.

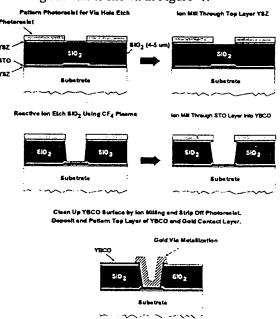


Figure 1. HTS via process.

Our research has centered around two layers of laser ablated YBa<sub>2</sub>Cu<sub>3</sub>O<sub>7-x</sub> (YBCO) interconnects separated by a multilayer dielectric consisting of SrTiO<sub>3</sub>/SiO<sub>2</sub>/YSZ. We are able to attain critical current densities > 5 x 10<sup>5</sup> A/cm<sup>2</sup> in both YBCO layers. The SrTiO<sub>3</sub> (STO) and YSZ (yttria-stabilized zirconia) layers being ~0.5 μm thick while the SiO<sub>2</sub> ranges between 4 and 5 μm.

The via fabrication process is as shown in Figure 1. The etching involves a 500 eV ion mill through the top YSZ buffer layer, which is followed by a reactive ion etch through the SiO<sub>2</sub> interlevel dielectric selectively stopping at the barrier layer of STO. To complete the etching process, a 500 eV ion mill is done to etch through the STO. The final milling is very nonselective and requires close observation to keep from overetching through the bottom layer of YBCO. When depositing the top layer of YBCO at ~700° C, whatever material is deposited on the via sidewalls is presumably corroded due to interdiffusion of Si from SiO2 into the YBCO but, presumably, does not effect the quality of the via. The subsequent in situ deposition of ~2000 Å of Au by laser ablation creates low resistance contacts without having to do a high temperature anneal in oxygen as was described by Ekin et al. [2]. In similar structures, contact resistivities of less than 10<sup>-7</sup> Ω-cm<sup>2</sup> have consistently been attained. An additional 1.5-2.0 µm of Au is deposited over the existing YBCO/Au and then patterned using ion milling and photoresist as a mask.

This type of via structure has several advantages over previously demonstrated superconducting vias for use in HTS MCMs [3,4]. Since HTS thin films need to be deposited on planar surfaces or gradual slopes to maintain a reasonable current density, due to grain boundary problems, they require gradually sloped via holes that take up a wide area. By using a noble metal, compact, high-aspect ratio vias can be fabricated reliably.

Ultrasonic AI wire bonds were then made between YBCO/Au bond pads on the substrate and a wire bondable PC board. Via chain resistance was measured using a conventional 4-point contact configuration and measuring the voltage drop across the vias while passing DC current through it. The resistance vs. temperature of a  $\sim 0.5$  cm long via chain structure with ten 40  $\mu$ m square vias interconnecting 50  $\mu$ m wide YBCO lines is shown in Figure 2. The room temperature resistance was measured to be about 515  $\Omega$ , and upon cooling to 78.5 K, the resistance

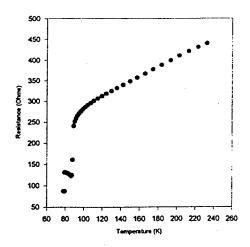


Figure 2. Temperature transition of a chain of ten 40 µm wide vias.

dropped to about 87  $\Omega$ . As is shown in Figure 2, there are two separate superconducting transitions occurring at about 89 K and 80 K which correspond to the top and bottom layer YBCO transitions. At 78.5 K, the interconnects had not yet become fully superconducting.

In summary, 40 µm YBCO/Au via chain structures have been characterized. The preliminary work shown here is to be improved upon by improving the quality of the YBCO layers, lowering the contact resistances, and possibly improving the step coverage of Au through the via by increasing its thickness.

### **ACKNOWLEDGEMENT**

This work was supported in part by NSF (DMR 9318946), U.S. Army Research Office (DAAH04-96-1-0455), and DARPA (MDA 972-93-I-0036).

### REFERENCES

- 1. S. K. Tewksbury, L. A. Hornak, L. A. Tewksbury, and L. Chen, Journal of Microelectronic Systems Integration, Vol. 4, No. 2, (1996).
- J. W. Ekin, S. E. Russek, C. C. Clickner, and B. Jeanneret, Appl. Phys. Lett., 62 369 (1993).
- M. J. Burns, K. Char, B. F. Cole, W. S. Ruby, and S. A. Sachtjen, Appl. Phys. Lett., 62 1435 (1993).
- 4. B. Santo, Electronic Engineering Times, August 10 (1992).



## 5th International Conference on Materials and Mechanisms of Superconductivity, and High-Temperature Superconductors

February 28-March 4, 1997, Beijing, China

Nov. 12, 1996

Dr. John W Cooksey University of Arkansas High Density Electronocs Ceter 600 W.20th St. Fayetteville, AR 72701 USA

Fax: 5015752719

Dear Dr. John W Cooksey,

We are pleased to inform you that your paper

Ref. No.:

US-012/A4a-002

Title:

Fabrication and Characterization of Vias for Contacting YBa2Cu3O7-

x Multilayers

Co-Authors: S. Afonso W D Brown L W Schaper S S Ang R K Ulrich G J Salamo

F T Chan

has been accepted for presentation at the M2S-HTSC-V Conference. The instruction for preparing the manuscript will be sent to you directly by Physica C, Elsevier Science B.V.. The deadline for submitting the manuscripts is extended to January 31, 1997, but the earlier submission is preferable. Please mention the reference number in the further communication.

As the chairmen of the conference, we would like to invite you for an active participation in the M<sup>2</sup>S-HTSC-V, which will be held in Beijing, Feb. 28-Mar. 4, 1997.

We will send you an official invitation letter for visa application after receiving your registration form, since your personal information (e.g. Passport Number etc.) is required in the letter. Please send us your registration form before December 1, 1996. If the registration form is not available, you may get it from the homepage of M<sup>2</sup>S conference at http://sun1.bham.ac.uk/hey/conferences/, or directly ask us for it.

We are looking forward to meeting you at the M<sup>2</sup>S-HTSC-V in Beijing.

Sincerely yours,

7. ylu Gan

Zi-Zhao GAN Guo-Zhen YANG Zhong-Xian ZHAO Co-chairmen of M<sup>2</sup>S-HTSC-V

# PRESENTATION: Paper



Fabrication techniques and electrical properties of YBa<sub>2</sub>Cu<sub>3</sub>O<sub>7-x</sub> multilayers with rf sputtered amorphous SiO<sub>2</sub> interlayers

aS. Afonso, aK. Y. Chen, aQ. Xiong, aF. T. Chan, aG. J. Salamo, bJ. W. Cooksey, bS. Scott, bS. Ang, bW. D. Brown, and bL. W. Schaper.

<sup>a</sup>Department of Physics and <sup>b</sup>Department of Electrical Enginneering/High Density Electronics Center, University of Arkansas, Fayetteville, AR 72701, USA

We have successfully fabricated YBa<sub>2</sub>Cu<sub>3</sub>O<sub>7-x</sub>/YSZ/SiO<sub>2</sub>/YSZ/YBa<sub>2</sub>Cu<sub>3</sub>O<sub>7-x</sub> multilayer structures on single crystal LaAlO<sub>3</sub> (100), substrates. The YBa<sub>2</sub>Cu<sub>3</sub>O<sub>7-x</sub>(YBCO) layers were deposited using pulsed laser ablation (PLD), the biaxially aligned YSZ (250 nm thick) layers were deposited using ion beam assisted PLD (IBAD-PLD), and an amorphous SiO<sub>2</sub> (1-2μm) layer fabricated via rf sputtering was sandwiched between the YSZ layers. Fabrication techniques and characterization results are reported for patterned layers in this work.

## 1. INTRODUCTION

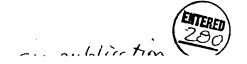
For high temperature superconductor multichip module(HTS-MCM) applications the basic building block is the HTS/Insulator (thickness > 1 \mu m)/HTS structure. MCM can be defined as a miniaturized version of a multilayered printed wiring board with superconducting interconnects. Previously such a HTS-MCM prototype using a YBCO/SrTiO<sub>3</sub>(500nm)/YBCO has been successfully fabricated by Burns et al [1]. Recently the use of ion beam assisted deposition to deposit biaxially aligned YSZ buffer layers on polycrystalline amorphous substrates allowed for good quality YBCO films on these substrates [2-5]. Reade et al [6] were able to demonstrate using the ion beam assisted pulsed deposition (IBAD-PLD) technique that it was possible to fabricate the YBCO/YSZ-/amorphousYSZ(5µm)/YSZ/YBCO multilayers on oriented YSZ substrates with the top YBCO Tc ~ 87 K. They also fabricated the same structure using amorphous SiO2, but cracks in the top YBCO layer did not permit electrical measurements of the top layer. The main advantage of SiO2 is its low dielectric constant (~ 3.89), which makes it an ideal insulator material for MCMs.

In this paper we briefly describe the method to fabricate and the results obtained

from the characterization of the YBCO/YSZ-/SiO $_2$ /YSZ/YBCO multilayers.

## 2. EXPERIMENTS

The first YBCO layer (300nm thick) was fabricated by pulsed laser deposition using standard conditions. After patterning, part of the pads were masked to allow for transport measurements later. Next a 250 nm thick YSZ layer was deposited via IBAD PLD using conditions described in [5]. After this a 1-2 µm thick SiO2 layer was deposited by reactively sputtering a Si target in oxygen ambient (the details of this process are described in [4]). Following the SiO<sub>2</sub> deposition another 250 nm thick biaxially aligned YSZ buffer/capping layer was deposited via IBAD PLD. Finally the masks were taken off and the top YBCO was deposited using the same conditions as the first YBCO except that the deposition temperature was kept ~ 20-30° lower. For the first set of multilayers the top YBCO layer was patterned into bridges over the underlying bridge patterns but shifted a little to the side so that the top bridge goes over step edges. The patterning was carried out by using photolithography and ion milling. For the second set of multilayers the top YBCO layer was patterned into



bridges whereas the bottom YBCO layer was not patterned. Finally in the third set the top YBCO layer was patterned into serpentine (meander) lines crossing over the patterned bottom YBCO serpentine lines

## 3. RESULTS

The X-ray diffraction pattern for an unpatterned multilayer in Fig. 1. shows that the films have good c-axis orientation. We also measured the top YBCO  $\phi$  scan full width at half maximum (FWHM) ~ 26° (for the (103) peaks), while for YSZ (111) peaks the FWHM was ~ 2-3° greater than that of the top YBCO.

For the first set, the bottom 40  $\mu m$  wide bridge the  $T_c \sim 90$  K and  $J_c \sim 2\times10^6$  A/cm² whereas for the top YBCO bridge 60  $\mu m$  wide (with step edges), the  $T_c \sim 86\text{-}87$  K and  $J_c \sim 3\times10^4$  A/cm². In the second set, the top YBCO bridge patterns of the same width without step edges the  $J_c \sim 10^5$  A/cm² with  $T_c \sim 87\text{-}88$  K. Finally in Fig. 2(A) is shown the resistance versus temperature plot for 20  $\mu m$  serpentine bottom YBCO line 19 cm long the  $T_c \sim 87$  K and  $J_c \sim 2\times10^5$  A/cm², whereas the same width serpentine line on the top layer showed semiconducting behavior as seen in Fig.2(B).

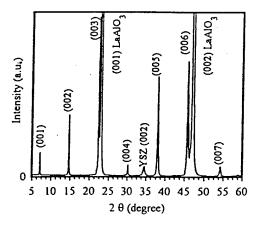


Fig. 1. X-ray diffraction pattern for a multilayer YBCO/YSZ/SiO<sub>2</sub>/YSZ/YBCO sample

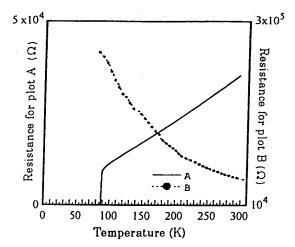


Fig. 2 Resistance versus temperature curves for
(A) 20 μm wide bottom YBCO serpentine line,
(B) 20 μm wide top YBCO serpentine line

## 4. CONCLUSIONS

Good quality YBCO layers separated by an amorphous SiO<sub>2</sub> interlayer have been fabricated by using biaxially aligned YSZ layers. However if the bottom YBCO is densely patterned then planarization is necessary to prevent degradation of superconducting properties at the step edges.

## ACKNOWLEDGEMENT

This work was supported in part by NSF (DMR 9318946), U.S. Army Research Office (DAAH04-96-1-0455), and DARPA (MDA 972-93-I-0036).

## REFERENCES

- M. J. Burns et al., Appl. Phys. Lett. 62,(1993) 1435.
- 2. Y. lijima et al., J. Appl. Phys. 74 (1993) 1905.
- X. Wu et al., Appl. Phys. Lett. 65 (1994) D1961
- R. G. Florence et al., Supercond. Sci. Technol. 8, (1995) 546.
- K.Y. Chen et al., Physica C 267 (1996) 355.
- R. P. Reade, et al., Appl. Phys. Lett. 66, (1995) 2001.



# 5th International Conference on Materials and Mechanisms of Superconductivity, and High-Temperature Superconductors

February 28-March 4, 1997, Beijing, China

Nov. 12, 1996

Dr. John W Cooksey University of Arkansas High Density Electronocs Ceter 600 W.20th St. Fayetteville, AR 72701 USA

Fax: 5015752719

Dear Dr. John W Cooksey,

We are pleased to inform you that your paper

Ref. No.:

US-012/A4a-002

Title:

Fabrication and Characterization of Vias for Contacting YBa2Cu3O7-

x Multilayers

Co-Authors: S. Afonso W D Brown L W Schaper S S Ang R K Ulrich G J Salamo

F T Chan

has been accepted for presentation at the M2S-HTSC-V Conference. The instruction for preparing the manuscript will be sent to you directly by Physica C, Elsevier Science B.V.. The deadline for submitting the manuscripts is extended to January 31, 1997, but the earlier submission is preferable. Please mention the reference number in the further communication.

As the chairmen of the conference, we would like to invite you for an active participation in the M<sup>2</sup>S-HTSC-V, which will be held in Beijing, Feb. 28-Mar. 4, 1997.

We will send you an official invitation letter for visa application after receiving your registration form, since your personal information (e.g. Passport Number etc.) is required in the letter. Please send us your registration form before December 1, 1996. If the registration form is not available, you may get it from the homepage of M<sup>2</sup>S conference at http://sun1.bham.ac.uk/hey/conferences/, or directly ask us for it.

We are looking forward to meeting you at the M2S-HTSC-V in Beijing.

Sincerely yours,

7. 8 h (nau

Zhong-Xian ZHAO Zi-Zhao GAN Guo-Zhen YANG Co-chairmen of M<sup>2</sup>S-HTSC-V

# PRESENTATION: Paper



## Recent Advances in High Temperature Superconductor Multichip Modules

J. W. Cooksey, S. S. Scott, W. D. Brown, S. S. Ang and R. G. Florence High Density Electronics Center/Department of Electrical Engineering University of Arkansas, Fayetteville, AR 72701 Phone: 501-575-8603 Fax: 501-575-2719 E-mail: jwc1@engr.uark.edu

S. Afonso
High Density Electronics Center/Department of Physics
University of Arkansas, Fayetteville, AR 72701

## **Abstract**

Two different techniques for fabricating high temperature superconducting (HTS) MCM-D substrates have been developed and tested. The first unit consists of two digital gallium arsenide bare die connected by YBa<sub>2</sub>Cu<sub>3</sub>O-<sub>-8</sub> (YBCO) HTS interconnects to form two ring oscillators on a 2.25 cm² MCM-D substrate. The interconnections consist of two wiring layers of YBCO separated by a 4-5  $\mu$ m silicon dioxide interlevel dielectric. The signal lines are routed between power and ground lines which form an interconnected mesh power system (IMPS) and, thereby, the module avoids the necessity of having two additional layers for power and ground planes. Connection between the two YBCO layers is accomplished with low contact resistance 40  $\mu$ m gold vias through the interlevel dielectric layer. The signal interconnects have 50  $\mu$ m linewidths and 75  $\mu$ m spacings. Electrical connections between the die and the MCM substrate and between the substrate and the PC board were made using ultrasonic Al wire bonds to low contact resistance gold/YBCO bond pads on the MCM substrate.

The second module, known as the Flip-Mesh superconducting MCM, provides an alternative to the multilayer MCM-D substrate described above. It involves using flip chip bonding techniques to connect multiple single-layer substrates, thereby reducing the processing complexity of fabricating multiple layers. X-plane and Y-plane interconnects are fabricated on separate substrates and interconnected using solder bumps. The IMPS topology is also utilized in this structure so that power, ground, and signals can be fabricated on two planes. The initial Flip-Mesh design incorporates 100 µm (4 mil) solder bump vias with similar spacings, which results in a low packing density for MCM-D technology, but a high density for I/O technology.

Key words: High temperature superconductors, MCM-D, Interconnected Mesh Power System (IMPS), YBCO

## Introduction

Unlike that of VLSI technologies where smaller feature sizes in successive generations allow interconnect lengths and power dissipation to be reduced, multichip modules (MCMs) will not have that same luxury. As the complexity of ICs advances, pinout count per IC increases, and operating frequencies increase, MCM normal interconnections will have to grow in length and will not be allowed to reduce in cross-sectional area. On MCM-D substrates, typical copper or aluminum interconnection dimensions are about 2 to 5 µm in thickness and between 15 and 30 µm wide. The resistivity of copper or aluminum decreases by at least a factor of 7 when decreasing the temperature from 300 K to 77 K (liquid nitrogen temperature), which allows smaller cross-section interconnections to be fabricated on cryo-cooled MCMs. In order to increase the wiring density in MCMs beyond that of cryo-cooled MCMs and improve the chip-to-chip bottleneck at high frequencies, alternatives to conventional metal interconnects must be considered [1].

High temperature superconductor (HTS) interconnections, with negligible resistivity at operating frequencies of several tens of GHz and lower, have great potential to reduce the interconnection line cross-section even further with typical thicknesses being less than 1 µm and widths could be reduced to less than 2 µm for MCM applications. The critical current density of HTS interconnects, which limits the line's minimum cross-section, is similar in value to the maximum current density allowed in Al interconnects to inhibit electromigration. These small, low resistance

interconnects offer significant performance advantages over normal metal interconnects for MCM-D technology using CMOS or GaAs integrated circuits which have enhanced chip level performance at liquid nitrogen temperatures (77 K). An added benefit of HTS lines is the reduced capacitive coupling between adjacent interconnections (due to their reduced thickness) which allows the lines to be spaced more closely together. The reduced cross-section of HTS interconnects should allow a significant increase in packing density and a corresponding decrease in the number of interconnect layers required to achieve the same functionality with normal metal interconnects.

We have been developing two separate HTS MCM prototypes. One is to be the first planar HTS MCM utilizing a thick layer of silicon dioxide as an interlevel dielectric and is based on MCM-D technology. The second prototype is based on interconnecting two layers of HTS interconnects on separate substrates via solder bumps and flip chip techniques. Our development has centered around the HTS material YBa<sub>2</sub>Cu<sub>3</sub>O<sub>7-8</sub> (YBCO) which has a transition temperature of about 91 K (well above the boiling point of liquid nitrogen, 77 K) and critical current densities typically greater than 5 x 10<sup>5</sup> A/cm<sup>2</sup>.

## I. HTS MCM-D Prototype

A cross-section of our proposed HTS MCM is shown in Figure 1.

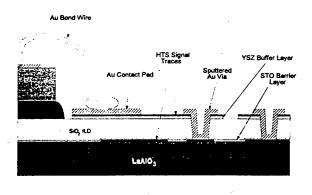


Figure 1. HTS MCM cross-section.

This novel structure has several key features that provide advantages over previously demonstrated HTS MCMs [2,3]. These advantages are:

(1) the utilization of an Interconnected Mesh Power System (IMPS) topology that is ideal for HTS multilayer fabrication because it allows an MCM to be constructed with only two layers of interconnects as opposed to the four that are traditionally used: x-signal, ysignal, and ground and power planes;

- (2) a thick ( $\sim 5~\mu m$ ) layer of SiO<sub>2</sub> that is sandwiched between a thin buffer layer dielectric and a thin diffusion barrier layer dielectric to form a composite interlevel dielectric that is compatible with multilayer YBCO processing while allowing controlled impedance ( $Z_o = 50~\Omega$ ) lines to be fabricated, which are necessary for high speed signal propagation;
- (3) chemical-mechanical polishing to create a planar SiO<sub>2</sub> surface for deposition of a high quality top level superconductor/buffer layer;
- (4) high-aspect ratio, low contact resistance vias that utilize noble metals to form contacts between the two layers of YBCO interconnects, as opposed to large area, low-aspect ratio superconducting vias that have been fabricated with marginal success previously.

Due to the grain boundary problems associated with making very wide, sloping superconducting vias through a thick dielectric layer, alternative methods have to be explored to create the compact, high-aspect ratio vias necessary for fast, high density HTS MCMs.

Yttria stabilized zirconia (YSZ) was chosen as the material for providing a diffusion barrier/buffer layer between the superconductor and the interlevel dielectric material, silicon dioxide, because of its diffusion barrier properties as well as having a close lattice spacing and coefficient of thermal expansion (CTE) match to YBCO. Silicon dioxide was chosen as the interlevel dielectric material because of its low dielectric constant and well developed deposition and etching processes.

## **Experimental Details**

Our MCM-D substrate was constructed of two layers of laser-ablated YBCO interconnects separated by a multilayer dielectric consisting of  $SrTiO_3/SiO_2/YSZ$ . We are able to attain critical current densities  $> 5 \times 10^5 \text{ A/cm}^2$  in both YBCO layers. The laser-ablated  $SrTiO_3$  (STO) and ion beam assisted laser-ablation deposited (IBAD) YSZ (yttria-stabilized zirconia) layers were  $\sim 0.5 \ \mu \text{m}$  thick while the reactively-sputtered  $SiO_2$  ranges between 4 and 5  $\mu \text{m}$  thick. The multilayered thin film structure is fabricated on 15 mm x 15 mm LaAlO3 and YSZ substrates.

The HTS MCM was layed out as shown in Figure 2 on the following page.

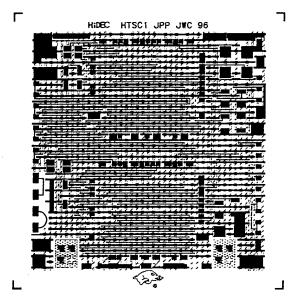


Figure 2. Layout of a 2 layer 15 mm x 15 mm HTS MCM-D substrate.

The 2.25 cm<sup>2</sup> substrate consists of two separate ring oscillators built using YBCO interconnects between two digital GaAs bare die (4.4 mm x 3.5 mm). The first ring oscillator is connected using the smallest possible interconnection, whereas, the second is connected by a much longer interconnect. performance comparison between the two oscillators is planned for future work. There are also bond pads on the substrate for mounting various sizes of surface mount decoupling capacitors and terminating resistors. A prototype of our ring oscillator using one of the GaAs bare die wirebonded to 20 mil wide copper traces on a PC board was tested at liquid nitrogen temperature and was found to oscillate at ~250 MHz. Based on this result, our HTS MCM ring oscillator is estimated to operate at about the same frequency.

The via fabrication process is shown in Figure 3. The etching involves a 500 eV ion mill through the top YSZ buffer layer, which is followed by a reactive ion etch (RIE) through the SiO2 interlevel dielectric selectively stopping at the barrier layer of STO. To complete the etching process, a 500 eV ion mill is done to etch through the STO and into the underlying YBCO. The final milling is very nonselective and requires close observation to keep from overetching through the bottom layer of YBCO. When depositing the top layer of YBCO at ~700° C, whatever material is deposited on the via sidewalls is presumably corroded due to interdiffusion of Si from SiO, into the YBCO but, presumably, does not affect the quality of the via. The subsequent in situ deposition of ~2000 Å of Au by laser ablation creates low resistance contacts without having to do a high temperature anneal in oxygen as was described by Ekin et al. [4]. This Au capping layer also acts as a passivation layer for the YBCO. In similar structures, contact resistivities of less than  $10^{-7}$   $\Omega$ -cm² have consistently been attained. An additional 1.5-2.0  $\mu m$  of Au is deposited over the existing YBCO/Au and then patterned using ion milling and photoresist as a mask.

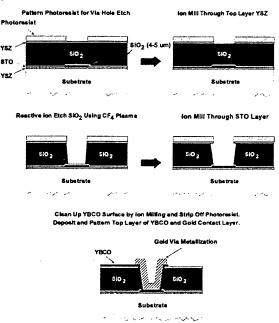


Figure 3. HTS via fabrication process.

This type of via structure has several advantages over previously demonstrated superconducting vias for use in HTS MCMs [2,3]. Since HTS thin films have to be deposited on planar surfaces or gradual slopes to maintain a reasonable current density, due to grain boundary problems, they require gradually sloped via holes that take up a wide area. By using a noble metal, compact, high-aspect ratio vias can be fabricated reliably.

Ultrasonic Al wire bonds were then made between YBCO/Au bond pads on the substrate and a wire bondable PC board. Via chain resistance was measured using a conventional 4-point contact configuration and measuring the voltage drop across the vias while passing DC current through it. The resistance vs. temperature of a ~0.5 cm long via chain structure with ten 40 µm square vias interconnecting 50 µm wide YBCO lines is shown in Figure 4. The room temperature resistance was measured to be about 515  $\Omega$ , and upon cooling to 78.5 K, the resistance dropped to about 87  $\Omega$ . As is shown in this figure, there are two separate superconducting transitions occurring at about 89 K and 80 K, which correspond to the top and bottom layer YBCO transitions. At 78.5 K, the interconnects had not yet become fully superconducting.

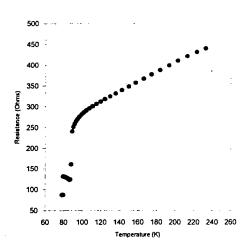


Figure 4. Temperature transition of a chain of ten 40 µm wide vias.

## II. Flip-Mesh HTS MCM

The Flip-Mesh Superconducting Multi Chip Module (MCM) is an alternative to the conventional multi-layer superconducting MCM. It is desired that a superconducting MCM be fabricated using High-Temperature Superconductor (HTS) materials, with which such an MCM can be cooled using liquid nitrogen. However, many difficulties arise in the formation of multiple superconducting planes separated by dielectric layers on a single substrate. The crystalline nature of HTS materials such as Yttrium-Barium-Copper-Oxide (YBCO) requires that the deposition surface be closely matched to the HTS material in crystalline structure.

The high temperatures needed to form HTS materials requires that the other HTS MCM materials be matched with the superconductor in coefficient of thermal expansion (CTE), and not crack or delaminate at such high temperatures. These requirements lead to a complex stack of materials in order to create a multiple-superconducting-plane MCM interconnect structure. This combination of materials also complicates selective patterning processes with respect to the HTS material.

## Flip-Mesh Basics

The fundamental concept of Flip-Mesh is that instead of depositing multiple HTS layers on a single substrate and connecting the layers by vias, single HTS layers are deposited on multiple substrates, and opposing superconducting layers on separate substrates

are connected by flip-chip technology. This reduces the number of high-temperature processing steps to one, eliminating most of the difficulties in the multi-layer structure. However, the use of I/O technology to form vias limits the ultimate density of the Flip-Mesh Superconducting MCM.

In the multilayer MCM, Ion Beam Assisted Deposition (IBAD) [5] is used to form an oriented buffer layer so that an HTS film can be grown on an amorphous surface. This also allows the use of an amorphous substrate. Since Flip-Mesh requires only one superconducting plane per substrate, it is an ideal application for depositing HTS films on amorphous substrates. Amorphous substrates are considerably less costly than single-crystal substrates.

## Flip-Mesh Substrate Arrangement

There are three substrates in a Flip-Mesh module. The main substrate contains x-plane interconnect and bonding sites for chips. Two smaller secondary substrates contain y-plane interconnect, and are "flipped" onto the main substrate. The chip bonding sites are between the secondary substrates. I/O pads are located on the outside edges of the main substrate. The Flip-Mesh substrate configuration is shown in Figure 5. As with the multilayer MCM, the Interconnected Mesh Power System (IMPS) topology [6] allows complete power, ground, and signals to be formed in two conducting planes. The term "Flip-Mesh" is derived from the flipping of IMPS-mesh interconnect planes to form an MCM interconnect structure.

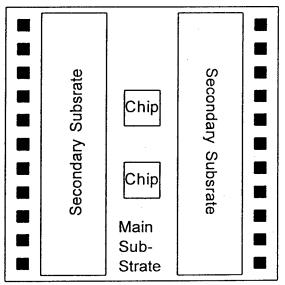


Figure 5. Flip-Mesh substrate configuration.

## Flip-Mesh Substrate Processing

YBCO films are formed by laser ablation [7] on 1/2" or 1" square single-crystal yttria-stabilized zirconia (YSZ) or IBAD YSZ-buffered alumina substrates. The YBCO films are then patterned by argon ion milling [8] using conventional photoresist as a mask. The fact that ion milling is non-selective is not important in Flip-Mesh, since the underlying layer is always the substrate, which can be over-etched. The ion milling system is equipped with a water cooled sample stage to prevent YBCO or photoresist damage due to excessive heating from the ion milling.

Gold pads are then formed where electrical contact to YBCO is desired. A lift-off process is employed in which 2  $\mu$ m of gold is sputter deposited onto a patterned photoresist layer. The Flip-Mesh substrates are exposed to a brief low-energy ion milling, which serves to prime the exposed YBCO surface for the gold deposition. After deposition, the photoresist layer is lifted off in an ultrasonic bath of acetone, leaving the gold pads on the YBCO. The lift-off process again avoids selective etching with respect to the YBCO. The Flip-Mesh substrates are then annealed at 600 °C for I hour in 500 Torr of oxygen to form a sturdy low-resistance contact.

The critical element of Flip-Mesh is the material used for the vias and the method used to form the interconnection. Figure 6 shows a cross-section of a Flip-Mesh via bump.

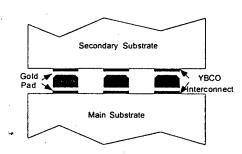


Figure 6. Flip-Mesh via cross-section.

The initial approach was to form gold balls using a ball bonding machine, and then press the substrates together while heating. Ball placement was found to be tedious, but workable. It was discovered, however, that the ball bonding process would often damage the underlying YBCO. This was not obvious unless the gold ball detached from the bonding pad. Ball detachment can be avoided by attaching to a bonding pad that is at least 1.5 times the size of the ball, but it is believed that this only disguises the damage.

Typical gold ball sizes range from 70  $\mu$ m to 100  $\mu$ m in diameter. The size of the Flip-Mesh bonding pad is 100  $\mu$ m. Since density is already a limiting factor in the Flip-Mesh approach, increasing the via size is not desirable. It was also found that the extreme heat and pressure required to make an acceptable contact between the Flip-Mesh substrates caused the YBCO to become non-superconducting. The YBCO could be repaired by annealing, but the substrates would detach in the process.

The second assembly method attempted was to individually place preformed indium spheres. Indium was chosen because of its decent conductivity and low melting point. It was quickly discovered, however, that indium is far too soft to be handled mechanically, and no modules could be formed using this method. Stencil printing was then determined to be the ideal method for placing Flip-Mesh via bumps. A batch process would certainly be desirable, but the small via size (4 mil) and pitch (8 mil) puts severe limitations on this technology.

The first material to be screen printed was conductive epoxy, but this material was unable to meet the density requirement. The epoxy bumps would flatten and create shorts. Further work with the viscosity of the epoxy may lead to a useful application.

The next stencil printing material used was tin/lead solder. A special high-density solder was acquired, and worked nicely, but standard tin/lead solder has a leaching problem with the gold contact pads. Modules fabricated in this process detached within hours due to the leaching. Another solder paste was then acquired, which contained an additional 2% silver to prevent gold leaching.

After screen printing solder pads to the main substrate, the secondary substrates are aligned to the main substrate, and the solder is reflowed. The current Flip-Mesh material components are laser-ablated YBCO on single-crystal YSZ substrates with gold contact pads interconnected by screen printed tin/lead/silver solder bumps.

## Initial Flip-Mesh Circuit

The initial Flip-Mesh circuit is a ring oscillator formed from 2 quad-XOR HCMOS chips. The first XOR gate has one input tied high, which turns it into an inverter. The other gates have one input tied low, which makes them buffers. This arrangement permits the number of gates in the loop to be adjusted from 2 to 8, allowing different speeds of oscillation.

The IMPS power and ground stripes are 250  $\mu$ m wide, the signals are 50  $\mu$ m wide, and the spacing between the two is 50  $\mu$ m. The main substrate is 10

mm x 10 mm, and the secondary substrates are 2.5 mm x 10 mm. As was discussed previously, the contact pads are 100  $\mu$ m x 100  $\mu$ m. The XOR chips are approximately 1mm x 1mm each.

## Flip-Mesh Assembly and Testing

After a Flip-Mesh substrate module is completed, the XOR chips are attached using thermoplastic tape. The leads of the chips are then aluminum wire bonded to the main substrate. The number of gates in the oscillator loop is selected by a wire bond in the center of the main substrate. The assembled Flip-Mesh module is then attached to a test board using thermoplastic tape. The I/O pads of the module are then aluminum wire bonded to the test board.

When complete, the test board is attached to an oscilloscope and power supply, measuring the output signal of the first XOR gate. The module is then slowly immersed in a small dewar of liquid nitrogen.

## Conclusions

In summary, 40 µm YBCO/Au via chain structures have been characterized for use in an MCM-D substrate. The preliminary work shown here is to be improved upon by improving the quality of the YBCO layers, lowering the contact resistances, and possibly improving the step coverage of Au through the via by increasing its thickness. We are hoping to have an HTS MCM-D substrate fabricated in the near future. The performance of this MCM will be compared to that of a nearly identical Al interconnect module operating at liquid nitrogen temperature.

Thus far, functional Flip-Mesh modules have been fabricated only with metal interconnects. These modules were built on glass substrates with gold/titanium-tungsten metallization, and the substrates were interconnected with gold balls formed by a ball bonder. These units were tested both at room temperature and while immersed in liquid nitrogen with 2 to 8 gates in the oscillator loop. As would be expected, the modules ran faster at cryogenic temperature. While the gold ball vias worked adequately for a metal module, they were found to be

incompatible with YBCO due to damage caused by the attachment process. The stencil printing processes discussed are under investigation to find a YBCO-compatible process. It will be interesting to compare the performance of the HTS Flip-Mesh to the cryogenic metal Flip-Mesh.

Despite the great processing complexity involved with fabricating an HTS MCM, great progress is being made toward achieving practical MCM substrates utilizing these novel materials.

## References

- [1] S. K. Tewksbury, L. A. Hornak, L. A. Tewksbury, and L. Chen, "A System-Level Evaluation of HTS Interconnections on MCMs for High Performance VLSI Systems", Journal of Microelectronic Systems Integration, Vol. 4, No. 2, (1996).
- [2] M. J. Burns, K. Char, B. F. Cole, W. S. Ruby, and S. A. Sachtjen, "Multichip module using multilayer YBa<sub>2</sub>Cu<sub>3</sub>O<sub>7-8</sub> interconnects", Appl. Phys. Lett., **62** 1435 (1993).
- [3] B. Santo, "Superconducting MCM demo'd", Electronic Engineering Times, August 10 (1992).
- [4] J. W. Ekin, S. E. Russek, C. C. Clickner, and B. Jeanneret, "In situ noble metal YBa<sub>2</sub>Cu<sub>3</sub>O<sub>7-8</sub> thin-film contacts", Appl. Phys. Lett., **62** 369 (1993).
- [5] G. Florence, "Fabrication and Characterization of Superconducting Yttrium Barium Copper Oxide Multilayer Structures", Ph.D. Dissertation, University of Arkansas, (1995).
- [6] L.W. Schaper, S. Ang, Y.L. Low, and D. Oldham, "Electrical Characterization of the Interconnected Mesh Power System (IMPS) MCM Topology", Proceedings of the 44th Electronic Components & Technology Conference, Washington, D.C., May 1-4, pp. 791-795, (1994).
- [7] S. Afonso et al., "Magnetic Field and Temperature Dependence of Critical Current Densities in Multilayer YBa<sub>2</sub>Cu<sub>3</sub>O<sub>7-a</sub>\_Films", Journal of Applied Physics, Vol. 79, No. 8, pp. 6593-6595, (1996).
- [8] S. Scott, "Ion Milling of Yttrium-Barium-Copper-Oxide for Interconnects in a Superconducting Multichip Module", M.S.E.E. Thesis, University of Arkansas, (1994).

6th International Conference and EXHIBITION ON Modules MULTICHIP The Adam's Mark Hotel, Denver, Colorado SPONSORED BY: THE INTERNATIONAL Microelectronics AND PACKAGING SOCIETY (IMAPS) THE INTERNATIONAL ELECTRONICS INDUSTRIES Association (EIA) IEEE/CPMT APRIL 2-4, 1997 COMPONENTS, PACKAGING, Manufacturing Technology SOCIETY

Scaling New Heights!

# PRESENTATION: paper



# FABRICATION AND CHARACTERIZATION OF A HIGH TEMPERATURE SUPERCONDUCTING MULTICHIP MODULE

J. W. Cooksey, W. D. Brown, L. W. Schaper, R. G. Florence and S. S. Scott High Density Electronics Center/Department of Electrical Engineering, University of Arkansas 600 W. 20th Street, Fayetteville, AR 72701

S. Afonso

High Density Electronics Center/Department of Physics, University of Arkansas Fayetteville, AR 72701

A process for fabricating high temperature superconducting (HTS) multichip module - deposited (MCM-D) substrates has been developed and tested. The module consists of two digital gallium arsenide bare die connected by  $YBa_2Cu_3O_{7.\delta}$  (YBCO) HTS interconnects to form two ring oscillators on a 2.25 cm² MCM-D substrate. The interconnections consist of two wiring layers of YBCO separated by a 4-5  $\mu$ m silicon dioxide interlevel dielectric. The 50  $\mu$ m wide signal lines are routed between 150  $\mu$ m power and ground lines with 75  $\mu$ m spacings to form an interconnected mesh power system (IMPS). Connection between the two YBCO layers is accomplished with low contact resistance 40  $\mu$ m gold vias through the interlevel dielectric layer. Ultrasonic Al wire bonds serve as electrical connections to gold/YBCO bond pads on the MCM substrate.

## INTRODUCTION

One of the most promising applications for high temperature superconductors (HTSs) is as signal interconnects between integrated circuits (ICs) on multichip module (MCM) substrates. Unlike that of VLSI technologies where smaller feature sizes in successive generations allow interconnect lengths and power dissipation to be reduced, MCMs will not have that same luxury. As the complexity of ICs advances, both the pinout count per IC and the operating frequency will increase. However, MCM normal metal interconnections will be required to grow in length and will not be allowed to reduce in cross-sectional area. On MCM-D substrates, typical copper or aluminum interconnection dimensions are about 2 to 5 µm in thickness and between 15 and 30 µm wide. The resistivity of copper or aluminum decreases by at least a factor of 7 when decreasing the temperature from 300 K to 77 K (liquid nitrogen temperature), which allows smaller cross-section interconnects to be fabricated on cryogenically cooled MCMs. In order to increase the

wiring density in MCMs beyond that of cryo-cooled MCMs and improve the chip-to-chip bottleneck at high frequencies, alternatives to conventional metal interconnects must be considered [1].

HTS interconnections with negligible resistivity at operating frequencies of several tens of GHz and lower have great potential to reduce the interconnection line cross-section further with typical thicknesses being less than 1 μm and widths less than 2 μm for MCM applications. The critical current density of HTS interconnects, which limits the line's minimum cross-section, is similar in value to the maximum current density allowed in Al interconnects to inhibit electromigration. These small, low resistance interconnects offer significant performance advantages over normal metal interconnects for MCM-D technology using CMOS or GaAs integrated circuits which have enhanced chip level performance at liquid nitrogen temperatures (77 K). An added benefit of HTS lines is the reduced capacitive coupling between adjacent interconnections (due to their reduced thickness) which allows the lines to be spaced more closely together. The reduced cross-section of HTS interconnects should allow a significant increase in packing density and a corresponding decrease in the number of interconnect layers required to achieve the same functionality with normal metal interconnects.

## HTS MCM DESCRIPTION

Our development has centered around the HTS material YBa<sub>2</sub>Cu<sub>3</sub>O<sub>7-8</sub> (YBCO) which has a transition temperature of about 91 K (well above the boiling point of liquid nitrogen, 77 K) and critical current densities typically greater than 5 x 10<sup>5</sup> A/cm<sup>2</sup>. A cross-section of our proposed HTS MCM is shown in Figure 1.

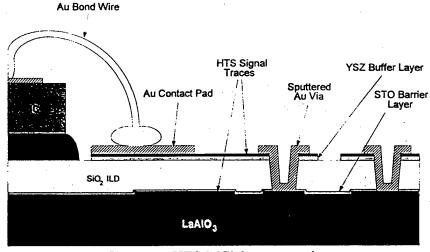


Figure 1: HTS MCM cross-section.

This novel structure has several key features that provide advantages over previously demonstrated HTS MCMs [2,3]. These advantages are:

- (1) the utilization of an Interconnected Mesh Power System (IMPS) topology [4] that is ideal for HTS multilayer fabrication because it allows an MCM to be constructed with only two layers of interconnects as opposed to the four that are traditionally used: x-signal, y-signal and ground and power planes;
- (2) a thick ( $\sim 5 \mu m$ ) layer of SiO<sub>2</sub> that is sandwiched between a thin buffer layer dielectric and a thin diffusion barrier layer dielectric to form a composite interlevel dielectric that is compatible with multilayer YBCO processing while allowing controlled impedance ( $Z_o = 50 \Omega$ ) lines to be fabricated, which are necessary for high speed signal propagation;
- (3) chemical-mechanical polishing to create a planar SiO<sub>2</sub> surface for deposition of a high quality top level superconductor/buffer layer;
- (4) high-aspect ratio, low contact resistance vias that utilize noble metals to form contacts between the two layers of YBCO interconnects, as opposed to large area, low-aspect ratio superconducting vias that have been fabricated with marginal success previously.

Due to the grain boundary problems associated with making very wide, sloping superconducting vias through a thick dielectric layer, alternative methods have to be explored to create the compact, high-aspect ratio vias necessary for fast, high density HTS MCMs.

Yttria stabilized zirconia (YSZ) was chosen as the material to provide a diffusion barrier/buffer layer between the superconductor and the interlevel dielectric material, silicon dioxide, because of its diffusion barrier properties as well as its close lattice spacing and coefficient of thermal expansion (CTE) match to YBCO. Silicon dioxide was chosen as the interlevel dielectric material because of its low dielectric constant and well developed deposition and etching processes.

## EXPERIMENTAL DETAILS AND RESULTS

The HTS MCM-D substrate was layed out as shown in Figure 2. The 2.25 cm<sup>2</sup> substrate consists of two separate ring oscillators built using YBCO interconnects to connect two digital GaAs bare die (4.4 mm x 3.5 mm). The first ring oscillator is connected using the shortest possible signal line, whereas the second is connected by a much longer interconnect. A performance comparison between the two oscillators is planned for future work. There are also bond pads on the substrate for mounting various size surface mount decoupling capacitors and terminating resistors. A prototype of our ring oscillator using one of the GaAs bare die wirebonded to 20 mil wide copper traces on a PC board was tested at liquid nitrogen temperature and was found to oscillate at ~250 MHz. Based on this result, our HTS MCM ring oscillator is estimated to operate at about the same frequency.

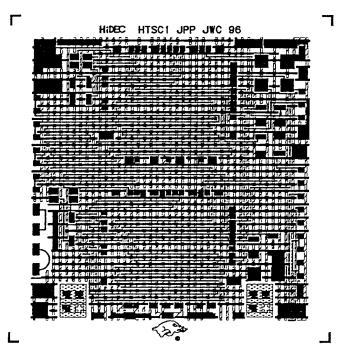
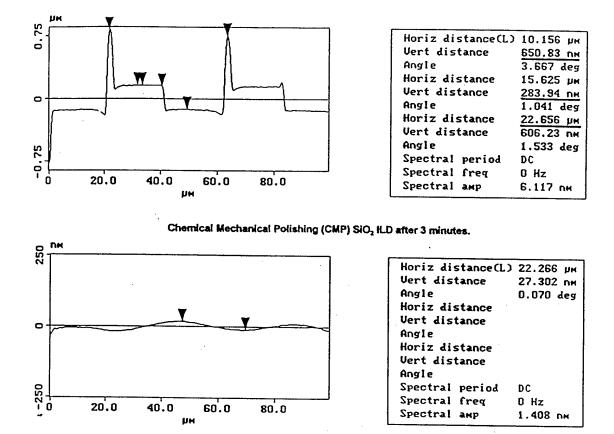


Figure 2: Layout of a 2 layer 15 mm x 15 mm HTS MCM-D substrate.

The HTS substrate was constructed of two layers of laser-ablated YBCO interconnects separated by a multilayer dielectric consisting of SrTiO<sub>3</sub>/SiO<sub>3</sub>/YSZ. The details of this technique will be described elsewhere [5]. The first layer of YBCO was deposited on a 15 mm x 15 mm single crystal substrate of LaAlO<sub>3</sub> or YSZ at a temperature of ~750° C to a thickness of 3000-3500 Å using a Lambda Physik LPX300 ArF excimer laser ( $\lambda = 193$  nm) focused onto a rotating 1" diameter stoichiometric YBCO target. For thin film YBCO deposition, a pulse energy density of ~3-4 J/cm<sup>2</sup> at a 6 Hz repetition rate was used in a deposition chamber maintained at an oxygen pressure of 150-200 mTorr. We are able to attain critical current densities > 5 x 10<sup>5</sup> A/cm<sup>2</sup> in both YBCO layers. The YBCO was patterned using photolithography and 500 eV ion milling with a 30 mA beam current. The 3000-4000 Å thick SrTiO<sub>3</sub> (STO) diffusion barrier layer was laser-ablated at a pulse energy density of ~3-4 J/cm<sup>2</sup> with an 8 Hz repitition rate at a substrate temperature of ~650° C. The SiO<sub>2</sub> interlevel dielectric was deposited to a thickness of 4-5 μm by reactively sputtering a 3" diameter pure silicon target at an RF power of 180 W in a gas mixture of 83% argon/27% oxygen at a deposition pressure of 16 mTorr. The films were deposited at room temperature at a deposition rate of ~0.55 µm/hr.

After the SiO<sub>2</sub> deposition, the sharp step edges at the surface of the dielectric from nonconformal coating of the patterned bottom layer of YBCO must be smoothed out or planarized. This process is necessary to minimize the YBCO grain boundary dislocations

that would occur at 90° step edges and thereby to insure good quality layers of IBAD YSZ and YBCO are formed in the top interconnect layer [6]. To accomplish the  $SiO_2$  step edge reduction, a chemical-mechanical polishing (CMP) process is performed using an alkaline (pH ~11) slurry consisting of ~100 nm silica particles in a mixture of potassium hydroxide and DI water [7]. The solution is dispersed onto a Rodel IC1000 porous, urethane polishing pad spinning at a rate of 50 rpm. The samples are mounted to a holder and rotated at a rate of 65-70 rpm opposite the direction of the polishing pad. Polishing at a force of 10 lb for 3 minutes results in a reduction of a 935 nm tall spike and a sharp 284 nm step edge to a 27 nm hump as shown in Figure 3.



<u>Figure 3</u>. Step height reduction using silicon dioxide chemical-mechanical polishing (CMP) process.

Following planarization and cleanup, a layer of YSZ was deposited using an ion beam assisted deposition (IBAD) technique along with laser-ablation to attain a textured film at room temperature [8]. Briefly, the technique involves positioning an ion gun at a distance of ~14 cm from the substrate and at an angle of 55° from the substrate normal. Argon gas is flowed through the ion gun at a rate of 20 sccm and directed at the sample at a beam

energy of 250 eV and beam current of 15 mA while the laser deposition is occurring. The final thickness of the YSZ film was ~3000-4000 Å.

The via fabrication process is shown in Figure 4.

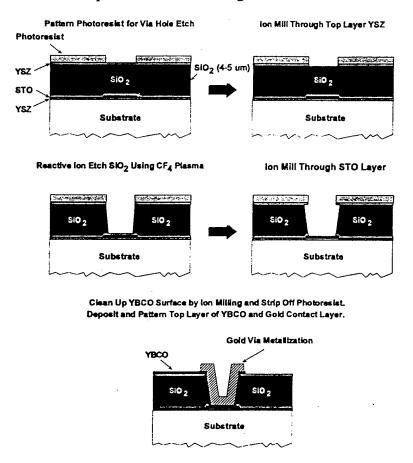


Figure 4: HTS via fabrication process.

The etching involves a 500 eV ion mill with a beam current of 30 mA through the top YSZ buffer layer, which is followed by a reactive ion etch (RIE) using a gas mixture of 85% CF<sub>4</sub>/15% O<sub>2</sub> through the SiO<sub>2</sub> interlevel dielectric selectively stopping at the barrier layer of STO. To complete the etching process, a 500 eV ion mill at a beam current of 30 mA is done to etch through the STO and into the underlying YBCO. The final milling is very nonselective and requires close observation to keep from etching through the bottom layer of YBCO. When depositing the top layer of YBCO at ~700° C, whatever material is deposited on the via sidewalls is presumably corroded due to interdiffusion of Si from SiO<sub>2</sub> into the YBCO [9] but, presumably, does not affect the quality of the via. The subsequent in situ deposition of ~2000 Å of Au by laser ablation creates low resistance contacts without having to do a high temperature anneal in oxygen as was described by Ekin et al. [10]. This

Au capping layer also acts as a passivation layer for the YBCO. In similar structures, contact resistivities of less than  $10^{-7} \,\Omega$ -cm² have consistently been attained. An additional 1.5-2.0  $\mu$ m of Au is deposited over the existing YBCO/Au and then patterned using ion milling and photoresist as a mask. This type of via structure has several advantages over previously demonstrated superconducting vias for use in HTS MCMs [2,3]. Since HTS thin films have to be deposited on planar surfaces or gradual slopes to maintain a reasonable current density, due to grain boundary problems, they require gradually sloped via holes that take up a wide area. By using a noble metal, compact, high-aspect ratio vias can be fabricated reliably. The additional resistance in the vias (series resistance and contact resistance) will be very small and will not give rise to unwanted RC delay provided there are not an excessive number of vias in the signal path.

Ultrasonic Al wire bonds were then made between YBCO/Au bond pads on the substrate and a wire bondable PC board. The via chain resistance was measured using a conventional 4-point contact configuration by measuring the voltage drop across the vias while passing DC current through it. The resistance vs. temperature of a ~0.5 cm long via chain structure with ten 40  $\mu$ m square vias interconnecting 50  $\mu$ m wide YBCO lines is shown in Figure 5. The room temperature resistance was measured to be about 515  $\Omega$ , and upon cooling to 78.5 K, the resistance dropped to about 87  $\Omega$ . As shown in this figure, there are two separate superconducting transitions occurring at about 89 K and 80 K which correspond to the top and bottom layer YBCO transitions. At 78.5 K, the interconnects had not yet become fully superconducting.

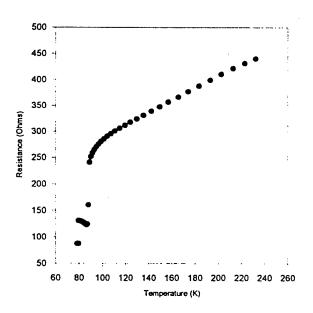


Figure 5: Temperature transition of a chain of ten 40 µm wide vias.

## **CONCLUSIONS**

In summary, 40  $\mu$ m YBCO/Au via chain structures have been characterized for use in an MCM-D substrate. The preliminary work shown here is to be improved upon by improving the quality of the YBCO layers, lowering the contact resistances, and possibly improving the step coverage of Au through the via by increasing its thickness. We are hoping to have an HTS MCM-D substrate fabricated in the near future. The performance of this MCM will be compared to that of a nearly identical Al interconnect module operating at liquid nitrogen temperature.

Despite the processing complexity involved with fabricating an HTS MCM, great progress is being made toward achieving practical MCM substrates utilizing these novel materials.

## REFERENCES

- [1] S. K. Tewksbury, L. A. Hornak, L. A. Tewksbury, and L. Chen, Journal of Microelectronic Systems Integration 4, 95 (1996)
- [2] M. J. Burns, K. Char, B. F. Cole, W. S. Ruby, and S. A. Sachtjen, Appl. Phys. Lett. 62, 1435 (1993)
- [3] B. Santo, Electronic Engineering Times, August 10 (1992)
- [4] L.W. Schaper, S. Ang, Y.L. Low, and D. Oldham, Proceedings of the 44th Electronic Components & Technology Conference, Washington, D.C., May 1-4, 791 (1994)
- [5] S. Afonso, K. Y. Chen, Q. Xiong, Y. Q. Tang, G. J. Salamo, F. T. Chan, J. Cooksey, S. Scott, R. G. Florence, S. Ang, W. D. Brown, and L. W. Schaper (unpublished)
- [6] F. C. Wellstood, J. J. Kingston, and J. Clarke, J. Appl. Phys. 75, 683 (1994)
- [7] W. J. Patrick, W. L. Guthrie, C. L. Standley, and P. M. Schiable, J. Electrochem. Soc. 138, 1778 (1991)
- [8] R. G. Florence, S. S. Ang, and W. D. Brown, Supercond. Sci. Technol. 8, 546 (1995)
- [9] H.-U. Habermeier, G. Mertens, and G. Wagner, Vacuum 4, 859 (1990)
- [10] J. W. Ekin, S. E. Russek, C. C. Clickner, and B. Jeanneret, Appl. Phys. Lett. 62, 369 (1993)

# PETTO CHE STORY OF THE STORY OF

## CALL FOR PAPERS

# FOURTH SYMPOSIUM ON LOW TEMPERATURE ELECTRONICS AND HIGH TEMPERATURE SUPERCONDUCTIVITY

191st Electrochemical Society Meeting, Montreal, Canada, May 4-9, 1997

This symposium is intended to provide a forum for discussion of the latest developments and evolutions in the field of Low Temperature Electronics and High Temperature Superconductivity. Beside providing an opportunity to review developments since the 3rd symposium, which took place two years ago in Reno, it will focus on new aspects of electronic materials, devices, and systems operating at cryogenic temperatures. The symposium will consist of both invited and contributed papers, and the publication of a proceedings volume is being considered.

Contributed papers are solicited in the following areas:

- 1. Fundamentals; theoretical limitations and restrictions (speed, power, performance), superconducting materials (high temperature superconductors, thin films preparation, physical phenomena, new low temperature effects)
- 2. Devices; semiconductor components (MOS, bipolar, SOI, MODFETs ...), superconducting devices, SQUIDs, infrared components, optoelectronic devices, hybrid and monolithic integration, nanostructures and novel devices, processing, modelling
- 3. Circuits; integrated circuits; digital and analog, charge coupled devices and read out circuits, low temperature systems, design considerations, superconducting circuits
- 4. Systems; packaging, assembly and interconnections, reliability performance, low-room temperature interfaces (electrical, mechanical, thermal), heat transfer and refrigeration systems, device and system testing
- 5. Applications; computer and telecommunications, space applications, infrared astronomy, instrumentation, low temperature measurement systems

An Extended Abstract must be submitted to one of the Symposium Organizers, not later than Number 1, 1996. The original of the abstract must be sent to the Electrochemical Society Headquarters office. Notification of acceptance and instructions for the preparation of the manuscripts will be given by December 15. The full manuscripts will be required by January 31, 1997. Suggestions and inquiries should be sent to the Symposium Organizers.

C.L. Claeys	5.1. Raider
IMEC	IBM, TJ W
Kapeldreef 75	P.O. Box 2
B-3001 Leuven	Yorktown
Belgium	NY 10598
Fax: 32 16 281214	Fax: 914 9
Tel: 32 16 281328	Tel: 914 94
clacys@imec.bc	raider@wa

S.I. Raider	M.J. Deen
IBM, TJ Watson	U. Simon Fraser
P.O. Box 218	Burnaby
Yorktown Height	British Columbia
NY 10598 USA	Canada V5A 1S6
Fax: 914 945-2018	Fax: 604 291-495
Tel: 914 945-3822	Tel: 604 291-3248
raider@watson.ibm.com	jamal@cs.sfu.ca

W.D. Brown	R.K. Kirschman
U. of Arkansas	P.O. Box 391716
Bell Eng. Centre	Mountain View
Fayetteville	CA 94039
AŘ 72701 USA	USA
Fax: 501 575-7967	Fax: 415 964-5763
Tel: 501 575-3005	Tel: 415 962-0200
wdb@engr.engr.vark.edu	randall@infoserv.co



## THE FLIP-MESH SUPERCONDUCTING MCM

S. S. Scott, S. S. Ang, W.D. Brown, L. W. Schaper, S. Afonso High Density Electronics Center University of Arkansas, Fayetteville AR 72701

One of the many possible applications of high-temperature superconducting (HTS) thin films is as interconnect in a hybrid multichip module (MCM). Such a module would consist of a substrate containing superconducting interconnect and conventional CMOS circuitry chips. Since HTS thin films are crystalline in nature and deposited at high temperatures, many difficulties arise in the formation of epitaxial multi-layer superconducting structures. The Flip-Mesh Superconducting MCM provides an alternative to a multi-layer substrate by interfacing multiple single-layer substrates, thereby reducing the epitaxy requirement to one layer per substrate. This substrate interfacing is accomplished by forming X-plane interconnect on one substrate and Y-plane interconnect on another, and connecting them using I/O technology. The reduced epitaxy requirement of Flip-Mesh also makes the implementation of amorphous substrates more The Interconnected Mesh Power System (IMPS) topology used so that power, ground, and signals can be fabricated on two planes.

## **FLIP-MESH BASICS**

The Flip-Mesh Superconducting MCM is an alternative to the conventional multilayer superconducting MCM. It is desired that a superconducting MCM be fabricated using HTS materials, with which such an MCM can be cooled using liquid nitrogen. However, many difficulties arise in the formation of multiple superconducting planes separated by dielectric layers on a single substrate. The crystalline nature of HTS materials such as yttrium-barium-copper-oxide (YBCO) requires that the deposition surface be closely matched to the HTS material in crystalline structure.

The high temperatures needed to form HTS materials requires that the other HTS MCM materials be matched with the superconductor in coefficient of thermal expansion (CTE), and not crack or delaminate at such high temperatures. These requirements lead to a complex stack of materials in order to create a multiple-superconducting-plane MCM interconnect structure. This combination of materials also complicates selective patterning processes with respect to the HTS material.

The fundamental concept of Flip-Mesh is that instead of depositing multiple HTS layers on a single substrate and connecting the layers by vias, single HTS layers are deposited on multiple substrates, and opposing superconducting layers on the separate substrates are connected by flip-chip technology. This reduces the number of high-temperature processing steps to one, eliminating most of the difficulties in the multi-layer structure. However, the use of I/O technology to form vias limits the ultimate density of the Flip-Mesh Superconducting MCM.

In the multilayer MCM, ion beam assisted deposition (IBAD) [1] is used to form an oriented buffer layer so that an HTS film can be grown on an amorphous surface. This also allows the use of an amorphous substrate. Since Flip-Mesh requires only one superconducting plane per substrate, it is an ideal application for depositing HTS films on amorphous substrates. Amorphous substrates are considerably less costly than single-crystal substrates.

## FLIP-MESH SUBSTRATE ARRANGEMENT

There are three substrates in a Flip-Mesh module. The main substrate contains x-plane interconnect and bonding sites for chips. Two smaller secondary substrates contain y-plane interconnect, and are "flipped" onto the main substrate. The chip bonding sites are between the secondary substrates. I/O pads are located on the outside edges of the main substrate. The Flip-Mesh substrate configuration is shown in Figure 1. As with the multilayer MCM, the IMPS topology [2] allows complete power, ground, and signals to be formed in two conducting planes. The term "Flip-Mesh" is derived from the flipping of IMPS-mesh interconnect planes to form an MCM interconnect structure.

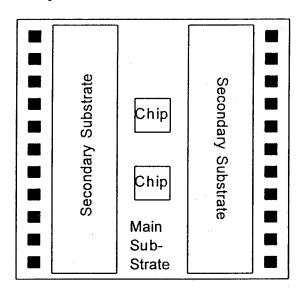


Figure 1: Flip-Mesh Substrate Configuration

## FLIP-MESH SUBSTRATE PROCESSING

YBCO films are formed by laser ablation [3] on 1/2" or 1" square single-crystal yttria-stabilized zirconia (YSZ) or IBAD YSZ-buffered alumina substrates. The YBCO films are then patterned by argon ion milling [4] using conventional photoresist as a mask. The fact that ion milling is non-selective is not important in Flip-Mesh, since the underlying layer is always the substrate, which can be over-etched. The ion milling system is equipped with a water cooled sample stage to prevent YBCO or photoresist damage due to excessive heating from the ion milling.

Gold pads are then formed where electrical contact to YBCO is desired. A lift-off process is employed, where 2  $\mu m$  of gold is sputter deposited on a patterned photoresist layer. The Flip-Mesh substrates are exposed to a brief low-energy ion milling, which serves to prime the exposed YBCO surface for the gold deposition. After deposition, the photoresist layer is lifted off in an ultrasonic bath of acetone, leaving the gold pads on YBCO. The lift-off process again avoids selective etching with respect to YBCO. The Flip-Mesh substrates are then annealed at 600 °C for 1 hour in 500 torr of oxygen to form a sturdy low-resistance contact.

The critical element of Flip-Mesh is the material used for the vias and the method used to form the interconnection. Figure 2 shows a cross-section of Flip-Mesh via bumps.

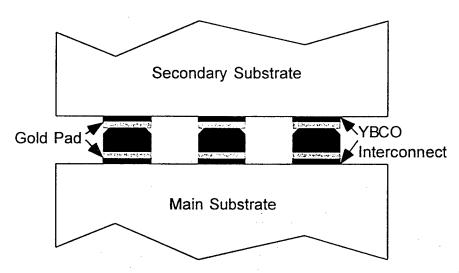


Figure 2: Flip-Mesh Via Cross-Section

The initial approach was to form gold balls using a ball bonding machine, and then press the substrates together while heating. Ball placement was found to be tedious, but workable. It was discovered, however, that the ball bonding process would often damage the underlying YBCO. This was not obvious unless the gold ball detached from

the bonding pad. Ball detachment can be avoided by attaching to a bonding pad that is at least 1.5 times the size of the ball, but it is believed that this only disguises the damage.

Typical gold ball sizes range from 70  $\mu m$  to 100  $\mu m$  in diameter. The size of the Flip-Mesh bonding pad is 100  $\mu m$ . Since density is already a limiting factor in the Flip-Mesh approach, increasing the via size is not desirable. It was also found that the extreme heat and pressure required to make an acceptable contact between the Flip-Mesh substrates caused the YBCO to become non-superconducting. The YBCO could be repaired by annealing, but the substrates would detach in the process.

The second assembly method attempted was to individually place preformed indium spheres. Indium was chosen because of its decent conductivity and low melting point. It was quickly discovered, however, that indium is far too soft to be handled mechanically, and no modules could be formed using this method. Stencil printing was then determined to be the ideal method for placing Flip-Mesh via bumps. A batch process would certainly be desirable, but the small via size (4 mil) and pitch (8 mil) puts severe limitations on this technology.

The first material to be screen printed was conductive epoxy, but this material was unable to meet the density requirement. The epoxy bumps would flatten and create shorts. Further work with the viscosity of the epoxy may lead to a useful application.

The next stencil printing material used was tin/lead solder. A special high-density solder was acquired, and worked nicely, but standard tin/lead solder has a leaching problem with the gold contact pads. Modules fabricated in this process detached within hours due to the leaching. Another solder paste was then acquired, which contained an additional 2% silver to prevent gold leaching.

After screen printing solder pads to the main substrate, the secondary substrates are aligned to the main substrate, and the solder is reflowed. The current Flip-Mesh material components are laser-ablated YBCO on single-crystal YSZ substrates with gold contact pads interconnected by screen printed tin/lead/silver solder bumps.

## INITIAL FLIP-MESH CIRCUIT

The initial Flip-Mesh circuit is a ring oscillator formed from 2 quad-XOR HCMOS chips. The first XOR gate has one input tied high, which turns it into an inverter. The other gates have one input tied low, which makes them buffers. This arrangement allows the number of gates in the loop to be adjusted from 2 to 8, allowing different speeds of oscillation. The IMPS power and ground stripes are 250  $\mu$ m wide, the signals are 50  $\mu$ m wide, and the spacing between the two is 50  $\mu$ m. The main substrate is 10 mm x 10 mm, and the secondary substrates are 2.5 mm x 10 mm. As was discussed

before, the contact pads are 100  $\mu m$  x 100  $\mu m$  . The XOR chips are approximately 1mm x 1mm each.

## FLIP-MESH ASSEMBLY AND TESTING

After a Flip-Mesh substrate module is completed, the XOR chips are attached using thermoplastic tape. The leads of the chips are then aluminum wire bonded to the main substrate. The number of gates in the oscillator loop is selected by a wire bond in the center of the main substrate. The assembled Flip-Mesh module is then attached to a test board using thermoplastic tape. The I/O pads of the module are then aluminum wire bonded to the test board. Figure 3 shows an assembled Flip-Mesh module connected to a test board. When complete, the test board is attached to an oscilloscope and power supply, measuring the output signal of the first XOR gate. The module is then slowly immersed in a small dewar of liquid nitrogen.

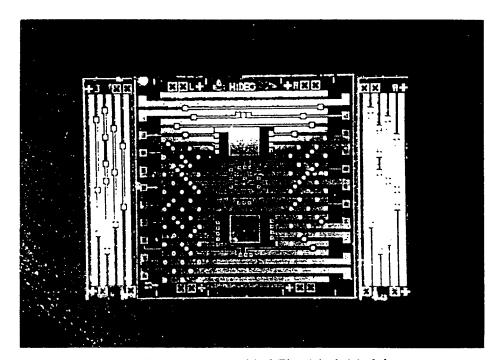


Figure 3: Assembled Flip-Mesh Module

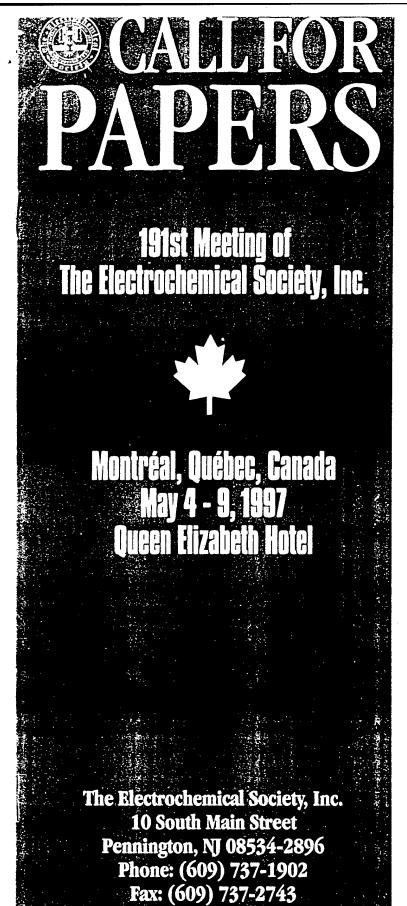
## CONCLUSION

Functional Flip-Mesh modules have been fabricated only with metal interconnect. These modules were built on glass substrates with gold/titanium-tungsten metallization, and the substrates were interconnected with gold balls formed by a ball bonder. These modules were tested both at room temperature and while immersed in liquid nitrogen with 2 to 8 gates in the oscillator loop. As would be expected, the modules ran faster at

cryogenic temperature. While the gold ball vias worked adequately for a metal module, they were found to be incompatible with YBCO due to damage caused by the attachment process. The stencil printing processes discussed are under investigation to find a YBCO-compatible process. It will be interesting to compare the performance of the cryogenic YBCO Flip-Mesh to the cryogenic metal Flip-Mesh.

## REFERENCES

- [1] R.G. Florence, S.S. Ang, W.D. Brown, G. Salamo, L.W. Schaper, and R.K. Ulrich, "Sputter-Deposited Yttrium Barium Copper Oxide Multilayer Structures Incorporating a Thick Interlayer Dielectric Material", Journal of Applied Physics, Vol. 79, No. 4, pp. 2003-2005, 1996.
- [2] L.W. Schaper, S. Ang, Y.L. Low, and D. Oldham, "Electrical Characterization of the Interconnected Mesh Power System (IMPS) MCM Topology", Proceedings of the 44th Electronic Components & Technology Conference, Washington, D.C., May 1-4, pp. 791-795, 1994.
- [3] S. Afonso et al., "Magnetic Field and Temperature Dependence of Critical Current Densities in Multilayer YBa<sub>2</sub>Cu<sub>3</sub>O<sub>7-8</sub> Films", Journal of Applied Physics, Vol. 79, No. 8, pp. 6593-6595, 1996.
- [4] S. Scott, "Ion Milling of Yttrium-Barium-Copper-Oxide for Interconnects in a Superconducting Multichip Module", M.S.E.E. Thesis, University of Arkansas, 1994.



e-mail: ecs@electrochem.org

Home Page: http://www.electrochem.org

and a forum for the exchange of information on the latest scientific and technical developments in the fields of electrochemical and solid-state science and technology. The 191st Meeting continues this tradition and serves as a major conference for the discussion of interdisciplinary research from around the world through a variety of formats, such as oral presentations, poster sessions, panel discussions, and tutorial sessions.

## Hotel & Meeting Registration

The 1997 Spring Meeting will be held at the Queen Elizabeth Hotel, 900 René Lévesque Blvd. West, Montréal, Québec, Canada H3B 4A5. The Queen Elizabeth is ideally located in the heart of downtown Montréal, with direct access to the train station, metro station, and the underground city. The shuttle bus from the downtown airport terminal stops at the hotel's door. The Queen Elizabeth is also within walking distance to many restaurants, business centers, shopping and cultural activities, such as historic "Old Montréal" with its cobblestone streets, horse-drawn carriages, and outdoor cafés. Since the Queen Elizabeth Hotel is the Headquarters Hotel, the Society has special discounted rates for our attendees. Please note that May is a busy month and space is limited, so we encourage you to make your reservation early to ensure your comfort and convenience. Be sure to mention that you will be attending the ECS Meeting to obtain the following special rates. The deadline for reservations is April 3, 1997.

\$132.00 Canadian Dollars ......Single Occupancy \$152.00 Canadian Dollars ......Double Occupancy

(At today's exchange rate, the single occupancy rate of \$132.00 in Canadian Dollars is approximately \$99.00 in US Dollars)

The Queen Elizabeth Hotel telephone number is (514) 861-3511 or toll free phone number (800) 441-1414 and the fax number is (514) 954-2256. A limited amount of additional rooms have been reserved at the Montréal Marriott Chateau Champlain. I Place du Canada, Montréal, Québec, Canada H3B 4C9 at the rate of \$130 Canadian Dollars for a single and \$150 Canadian Dollars for a double. The Montréal Marriott is approximately 3 blocks from the Queen Elizabeth Hotel and the phone numbers are (514) 878-9000 and (800) 228-9290 (toll free): the fax number is (514) 878-6761. Meeting registration and additional hotel reservation information will be sent to all members, authors of papers, and technical session co-chairs in February 1997.

## Abstract Submission

Submit one original, properly formatted, Meeting Abstract either electronically or on paper by January 2, 1997 to the Society Headquarters Office, with a second copy to the appropriate Symposium Organizers (see back cover for complete instructions). Abstracts should explicitly state objectives, new results, and conclusions or significance of the work. Programming for this Meeting will occur in January 1997, with some papers scheduled for poster presentation. All presenting authors will receive a letter from the Society Headquarters Office notifying them of the date and time of their presentation. You may also check the ECS Home Page for further program details.

# **Manuscript Preparation**

All Meeting Abstracts will be published in the Meeting Abstracts Volume, copyrighted by The Electrochemical Society, Inc. and become the property of the Society upon presentation. Acceptance of an abstract in a symposium for which a proceedings volume is planned obligates the author to submit a camera-ready copy of the full manuscript to the Symposium Organizers. To publish in the Journal of The Electrochemical Society a full manuscript must be submitted within six months of the symposium date. "Instructions to Authors" are available from the Society Headquarters Office, the Journal, or the ECS Home Page. If publication elsewhere is desired after presentation, written permission from the Society Headquarters Office is required.